AN ABSTRACT OF THE THESIS OF

Young-kong Lei for the degree of Doctor of Philosophy

in Department of Forest Products presented on October 17, 1977

Title: ON THE FRACTURE MECHANICS OF ORIENTED FLAKEBOARD

Abstract approved:

James B. Wilson

For an oriented flakeboard it is hypothesized that its fracture toughness (K_{IC}) is determined by the size and frequency of the inter-flake voids and non-bonded areas that occur in the board. This hypothesis is verified with a carefully controlled experiment. In accordance with the experimental observation a two-dimensional analytical model is subsequently constructed to depict the effect of inter-flake voids and non-bonded areas upon K_{IC}. Finally, the proposed analytical model is experimentally verified.

In addition to the inter-flake voids and non-bonded areas, the parameter effects of original solid wood, resin solids spread rate, board density, flake dimensions, and loading speed are also experimentally evaluated in terms of four different fracture modes, namely RL, TL, TR, and RT modes. Among the parameters studied, only the effect of inter-flake crack (void plus non-bonded area) shows a consistent trend on the K_{IC} of oriented flakeboard.

The establishment of the proposed model consists of two major parts. The first part is to analytically model the effect of an expected inter-flake crack length (Δc) in terms of fracture-strength

reduction factor in an oriented flakeboard. The second part is to incorporate into the model a proportional variable (g), which is obtained by pure deduction according to the experimental observation, to improve the flexibility of the model. This analytical model is experimentally verified at an average error of 6.9 percent.

The study concludes that the K_{IC} of a Douglas-fir oriented flakeboard is determined by the inter-flake crack length and the distance between cracks in the board, assuming that the flakes were not severely damaged and that the resin was properly applied.

ON THE FRACTURE MECHANICS OF ORIENTED FLAKEBOARD

by

Young-kong Lei

A THESIS

submitted to

Oregon State University

in partial fulfillment of
the requirements for the
degree of

Doctor of Philosophy

Completed (October 17, 1977)

Commencement June 1978

APPROVED:

Redacted for privacy

Assistant Professor of Forest Products
in charge of major

Redacted for privacy

Head of Department of Forest Products

Redacted for privacy

Dean of Graduate School

Date thesis is presented October 17, 1977

Typed by Chi-mei Lei for Young-kong Lei

TABLE OF CONTENTS

TABLE OF CONTENTS (continued)

LIST OF TABLES

LIST OF FIGURES

LIST OF FIGURES (continued)

LIST OF FIGURES (continued)

ACKNOWLEDGEMENTS

I wish to express my sincere appreciation to my major professor, Dr. J. B. Wilson, for his assistance, encouragement, and patience throughout this research program.

Appreciations are also due to Dr. A. Polensek, Dr. J. D. Wellons, and Dr. C. E. Smith for their serving on the committee, and especially for their constructive criticisms on the final draft of the thesis.

Special thanks go to Dr. F. L. Ramsey, Miss S. Tarng, and Dr. P. H. Kanarek for their help in statistical modelling and analysis.

Lastly, I wish to express my hearty gratitude to my parents for their continued encouragement and sacrifices throughout my education, and to my wife for her help in typing the drafts and the final copy of this thesis.

ON THE FRACTURE MECHANICS OF ORIENTED FLAKEBOARD

I. INTRODUCTION

The age for the forest products industry of generating high-grade lumber from old-growth trees will soon be ending. Fast-growth, juvenile, or previously low valued trees are becoming the major source for wood structural components and commodities. The effect of natural defects which are prevalent in these trees thus becomes a serious problem in terms of generating good quality lumber out of lower quality trees. In order to minimize the effect of natural defects an increasing use of reconstituted wood composites, in which natural defects are reduced in size and uniformly dispersed throughout the product, should be a foreseable trend. Thus, the responsibility that challenges the wood scientists is to design engineered wood composites to replace the decreasing availability of high-grade lumber.

Viewing current commercial wood composites, one can categorize their principles of design into process and use aspects. The process principle is to re-distribute the natural defects and to reduce the inherent directional effect from solid wood, such as the design of particleboard and plywood. For the use aspect, simple beam theory is often used, which states that the outermost layers in a beam sustains the maximum stress. This is the mechanical principle mostly applied in the design of wood products, such as the formation of a veneer-flakeboard sandwich panel (com-ply) and a layered particleboard.

Although the adoption of the simple beam concept in designing layered wood composites makes them more comparable in flexural

strength to solid wood, these composites, however, are still weak in their normal tensile strength (tensile strength perpendicular to surface, or familiarly called the internal bond strength). A laboratory-made Douglas-fir flakeboard or com-ply usually retains one-third the normal tensile strength of the same species of solid wood (Lehmann 1973, Wood Handbook 1974).

The normal tensile strength of wood or a wood composite is no longer just a property figure in the Wood Handbook (1974). The occurrence of normal tension failures of curved beams in service led to the recommendation that the normal tensile stress be limited to 15 psi for Douglas-fir (Hanrahan 1966). This has become part of the current National Design Specification for Stress-Grade Lumber and Its Fastening (National Forest Products Association 1973).

Theoretically, a normal tensile stress can occur in any structural member which is not perfectly straight when subjected to end compressive forces. If the trend of increasing usage of wood composites for structural purposes is unavoidable, then there exists a need for investigating and improving the normal tensile strength property of wood composites.

Failure in solid wood generally initiates from natural defects such as knots. In wood composites, depending on the size of their individual wood constituents, the natural defects of the solid wood are generally reduced in size and dispersed. Whereas, the processing defects, such as mechanically damaged wood constituents, inter-flake voids, and non-bonded areas between constituents become the obvious failure-initiation nuclei. Thus, the analysis of wood-composite

strength is actually an investigation of the effects of these processing defects. To deal with these kinds of effects, the application of fracture-mechanics concept, which will be explained in the next paragraph, is ideal.

A basic assumption in the study of fracture mechanics is the existence of at least one flaw within the material. The analysis of failure involves the size of this flaw and the resistance of the material to generate a new surface area at the tip of the flaw. Thus, the concept of fracture mechanics is more mechanistic than phenomenological. It can provide a theoretical basis for understanding failure in wood composites.

Because the normal tensile strength of a material is actually the fracture toughness (K_{IC}) of the material in the terminology of fracture mechanics, the main scope of this study, therefore, is to investigate the fracture toughness (K_{IC}) of oriented flakeboards.

II. OBJECTIVE

1. To experimentally identify the critical parameters among flake grain orientation, flake dimensions, board density, resin solids spread rate, and loading speed which affect the fracture toughness (K_{IC}) of oriented flakeboard.

2. To construct an analytical model which, considering the effects of the critical material parameters, quantitatively depicts the fracture toughness (K_{IC}) of oriented flakeboard.

3. To experimentally verify the analytical model.

III. LITERATURE REVIEW

Wood Composites

Flakeboard is a specific type of wood composite. According to Dietz (1972), "composites are considered to be combinations of materials in which the constituents retain their identities in the composite on a macro scale, that is, they do not dissolve or otherwise merge into each other completely, but they do act in concert." The most familiar composites of woody material can be classified into two major kinds: fibrous composites which include paper and fiberboard; and solid wood composites which include glulam, microlam, plywood, com-ply, flakeboard, and particleboard. Glulams are manufactured by laminating smaller pieces of lumber together to a desired larger dimension. Both plywood and microlam are also laminated products, with thin, rotary-peeled or sliced veneers assembled either with alternate layers at right angles to form plywood or laid up in a parallel alignment to fabricate microlam. Flakeboard is made from engineered particles of uniform length, thickness and width, whereas particleboards are made from particles of irregular shapes and dimensions. Com-ply is a sandwich product with veneer surface layers and a flake- or particleboard core. In this review, however, only the empirical and theoretical findings on flakeboard are emphasized.

Material Parameters Affecting Mechanical Properties of Flakeboard

Specific Gravity of Wood Flakes

High specific gravity or density has long been regarded as an indicator of good strength properties for solid wood (Wood Handbook 1974). However, a given density flakeboard produced from low density wood flakes is usually stronger in normal tensile and bending strengths than one produced from higher density wood flakes (Larmore 1959, Stayton et al 1971). This behavior is attributed to the higher compaction ratio for a given weight of low density flakes, resulting in increased contact between surfaces of flakes, a necessary condition for an increase in resin bond formations.

Flake Dimensions

The effects of flake dimensions on the mechanical properties of board have been studied by many investigators (Turner 1954, Post 1958, 1961, Brumbaugh 1960, Lehmann 1974). The general observations are: flakes up to four inches long produce better boards in bending strength; flakes up to .045 inch thick result in higher normal tensile strength; flake length to thickness ratio (slenderness ratio) is a good indicator of optimum flake dimensions with a proposed optimum slenderness ratio range from 100 to 300.

Resin Content

Resin content is defined as the weight percentage of resin solids to oven-dried wood flakes in a board. An increase of resin content from two to eight percent does show a tendency of increasing bending and normal tensile strength of flakeboard (Lehmann 1970, 1974). However, the effect of resin content is easily overshadowed by the

influences of board density (Turner 1954), specific gravity of wood flakes (Larmore 1959), and flake dimensions (Post 1958, 1961). A resin spread of at least one pound of resin solids per thousand square feet of flake surface area has been proposed by Lehmann (1974) as an optimum amount for overall board properties.

Flake Orientation

Flake orientation has become an important subject lately, both in the field of academic research (Lehmann 1974) and commercial research (McKean et al 1975), mainly because, flakeboard with controlled directional properties may offer advantages for specific engineering applications. Flakeboards with increased bending strength and stiffness in one board direction might be obtained by orienting the flakes within the board. This practice, however, would sacrifice strength in the transverse board direction (Lehmann 1974).

Board Density

Board density is a direct indicator of the substance that a board contains and the degree of contact between the flakes. These in turn affect all the mechanical properties of the flakeboard. Turner (1954) suggested that board density had primary influence in controlling the bending strength of flakeboard. The same tendency is also observed for all the mechanical properties other than bending strength (Lehmann 1970, 1974). However, an average board density is by no means an independent variable which determines the mechanical properties of a flakeboard. Its effect is not only closely related to the uniformness

of the density throughout a board, but also greatly affected by all the material parameters discussed previously.

There are other material parameters such as wood species and resin type, and processing parameters such as press temperature, press cycle, press closing time, and mat moisture content, also affecting the mechanical properties of board (Moslemi 1974, Kelly 1975). These parameters, however, are less subject to change in a given circumstance than those discussed previously. Therefore, they are treated as constants in this study.

Theoretical Strength Analysis of Flakeboard

Strength analysis can usually be treated as an extension of stiffness analysis by imposing a predetermined stress limit or a failure theory in the stiffness analysis. The maximum force a composite can sustain is thus obtained when the internal stress reaches the imposed limit. This predetermined stress limit, however, is usually obtained from experimental tests of the uniaxial strength properties of the material to be analyzed. In other words, theoretical strength analysis is usually similar to stiffness analysis, unless the combined stresses are involved in the loading condition, then a failure theory is needed. Therefore, the presentation in this section of the theoretical strength analysis of wood composites is given with the stiffness analysis.

In contrast to an ordinary laminated composite which has continuous layered structure or laminae, flakeboard has discontinuous laminae and interspersed voids. In spite of these differences,

flakeboard has often been treated as a laminated composite to make the theoretical analysis possible (Keylwerth 1958, Suchsland 1960, Plath 1971). Theoretical analysis of laminated composites covers a very broad field and numerous subject matters. Here, only the analysis of fiber-reinforced laminates, which are similar to wood composites, will be briefly discussed. For further in-depth information, books written by Jones (1975), Garg et al (1973), and Vinson and Chou (1975) are recommended.

"Mechanics analysis in general requires a mathematical model. The model is intended to depict a behavior of an actual material." (Tsai 1966 P.1). In order to depict a physical behavior in simple mathematical terms, the first step is to identify the problem, and then to make appropriate assumptions. For fiber-reinforced composites, which usually consist of laminations of fiber-matrix laminae, the following assumptions are usually needed to be made (Jones 1975): "The lamina is macroscopically homogeneous, linearly elastic, macroscopically orthotropic, initially stress-free. The fibers are homogeneous, linearly elastic, isotropic, regularly spaced, perfectly aligned. The matrix is homogeneous, linear elastic, isotropic. In addition, no voids can exist in the fibers or matrix or in between them (i.e. the bonds between the fibers and matrix are perfect)." Also, the strains in the fiber direction of an unidirectional fibrous composite are the same in the fibers as in the matrix. With all the above assumptions, a simple but well-known model called the "law of mixtures" has been proposed to depict the elastic property of a lamina. For a specified direction (Figure 1a), the law

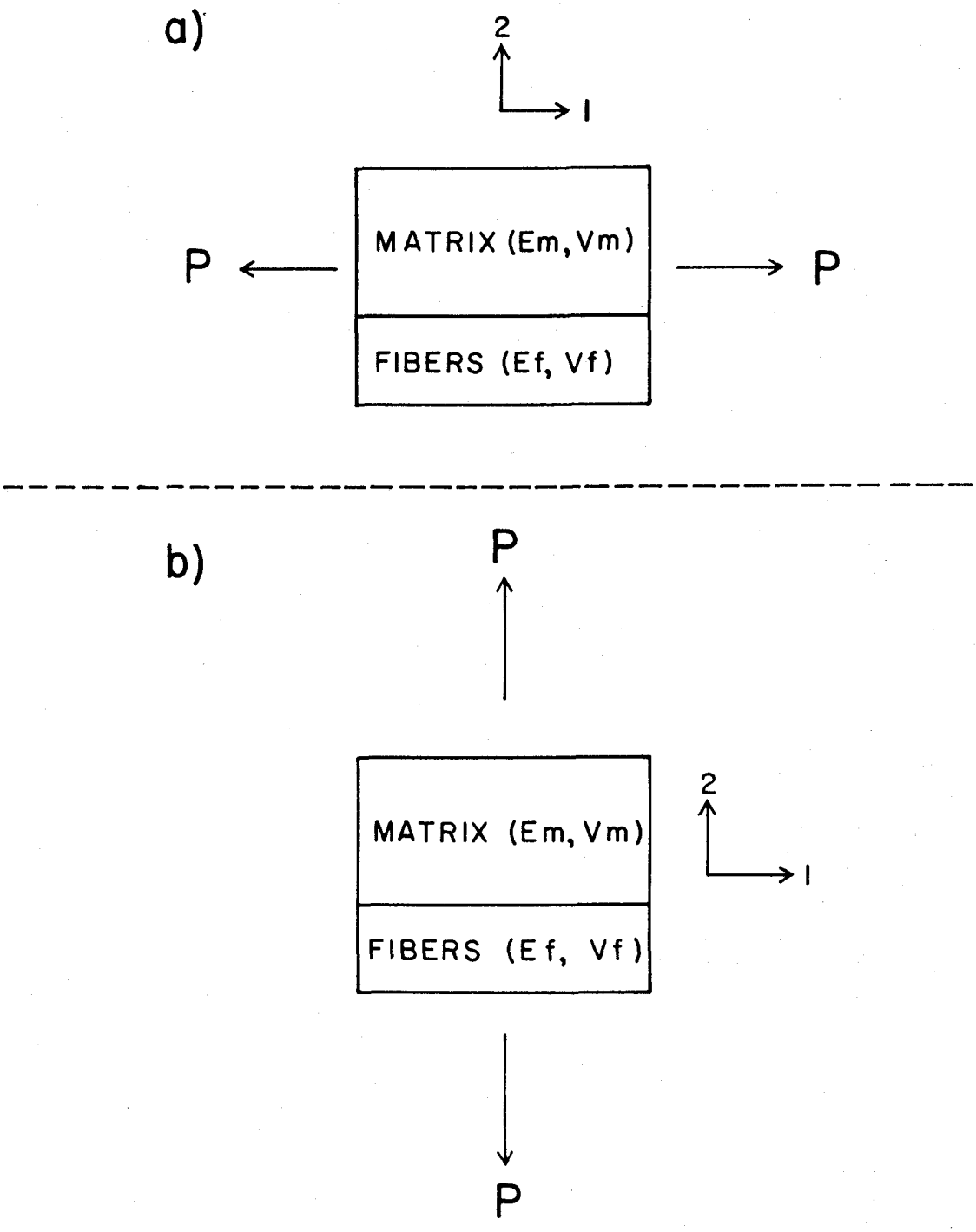

Figure 1. Composite model for the law of mixture. a) parallel loading, and b) transverse loading

of mixtures can be written in terms of Young's modulus (E) as

$$E_1 = E_f V_f + E_m V_m \qquad \text{(Jones 1975 P.91)} \tag{1}$$

or in terms of stresses as

$$\sigma_1 = \sigma_f V_f + \sigma_m (1-V_f) \qquad \text{(Garg 1973 P.19)} \tag{2}$$

with the assumption that the strains $\varepsilon_1 = \varepsilon_m = \varepsilon_f$ are in the direction of loading. In the derivation of Equation (1) or (2), the stresses generated due to Poisson's ratio differences in the two materials were neglected. In Equation (1) and (2),

E_1, E_f, E_m = Young's modulus of laminated composite, fiber, and matrix in loading direction

V_f, V_m = volume fraction of fiber and matrix

σ_1, σ_f, σ_m = stress of laminated composite, fiber, and matrix in loading direction

ε_1, ε_f, ε_m = strain of laminated composite, fiber, and matrix in loading direction

The law of mixtures simply states that the constituent materials contribute to the composite stiffness or strength in proportion to their own stiffness or strength and volume fractions.

Although the law of mixtures can be applied to a simplified model for a specified loading direction (Figure 1a), complications would be encountered if a transverse load is considered (Figure 1b). It is logical to assume that a load P applied in the transverse direction to the laminated composite would result in equivalent stresses σ_2 in both fiber and matrix in the loading direction (Figure 1b). Then the strains of fiber and matrix in the same direction are given by

$$\varepsilon_f = \frac{\sigma_2}{E_f} \quad , \quad \varepsilon_m = \frac{\sigma_2}{E_m} \tag{3}$$

Equation (3) actually represents a mismatch in strains at the boundary. Thus, the assumption of perfect bonding between fiber and matrix in the composite is violated in the case of transverse loading. In other words, in order to depict a physical behavior in simple mathematical terms, it is necessary to make idealistic assumptions on the boundary conditions, however the simplier the model, the harder it is to maintain consistency in the assumptions. The seriousness of such inconsistencies can usually be measured by comparison with experimental results or with more sophisticated models.

A complete match of strains across the boundary between the fiber and the matrix would constitute a rigorous solution that could be solved by the theory of elasticity. Many of the available papers, however, are quite abstract and of little direct applicability to practical analysis at this stage of development for elasticity approaches (Jones 1975 P.108).

Generally speaking, even using an elasticity approach, the volumetric fractions of matrix, fiber, and their respective elastic constants are usually the necessary terms in the derivations of the theoretical equations and in the resulting equations. In other words, the concept of law of mixtures is often a major gradient in the elasticity analysis. If the same approach applies to flakeboard, immediate difficulties will be encountered, since the matrix (resin) in flakeboard is almost volumeless and its functioning elastic properties are practically unknown. Although flakeboard has been

treated as a layered laminate for theoretical analyses, some of the considerations have to be different from that of the fiber-reinforced composites.

Keylwerth (1958) probably was the first to theoretically analyze the elastic properties of a three-layered particleboard model. The analysis was to relate the thickness and elastic properties of each layer to the elastic properties of the board. The mathematical relationships between board and layer properties under bending were established as

$$E = E_f - (1-\lambda)^3(E_f-E_c) \tag{4}$$

$$G = G_f - (1-\lambda)^3(G_f-G_c) \tag{5}$$

where

E, G = Young's and shear modulus of board

E_f, G_f = Young's and shear modulus of face layers

E_c, G_c = Young's and shear modulus of core layer

$$\lambda = \text{shelling ratio} = \frac{\text{face layers thickness}}{\text{core layer thickness}}$$

These relationships were examined with reference to density, moisture content, and resin content. As far as the material parameters are concerned, the moduli, density, and thickness of each layer are more important than the other in determining the overall board properties.

Suchsland (1960) used the relationship in Equation (4) to obtain Young's modulus (E) of the face layers because it was difficult to experimentally measure the E of a thin face layer in a three layered flakeboard. Then, an empirical relationship between densities and E

of each layer was used to substitute back into Equation (4), which results in a semi-empirical equation to predict board E.

By further extending Keylwerth's (1958) model to a three-layered particleboard, Plath (1971) used parabolic and sinusoidal functions to represent the continuous transition of density profiles across the thickness of a particleboard, and then combined this with the expanded version of the law of mixtures. The resulting equation for bending can be written as

$$E = \frac{E_M}{e_M} f(e) \qquad (6)$$

where

E = Young's modulus of board in bending

E_M = maximum value of E--profile which can be found at the point of the greatest density e_M

f(e) = a factor dependent on the gross density profile

Then the idea is to optimize Equation (6) in order to obtain the maximum Young's modulus of the board. Unfortunately, the process of optimization cannot be done analytically. No strength analysis is involved in either Keylwerth's (1958) or in Plath's (1971) work.

Based on the Hankinson's formula and the strength of material principle, Bryan (1962) calculated the maximum in-plane tensile and compressive strength as well as the bending strength of particleboard. Unfortunately, the assumptions he made on the use of the Hankinson's formula and on the failure mechanism of particleboard lack empirical evidence. Also, little consideration had been given to the internal

structure of actual particleboard. The resulting equations, therefore, do not reveal useful information for design purposes.

Rackwitz (1963) observed the difficulties of obtaining an analytical model which could quantitatively describe the influence of flake dimensions on flakeboard properties. Therefore, he set up a series of geometric models to discuss the effects of flake dimensions qualitatively. Rackwitz proposed that a flakeboard would reach its in-plane tensile strength when either the resin layer could no longer sustain the shear force or the wood flake failed to resist the tensile force. Starting at zero for increasing length of flake overlap, the failure first occurred at the resin layer, till an optimum overlapping length was reached. Failure then occurred in the wood flake (Figure 2). He also suggested that a further increase of overlapping length would not further increase the strength of flakeboard. The optimum overlapping length should be decided at the point of intersection of tensile and shear lines (Figure 2). To express this relationship mathematically, then

$$T = \sigma_w \cdot b \cdot t \tag{7}$$

$$V = \tau_r \cdot b \cdot 2L \tag{8}$$

At the intersection, since

$$T = V \tag{9}$$

then,

$$\sigma_w \cdot b \cdot t = \tau_r \cdot b \cdot 2L \tag{10}$$

therefore,

$$\frac{L_{opt}}{t} = \frac{1}{2} \cdot \frac{\sigma_w}{\tau_r} \tag{11}$$

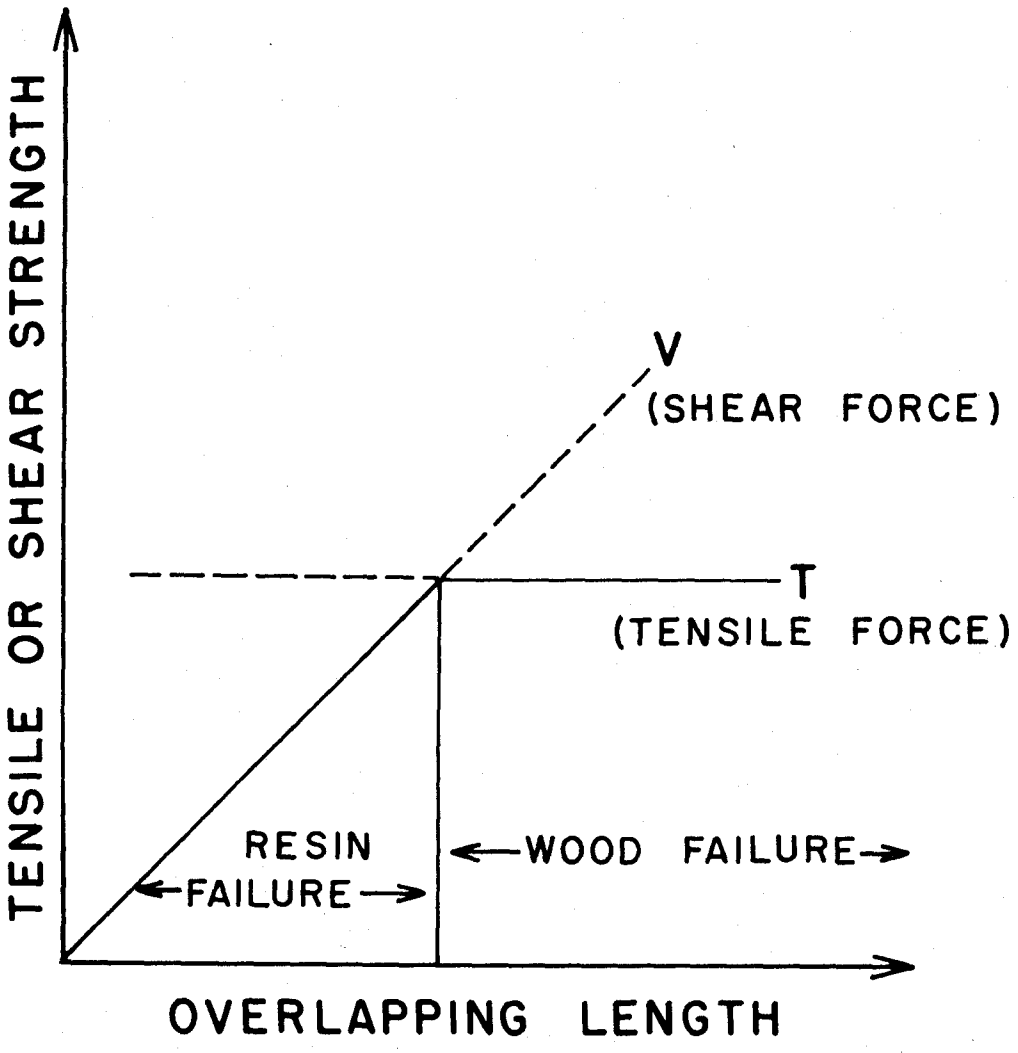

Figure 2. Relationship of flake bonding strength with the flake overlapping length

where

T, V = tensile and shear forces

σ_w = horizontal or in-plane tensile stress in wood

τ_r = shear stress in resin joint

L = flake overlapping length

b, t = flake width and thickness

L_{opt} = optimum overlapping length

From Equation (11), Rackwitz proposed, without explanation, that the optimum overlapping ratio is reached, if

$L_{opt} = 1/2\ (L - d)$, because $d \ll L$ so that $L_{opt} \simeq L/2$

where d is an interval between two flakes. In other words, the optimum overlapping length is one-half of each flake length.

Rackwitz (1963) also proposed that normal tensile strength of flakeboard increased with the resin strength σ_{rn} of resin layers loaded perpendicular to board surface, but decreased with the increasing magnitude of interspace d between flakes, and further decreased with a smaller flake length because the number of interspaces increased. Thickness and width of the flake were not considered as having any influence. Again, without explanation, Rackwitz found an equation for the normal tensile strength of flakeboard as

$$\sigma_w = \sigma_{rn} \cdot \frac{1}{1+\frac{d}{L}} \qquad (12)$$

where

σ_w = normal tensile strength of board

d = interspace between flakes

σ_{rn} = normal tensile strength of resin layer

L = flake length

Kusian (1968) also did a theoretical study on the influence of flake size on the structure and strength properties of flakeboard by using idealized geometric models combined with probability theory. Kusian's analysis is quite extensive, but the reasoning in some of his derivations for the models is difficult to understand. In contrast to the theoretical studies done by the other investigators, Kusian's discussion on the two-dimensional analysis is for the length-width plane rather than the length-thickness plane. Therefore, the flake width automatically becomes an important factor in determining the theoretical normal tensile strength of flakeboard. The resulting equation for normal tensile strength is

$$\sigma_n = \sigma_{wn} \cdot 2\left[\left(\frac{m}{m^2+1}\right) - \left(\frac{m}{m^2+1}\right)^2\right] \qquad (13)$$

when $\sigma_{rn} > \sigma_{wn}$,

or

$$\sigma_n = \sigma_{rn} \cdot 2\left[\left(\frac{m}{m^2+1}\right) - \left(\frac{m}{m^2+1}\right)^2\right] \qquad (14)$$

when $\sigma_{wn} > \sigma_{rn}$,

where

σ_n = normal tensile strength of flakeboard

σ_{rn} = normal tensile strength of resin layer

σ_{wn} = normal tensile strength of solid wood

$$m = \text{width ratio} = \frac{\text{flake width}}{\text{flake length}}$$

From Equation (13) and Equation (14), Kusian suggested that normal

tensile strength of flakeboard decreases with increasing width ratio of flakes.

Hunt (1970) used the finite element method to analyze the elastic properties of a structural analog of a flakeboard specimen subjected to an in-plane tensile load. Two types of elements were used: prismatic beam elements to represent the resin phase, and rectangular plate elements to represent the wood flake phase. Because the plate elements represented the wood flake phase, each plate was considered to have a randomly oriented grain direction. In order to model the elastic behavior of an actual tensile specimen, the structural idealization was completed by imposing a tensile load vector on the analog. This was not the actual load applied to the tensile specimen, but was actually the load adjusted for board density, moisture content, and weights of wood furnish and resin. A series of force and displacement results could be obtained to calculate the elastic properties of the analog. Strength analysis of flakeboard was not considered by Hunt.

The author of this thesis has conducted preliminary investigations on the strength analysis of flakeboard using the finite element approach. However, due to a lack of expertise by the author in finite element analysis, the solutions to the following three problems which are necessary to precede with the investigations were not found. These problems are: 1. modeling the contact effect between flakes, or the effect of flake density on board strength; 2. modeling the bonding mechanism between flakes; 3. identifying and modeling a failure criterion to match experimental observations for the normal tensile strength of flakeboard.

In this review of the literature, emphasis has been given to the theoretical analyses of flakeboard, especially to the end results or equations of analyses. The purpose is to describe the theoretical works which have been done for flakeboard and how the material parameters theoretically affect the flakeboard properties. Some of the analytical results might be useful for the purpose of designing better flakeboard, others might only be good for academic discussion. However, the concept or approach which has already been used to theoretically analyze a flakeboard should be borne in mind by the researchers who are interested in the theoretical analysis of flakeboard.

From this review, one should observe a distinct fact that none of the analyses on flakeboard strength has dealt with the processing defects in making flakeboards, such as inter-flake voids, non-bonded areas, or mechanically damaged wood flakes. Because the published strength properties of flakeboard are consistently lower than those of clear solid wood, it is ironical not to consider these processing defects in flakeboard, which have to be detrimental to flakeboard strength, when doing the theoretical strength analysis of flakeboard. For this reason, the concept of linear-elastic fracture mechanics will be used in this research to analyze the effect of processing defects on the normal tensile strength or fracture toughness of oriented flakeboard.

IV. LINEAR-ELASTIC FRACTURE MECHANICS

The history of studying the possible material-flaw effects on material strength can be traced back to the time of Leonardo da Vinci (1452-1519). He tested beams of uniform cross section and varying lengths, and concluded that the strength of a beam supported at both ends varies inversely to the length (Timoshenko 1953). Extensive investigations on fracture effects, however, were not initiated until World War II. Then, due to the increasing use of high-strength material, numerous fractures had occurred in gas transmission lines, in pressurized cabins of commercial jet planes, and in pressure vessels of many kinds. Each incident occurred unexpectedly. In each case it was felt that conventional engineering design practice had been followed sufficiently. The causes of these fracture failures have been attributed to the effects of flaws and stress concentrations (Broek 1977). Therefore, we could say that the occurrence of low stress fracture in high strength materials induced the development of fracture mechanics. The term "fracture mechanics" was not formally used until the early 1950's.

In contrast to the relative completeness in the development of linear elasticity theory, fracture mechanics is still in a developmental stage. The analysis of fracture mechanics primarily covers two broad fields: linear and nonlinear. Linear elastic fracture mechanics mainly deals with the brittle fracture, whereas nonlinear analysis is concerned with the influence of a large amount of plastic flow at the crack tip prior to failure. Nevertheless, the

fundamentals of analyses originated mainly from two important concepts, namely, the Griffith energy-balance concept and the Irwin crack-extension-force concept.

Griffith Energy-Balance Concept

The idea of the Griffith energy-balance concept is to set up a model for a crack system in terms of a reversible thermodynamical process (Figure 3), then to search for the configuration which minimizes the total free energy of the system; the crack would then be in a state of equilibrium, and thus on the verge of extension.

In order to minimize the total free energy in the system (Figure 3), we need to consider the total energy U in its individual terms which change as a result of crack formation. First, the applied load would deform the cracked body and does an amount of work W_L to the system. Second, the deformation will result in a storing of the strain potential energy U_E in the system. Third, the act of creating new crack surfaces generates the free surface energy U_S. For a static crack system, the total energy U is then the sum of these three individual energies, therefore

$$U = (-W_L+U_E) + U_S \tag{15}$$

Because the loading system and elastic medium jointly provide the agency through which forces are transmitted to the crack region, it is convenient to refer to the composite bracket term in Equation (15) as the mechanical energy of the system.

Thermodynamic equilibrium is then attained by balancing the mechanical and surface energy terms over a virtual crack extension δc

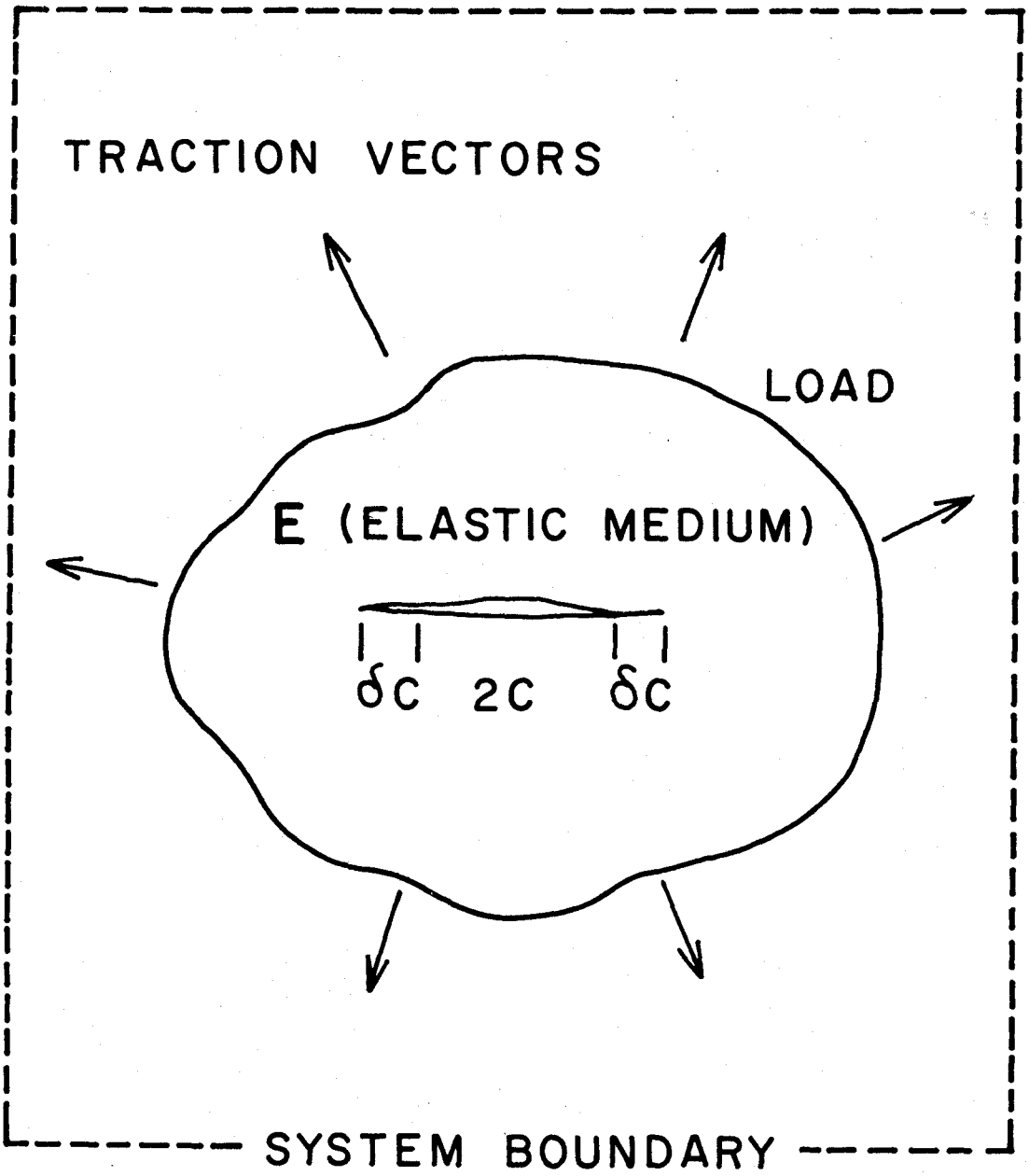

Figure 3. Static plane-crack system

(Figure 3). It is not difficult to see that the surface energy term must increase with the extension of the crack. Meanwhile, the mechanical energy must decrease in order to minimize the total energy U. Thus, the first (composite) term favors crack extension (note that W_L is always larger than or equivalent to U_E for the cracked body), while the second opposes it. This is then the Griffith energy-balance concept, a formal statement of which is given by the standard equilibrium requirement

$$\frac{dU}{dc} = 0 \tag{16}$$

Equation (16) is then a criterion for predicting the fracture behavior of a cracked body. A crack would extend or close up reversibly for small displacements from the equilibrium length, according to whether the $\frac{dU}{dc}$ is negative or positive.

When the Griffith energy-balance concept is applied to a cracked body under the influence of a constant tensile load at infinite ends, then

$$W_L = 2U_E \qquad \text{(constant load)} \tag{17}$$

For a thick plate (plane strain) of uniform width, the strain energy is

$$U_E = \pi(1-\nu^2)c^2\sigma_L{}^2 \,/\, E \qquad \text{(Lawn and Wilshaw 1975)} \tag{18}$$

Here ν is Poisson's ratio, c is half crack length, E is Young's modulus, and σ_L is applied tensile stress normal to the crack plane.

The surface energy of the crack system with a unit width is

$$U_S = 2c \cdot 2r = 4cr \tag{19}$$

where r is the free surface energy per unit area. The total system energy thus becomes, for the case of plane strain, say,

$$U = -W_L + U_E + U_S$$
$$= -U_E + U_S$$
$$= -\pi(1-\nu^2)c^2\sigma_L{}^2 / E + 4cr \qquad (20)$$

Applying Equation (16) to Equation (20), then

$$\sigma_L = [\frac{4Er}{\pi c(1-\nu^2)}]^{\frac{1}{2}} \qquad \text{(plane strain)} \qquad (21)$$

gives a critical condition for fracture at a constant load. Because $\frac{d^2U}{dc^2}$ has a negative value, the system's energy is a maximum at equilibrium, so the configuration is unstable. In other words, if the applied stress exceeds the critical level of Equation (21), the crack is free to propagate spontaneously without limit. Griffith used glass, which behaves as a perfectly brittle material, to verify his analysis. The experimental results agreed with his analysis. The above discussion of the Griffith energy-balance concept mainly is drawn from the discussion by Lawn and Wilshaw (1975) on fracture of brittle solids.

Irwin Crack-Extension-Force Concept

Griffith proposed that crack propagation would occur with an increase of tensile load when the mechanical energy release rate became greater than the surface tension of the solid. Unfortunately, the surface tension for solids is a quite abstract term to use in practical analysis. In addition, Griffith's analysis ignored a large dissipation of strain energy in the plastic flow which normally accompanies crack extension in any imperfect brittle material, such as metals. Therefore, Irwin (1960) proposed an

imaginary force called the crack-extension force (G), which motivated and propelled crack extension. It relates only to the applied force, crack length, and specimen dimensions.

Irwin (1962) defined the crack-extension force (G) as "the work per unit area done in closing the crack along a border segment," or as "the release of stress field energy per unit area as the borders of the crack expand." In order to fully understand the meaning of G, and to appreciate the advantage of using the Irwin crack-extension-force concept over that of the Griffith energy-balance concept in analyzing a cracked body, one has to relate Irwin's concept to the result of stress analysis on a cracked body when using the elasticity solution.

Stress Analysis of a Cracked Plate: Isotropic Material

For an isotropic elastic body having a crack at its edge, the free surface of the crack can penetrate the material in three different modes of crack-surface displacements (Figure 4). Mode I (opening mode) corresponds to normal separation of crack walls under the action of tensile stresses; mode II (sliding mode) corresponds to mutual shearing of the crack walls in a direction normal to the crack front; mode III (tearing mode) corresponds to mutual shearing parallel to the crack front.

From experimental observation (Irwin 1960), the plane of fracture propagation is usually perpendicular to the direction of greatest tension, implying that the opening mode usually develops more rapidly than the others for the same applied component of crack-extension-force. In other words, opening-mode fracture is usually more critical

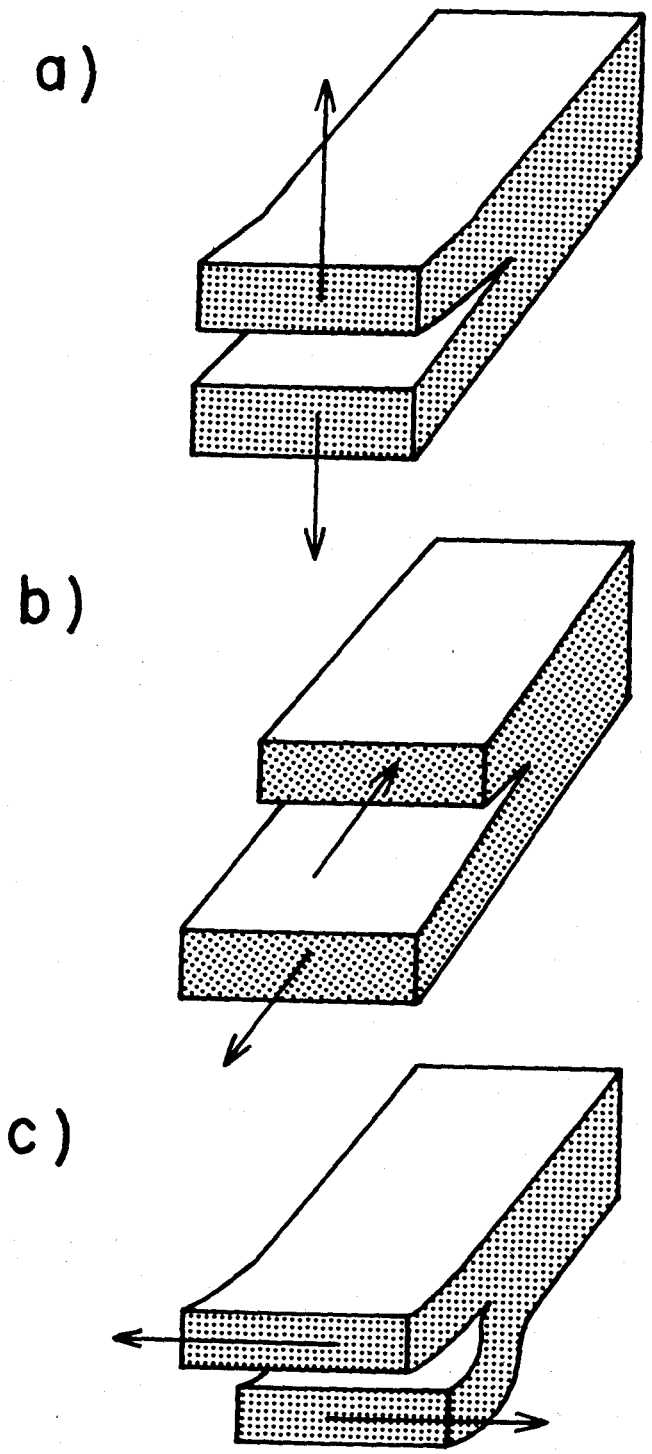

Figure 4. The three modes of fracture. a) opening mode, b) sliding mode, and c) tearing mode

than the other two modes. In this study, only the mode I or opening mode fracture will be discussed. Therefore, the repeated mentioning of "mode I" will be eliminated to avoid redundancy.

Elasticity solution of a cracked plate under uniform tension at infinity (Figure 5) is given as (Paris and Sih 1965)

$$\sigma_x = \frac{K_I}{\sqrt{2\pi r}} \cos\frac{\theta}{2} \left(1 - \sin\frac{\theta}{2} \sin\frac{3\theta}{2}\right)$$

$$\sigma_y = \frac{K_I}{\sqrt{2\pi r}} \cos\frac{\theta}{2} \left(1 + \sin\frac{\theta}{2} \sin\frac{3\theta}{2}\right) \tag{22}$$

$$\tau_{xy} = \frac{K_I}{\sqrt{2\pi r}} \sin\frac{\theta}{2} \cos\frac{\theta}{2} \cos\frac{3\theta}{2}$$

or

$$\sigma_{ij} = \frac{K_I}{\sqrt{2\pi r}} f_{ij}(\theta) \tag{23}$$

where σ_x, σ_y, and τ_{xy} are respectively the two normal stresses and shear stress in xy plane; r and θ are variables in polar coordinate system defined in Figure 5; and

$$K_I = \sigma\sqrt{\pi c} \tag{24}$$

is the so-called the opening mode (mode I) stress intensity factor in a unit of psi$\sqrt{\text{in}}$ or its equivalence.

Several points of interest arise from these solutions. First, we may emphasize the simple form of the expression in Equation (23) for stresses in which the coordinal features of the field appear as separable elements. The stress-intensity factor (K_I) depends only on the applied load and crack length. Physically, K_I may be interpreted as a parameter which reflects the redistribution of stress in a body

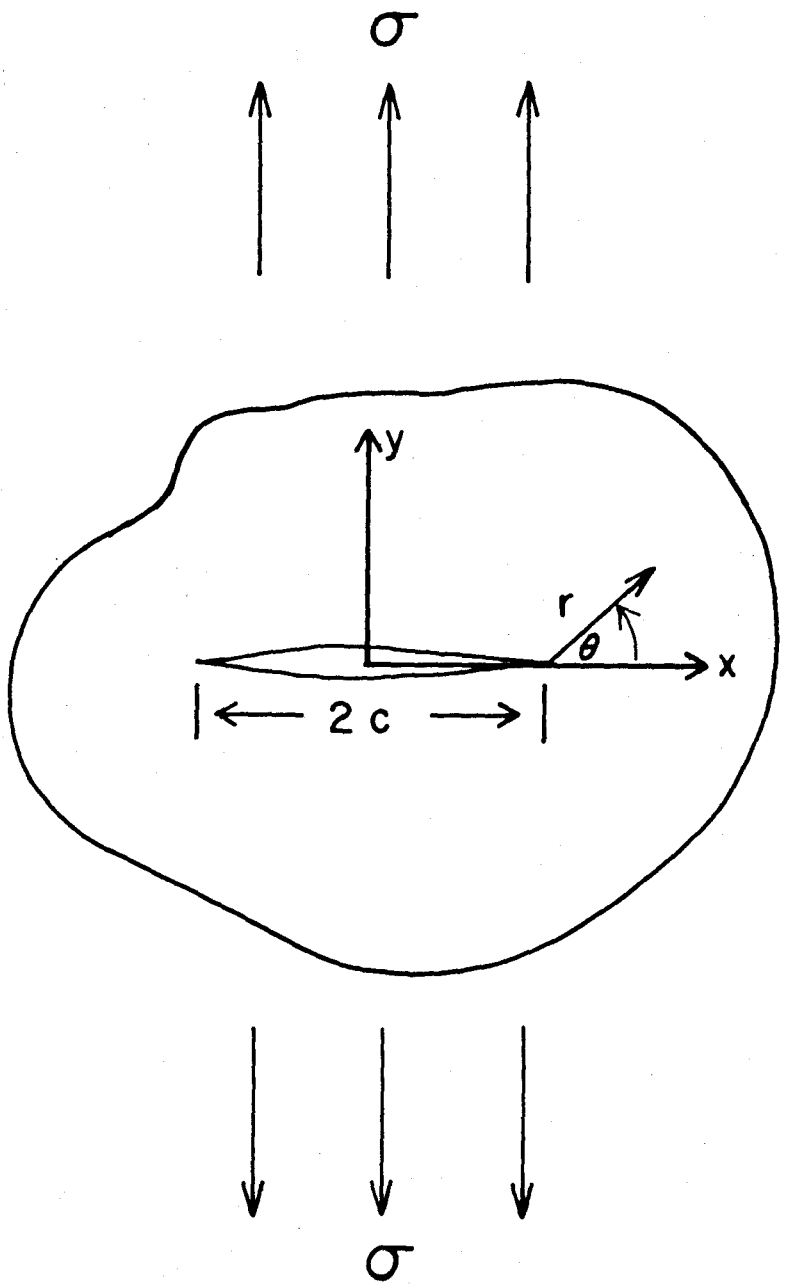

Figure 5. Cracked body under uniform tension at infinity

due to the introduction of a crack. In particular, K_I indicates the magnitude of force transmission through the crack tip region.

Second, we should be aware that higher order terms have been neglected in the derivation of Equation (22), and these terms need to be included if the stress field is to match the outer boundary conditions.

Third, because the crack-tip plastic zone is assumed to be small compared with specimen size, or the cracked body is assumed to be elastic in nature, the principles of superposition can be used in adding the stresses. It follows that the stress intensity factor for a given fracture is additive.

Finally, we can observe from Equation (24) that, with a certain crack length, for every stress level σ there corresponds a K_I. Through increases in applied load, σ will reach a critical level σ_C where the unstable crack starts, and simultaneously K_I will also reaches its maximum value (K_{IC}). In plane strain fracture testing, K_{IC} is the so-called "fracture toughness", a most widely used term in practice. Mathematically, then

$$K_{IC} = \sigma_C\sqrt{\pi c} \tag{25}$$

With the background of stress analysis of a cracked body in mind, we can now continue our discussion of the crack extension force G. Irwin (1962) postulated that the energies consumed for opening or closing a crack of fixed length are the same. He further proposed, that in the opening mode fracture, the only stress involved in crack opening was the stress perpendicular to the crack surface or σ_y in Equation (22). Then it can be shown that the work (cG_I) needed to

open up a crack in an isotropic plate is

$$cG_I = c \frac{1-\nu^2}{E} K_I^2 \qquad \text{(plane strain)} \tag{26}$$

where 2c is crack length, ν is Poisson's ratio. By substituting Equation (24) into Equation (26), then

$$G_I = \frac{\pi c(1-\nu^2)\sigma^2}{E} \qquad \text{(plane strain)} \tag{27}$$

Thus G is actually an imaginary force which is assumed to be responsible for propelling the crack in a cracked body. Its unit is in force per unit crack length. However, the crack propagation will not occur until G_I reaches a critical value G_{IC} called critical crack-extension force. G_{IC} can be evaluated experimentally.

In terms of energy, the crack-extension force G can also be defined as the derivative of mechanical energy release with respect to crack area (Lawn and Wilshaw 1975), or

$$G = -d(-W_L+U_E) \;/\; dc \qquad \text{(unit thickness)} \tag{28}$$

The advantage of expressing G in this manner is that it can be shown that the value of G is independent of loading configuration. In other words, for experimental evaluation, G can be obtained either by dead weight loading or by fixed grips loading.

Apparently, Equation (28) does not reveal much more than what we have already learned about Griffith's and Irwin's concepts. But it does show the connection between Griffith's concept and Irwin's concept, and the contribution of Griffith to the field of fracture mechanics.

Stress Analysis of a Cracked Plate: Orthotropic Material

For an orthotropic elastic body having a crack at its edge, the three major fracture displacement modes shown in Figure 4 are still maintained. However, due to the orthotropic nature, further distinctions have to be attached to these major modes. Six opening modes for orthotropic material have been shown in Figure 6 as K_{ILT}, K_{ILR}, K_{IRL}, K_{ITL}, K_{ITR}, and K_{IRT}, where the first subscript represents the fracture mode; the second subscript represents the loading direction which is normal to the crack plane; the third stands for the direction of crack propagation.

Elasticity solutions of a two-dimensional orthotropic cracked plate under uniform tension at infinite ends (Figure 5) were summarized by Wu (1962) as

$$\sigma_x = \frac{K_I}{\sqrt{2\pi r}} \left(\frac{\alpha^2+\beta^2}{2\alpha}\right) \left[\frac{\alpha\cos\frac{\phi_1}{2}+\beta\sin\frac{\phi_2}{2}}{\sqrt{(\cos\theta+\alpha\sin\theta)^2+(\beta\sin\theta)^2}} + \frac{\alpha\cos\frac{\phi_2}{2}-\beta\sin\frac{\phi_2}{2}}{\sqrt{(\cos\theta-\alpha\sin\theta)^2+(\beta\sin\theta)^2}}\right]$$

$$\sigma_y = \frac{K_I}{\sqrt{2\pi r}} \left(\frac{1}{2\alpha}\right) \left[\frac{\alpha\cos\frac{\phi_1}{2}-\beta\sin\frac{\phi_1}{2}}{\sqrt{(\cos\theta+\alpha\sin\theta)^2+(\beta\sin\theta)^2}} + \frac{\alpha\cos\frac{\phi_2}{2}+\beta\sin\frac{\phi_2}{2}}{\sqrt{(\cos\theta-\alpha\sin\theta)^2+(\beta\sin\theta)^2}}\right] \quad (29)$$

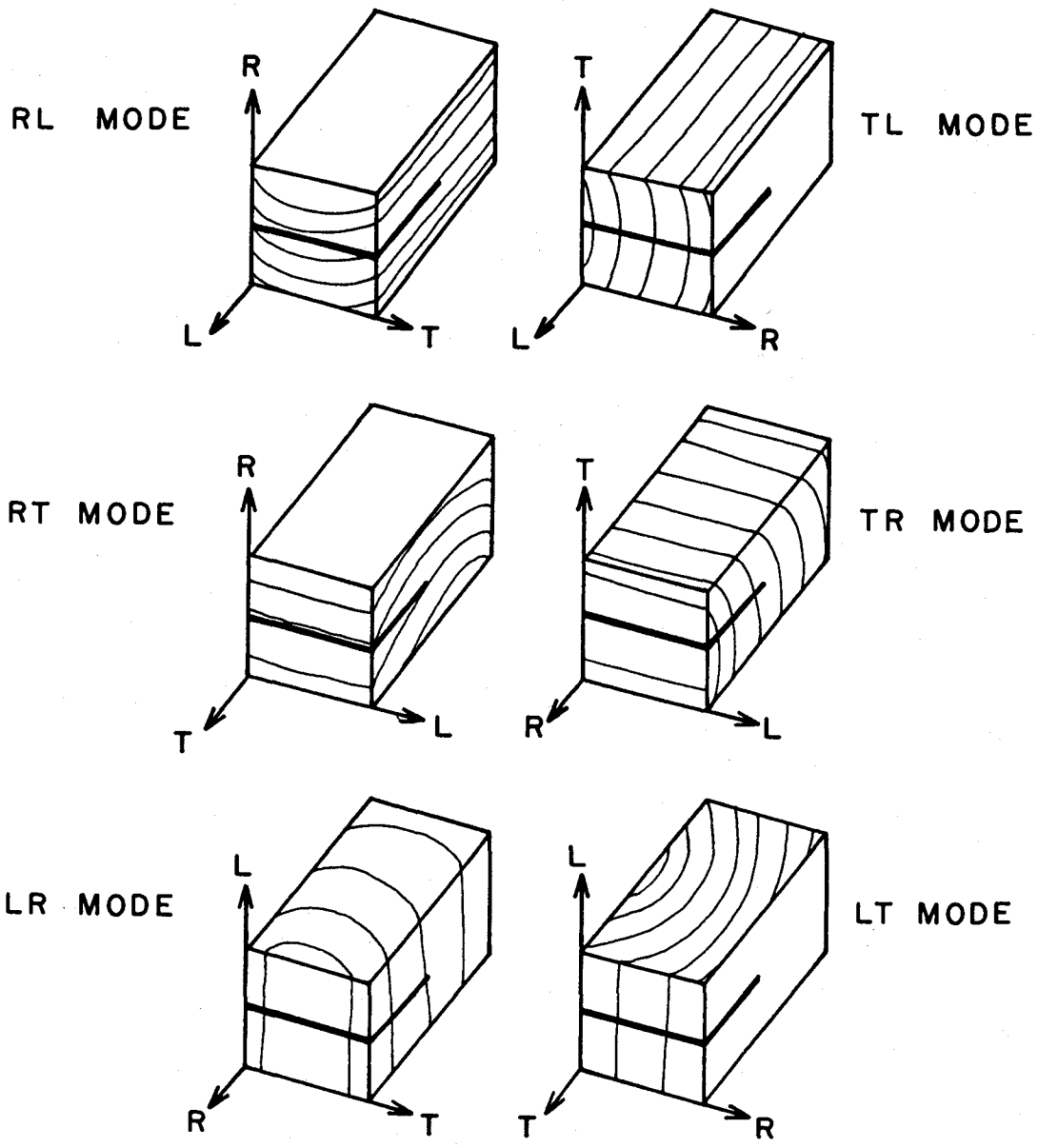

Figure 6. Six opening modes for orthotropic material (solid wood)

$$\tau_{xy} = \frac{K_I}{\sqrt{2\pi r}} \left(\frac{\alpha^2+\beta^2}{2\alpha}\right) \left[\frac{\cos\frac{\phi_1}{2}}{\sqrt{(\cos\theta+\alpha\sin\theta)^2+(\beta\sin\theta)^2}} - \frac{\cos\frac{\phi_2}{2}}{\sqrt{(\cos\theta-\alpha\sin\theta)^2+(\beta\sin\theta)^2}}\right]$$

where

$K_I = \sigma\sqrt{\pi c}$ (mode I stress intensity factor)

$\alpha, \beta = f(E_{11}, E_{22}, \nu_{12}, \nu_{21}, G_{12})$

$\phi_1, \phi_2 = f(\alpha, \beta, \theta)$

Comparing Equation (29) to Equation (22), the most distinct difference between the state of stress around the crack tip in an orthotropic plate and that in an isotropic plate is that the former is dependent on the elastic constants of the material while the latter is not. However, both orthotropic and isotropic cracked bodies have an identical mode I stress intensity factor.

The calculation of crack-extension force G_I for an orthotropic material is similar to that of an isotropic material. The resulting relationship between G_I and K_I can also be written in a similar form as

$$G_I = \pi C K_I^2 \tag{30}$$

For an isotropic material

$$C = \frac{1 - \nu^2}{E}$$

whereas for an orthotropic material

$$C = \sqrt{\frac{a_{11}a_{22}}{2}} \left(\sqrt{\frac{a_{22}}{a_{11}}} + \frac{a_{66}+2a_{12}}{2a_{11}}\right)^{\frac{1}{2}} \tag{31}$$

where

$$a_{11} = \frac{1}{E_{11}} \quad , \quad a_{22} = \frac{1}{E_{22}}$$

$$a_{12} = \frac{\nu_{12}}{E_{22}} \quad , \quad a_{66} = \frac{1}{G_{12}}$$

From the above discussion, we know that the same evaluation procedure can be applied to obtain K_I and K_{IC} for both isotropic and orthotropic materials. However, different considerations have to be made when evaluating G and G_{IC} for isotropic and orthotropic materials.

Applications

The Griffith energy-balance concept and the Irwin crack-extension-force concept are the fundamental concepts used to explain the crack propagation mechanism in a cracked body under stress. However, because of the assumptions of idealistic conditions used in their derivations (such as the use of surface energy of solid, or loading at infinity), they are not directly applicable to practical situations.

Generally speaking, cracks in plates of finite size are of greater practical interest, but for these cases no closed-form solutions are available. The problems are difficult because of the boundary conditions. Therefore, approximate solutions were derived by many investigators and were compiled by Paris and Sih (1965).

For design purposes, the plane strain fracture toughness K_{IC} is one of the most important factors to be determined because it decides

the maximum load a cracked body can sustain before fracture failure occurs. K_{IC} is also expected to be a material parameter which is not dependent upon the crack length in the material. Like some other material parameters, such as strength, the K_{IC} of a material can usually be obtained only by experimental evaluation of the cracked material. The test procedure for K_{IC} of metals is standardized by the American Society for Testing and Materials in Designation: E 399-74 "Standard Method of Test for Plane-Strain Fracture Toughness of Metallic Materials" (1974).

The subject matter of fracture mechanics covers an extremely broad field including those on static and fatigue cracks, on size of plastic zones, on speed of crack growth, on testing conditions, and on dynamics and crack arrest. Hundreds of published papers on analyses and applications are collected in two specific journals (International Journal of Fracture Mechanics, Engineering Fracture Mechanics) and many other engineering journals (Journal of Composite Materials, Experimental Mechanics). The significance of fracture mechanics, however, can be generalized in such a way that it should be able to answer the following questions (Broek 1975):

1. What is the residual strength as a function of crack size?
2. What size of crack can be tolerated at the expected service load; i.e. what is the critical crack size?
3. How long does it take for a crack to grow from a certain initial size to the critical size?
4. What size of pre-existing flaw can be permitted at the moment the structure starts its service life?

5. How often should the structure be inspected for cracks?

The works done on the application of fracture mechanics to solid wood, wood-resin bonds, and wood-resin joints (including resin layer and wood-resin interphases) are relatively limited (Atack et al 1961, Wu 1963, Porter 1964, Debaise et al 1966, Wu 1967, Tomin 1972, Johnson 1973, Schniewind and Pozniak 1973, Schniewind and Centeno 1973, Schniewind and Lyon 1973, Komatsu et al 1974, Mai 1975, Mindess et al 1975, 1976, Komatsu et al 1976, White 1976, 1977). By no means the above papers are exclusive. They are, however, the ones that are most referenced in the wood science field in the United States. The most noticeable results from these papers are:

1. Fracture toughness K_{IC} or critical crack-extension force G_{IC} is a material parameter of wood (Porter 1964, Johnson 1973, White 1976).
2. G_{IC} is independent of specimen geometry and crack length (Porter 1964).
3. K_{IC} or G_{IC} is temperature, moisture content, grain orientation and strain-rate dependent (Porter 1964, Debaise et al 1966, Johnson 1973).
4. Morphology or structure of wood influences K_{IC} (Debaise et al 1966, Johnson 1973).
5. K_{IC} of wood-resin joint (southern yellow pine and resorcinol-formaldehyde resin) is lower than that of solid wood (White 1976).
6. K_{IC} of resin bonds (resorcinol-formaldehyde) is lower than that of their substrates (loblolly pine) (White 1977).

There is no work reported on the application of fracture mechanics to flakeboard or any other wood composites.

V. PROBLEM ANALYSIS AND HYPOTHESIS

Background

The published values for the normal tensile strength of flakeboards are consistently inferior to that of clear, solid wood of the same species. We want to investigate whether and how this situation can be improved.

The structure of this problem needs to be analyzed in order to establish its solution. The final result of this study, however, is expected to provide an analytical model of the normal tensile strength or fracture toughness of flakeboards, which can be used as a design criterion for manufacturing flakeboards.

Scientific findings are usually the products of repeated alternations between hypotheses and experimental observations. In studying the process of manufacturing flakeboards, one could hypothesize that each of the material parameters such as flake property, resin property, and the process parameters such as pressure and temperature, must have its effect on the final strength of flakeboards. This hypothesis has already been tested in many experimental works cited in the LITERATURE REVIEW section. In these experiments, one of the parameters was treated as a variable while the others were held constant to test the effect of that particular variable. If there was an empirical relationship obtained by this experimental approach, the empirical relationship could only be used for the specified conditions.

Although there were also works done to theorize the hypotheses or experimental findings on the strength of flakeboards, the theoretical derivations were either limited to the effect of board density or limited to the effect of flake dimensions. Because the theoretical treatments deal only with the individual parameter effects, the discussion on the interactions between parameters could only be in a qualitative sense instead of quantitatively. Moreover, some of the most detrimental factors regarding flakeboard strength are processing defects, including inter-flake voids and non-bonded areas. These have been consistently ignored in both theoretical and experimental treatments, while natural defects such as knots in solid wood have always been of primary importance in the discussion of solid-wood strength. Therefore, new hypotheses regarding the flakeboard strength properties in terms of processing defects are needed. In this study, however, the discussion is confined to the fracture toughness of flakeboard.

Fracture Toughness of Flakeboard

In the process of manufacturing flakeboard, one applies resin onto the flakes, felts the flakes into a forming box to form a mat, and then compacts the mat under pressure and temperature to form a flakeboard of nominal thickness. The processing defects, such as inter-flake voids caused by mismatch among flakes, and non-bonded areas between flakes due to the uneven distribution of flakes, are a result of the reconstituting process and so become an inherent characteristic of flakeboard. From the viewpoint of strength-of-

materials, these processing defects, which cause stress concentrations in flakeboard, are most likely the failure initiation nuclei.

When thinking in terms of the fracture-mechanics concept, the normal tensile strength of flakeboard is actually the fracture toughness (K_{IC}) of a flakeboard if the size of the most critical inter-flake void, or non-bonded area, or their combination, is known. In other words, if we can relate the effects of flake dimension, resin spread rate, and board density to the sizes or distributions of inter-flake voids and non-bonded areas in flakeboard, then the given problem on the analysis of normal tensile strength of flakeboard becomes a fracture-mechanics problem in determining the K_{IC}.

There are several advantages if the given problem is analyzed in this manner. First, the interaction effects among parameters might be reflected by the inter-flake void sizes and distributions. Second, it is more probable to construct an analytical model relating the fracture toughness of a flakeboard only to its inter-flake void sizes and distributions rather than to establish an analytical model connecting all the individual material parameters to the flakeboard strength. And third, the sizes and distributions of inter-flake voids can be measured non-destructively.

In this study, the discussion of non-bonded areas is limited to the areas which directly link to the inter-flake voids and are not detectable by visual means from the edge surface. The inter-flake voids and possibly related non-bonded areas are illustrated in Figure 7. From this point on, the combination of inter-flake void and its

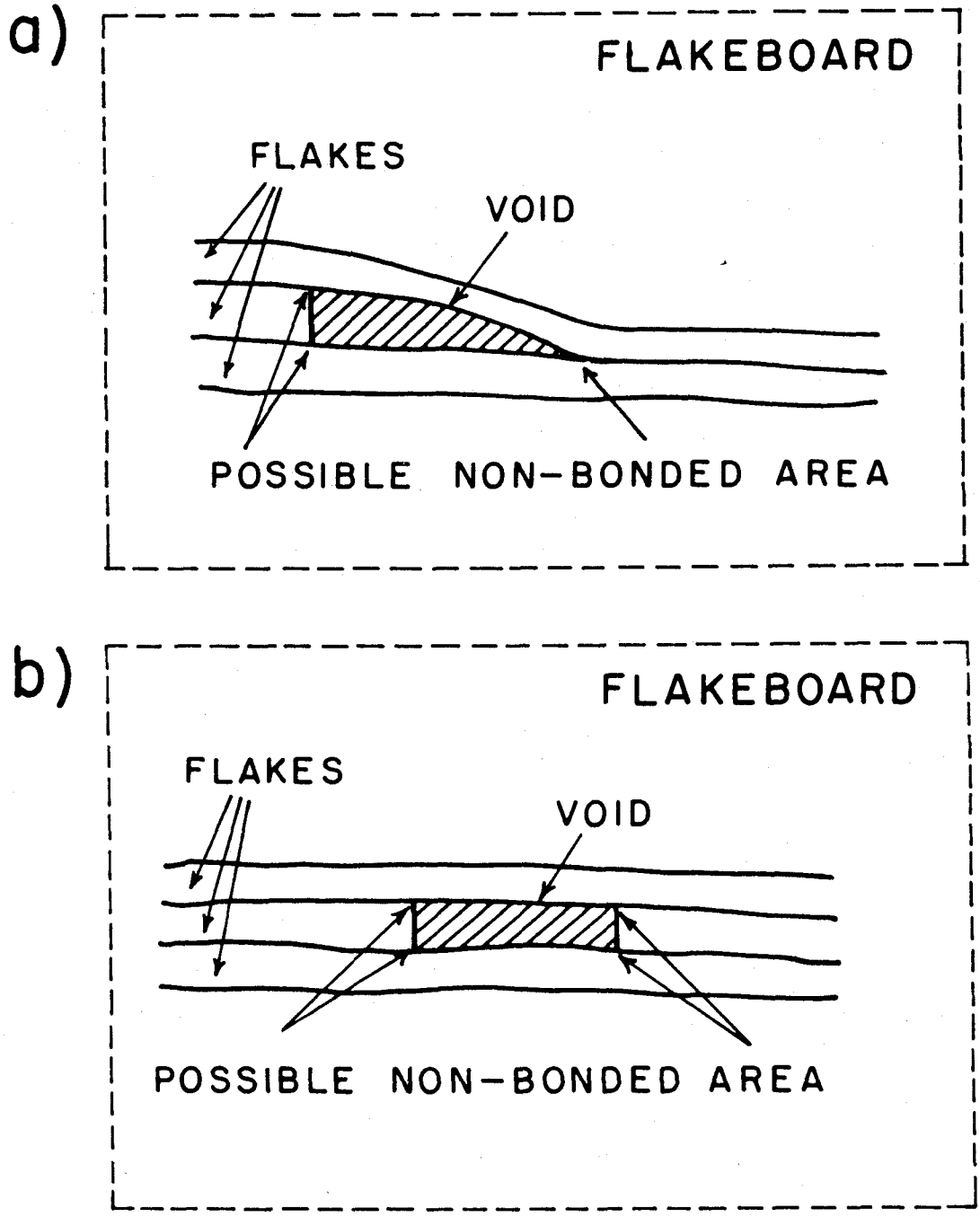

Figure 7. Inter-flake voids and non-bonded areas in flakeboard. a) triangular void and possible non-bonded area, and b) rectangular void and possible non-bonded area

tail-part non-bonded area will be referred to as the crack in the flakeboard.

When considering a critical crack in a flakeboard, we can assume that this crack would grow stably with an increase of loading and unstably when the crack-extension force reaches the critical value for the material. The parameters which resist the crack growth are the materials surrounding the crack front and the circumference of the crack. We can suppose that any crack in a flakeboard can be encompassed only by some combination of four (or five) kinds of materials. They are: solid wood, wood-resin joint (including wood-resin interphases and resin layer), non-bonded area, and other inter-flake voids.

The major function of resin in wood composites is to connect the wood constituents to form a continuum. With the amount of resin solids used in flakeboard manufacturing (4 to 10 percent, ovendry wood-weight basis, or roughly 1 to 3 lb/1000 sq ft of surface-area basis), there is no evidence to show that the applied resin forms continuous layers which could resist the fracture propagation in wood or could confine the fracture path between the resin layers. Actually, it should be the wood grain that dictates the fracture direction.

There is also no indication that this small amount of resin penetrated into wood cell walls could reinforce the fracture resistance of the wood cell walls. White (1976) applied resorcinol-formaldehyde resin to the surfaces of southern yellow pine and found

that the fracture resistance of the wood-resin joint was lower than that of the wood.

Because the resin layer or the wood-resin joint cannot enhance the fracture resistance of flakeboard, also because both the inter-flake voids and non-bonded areas cannot resist crack propagation, it is then the percentage of solid wood ahead of a crack front that actually resists the crack propagation.

Hypothesis

From the above induction we can make the following hypothesis: it is the size and distribution of the inter-flake cracks that determines the fracture toughness (K_{IC}) of the flakeboard with the condition that there is adequate bonding between the flakes having close contact for the failure to occur in the wood.

VI. EXPERIMENTS

Experimental-Design Requirements

In order to experimentally test the hypothesis that the fracture toughness (K_{IC}) of flakeboard is a function of the size and distribution of inter-flake cracks in the board, there are requirements that must be met for the design of such experiments before the results can be used to evaluate the hypothesis. The requirements are: 1. different fracture modes of K_{IC} of the solid wood from which the flakeboard is derived have to be known as references; 2. the flakes should be controlled in dimensions and grain orientation, and relatively undamaged; 3. the resin spread rate has to ensure adequate bonding between flakes (100% wood failure when testing) where sufficient contact pressure is present between the flakes.

To satisfy the first requirement that for every K_{IC} of flakeboard tested, the K_{IC} of the solid wood from which the flakeboard is made needs to be known, we obtained 40 pieces of clear, straight grain, green lumber (with a nominal size of 4 in by 4 in by 12 ft each) donated by Willamette Industries Inc. at Dalles, Oregon. The lumber were old-growth Douglas-fir with a range of 9 to 44 annual rings per inch (an average of 20 annual rings per inch). The reason for using this kind of lumber is that only straight-grain lumber from old-growth trees can meet both the flake-grain-orientation and flake-quantity (from each piece of lumber) requirements needed for the design of this experiment.

Each piece of green lumber was sawn into two flat-grain and two edge-grain planks, then planed to uniform dimensions (1.6 in by 4 in by 6 ft each) and subsequently labelled before kiln-drying. The cutting pattern is shown in Figure 8. One hundred and sixty planks, dimensions of 1.6 in by 4 in by 6 ft, were then kiln-dried to 12 percent equilibrium moisture content in a period of 15 days. The highest temperature in the kiln was 110°F. Soon after moving the planks out of the kiln, specimens designated for testing the K_{IC}, moisture content (M.C.), and density of each plank were cut (Figure 8). These solid wood specimens and the remaining planks were stored away in a standard conditioning room (72°F, 65% R.H.) before testing or further use.

In order to satisfy the second requirement that flakes have to be controlled in dimensions and grain orientation, and not severely damaged, we selected the sets of planks with the best straight grain out of the group, and used a table saw with a 60-tooth carbide-tip blade 9 inches in diameter to saw all the needed flakes to a dimension of 2 in by 11/16 in by 1/32 in (thickness). Two kinds of flakes were produced from each set of planks; flat-grain flakes, and edge-grain flakes. The selection of flake length followed the recommendation of Lehmann (1974). The selection of flake width and thickness are, however, arbitrary.

In order to fulfill the third requirement that good bonding between flakes should be ensured in the flakeboard wherever sufficient contact pressure is present, a series of microlams were made by varying the resin spread rate and assembly time, and testing with

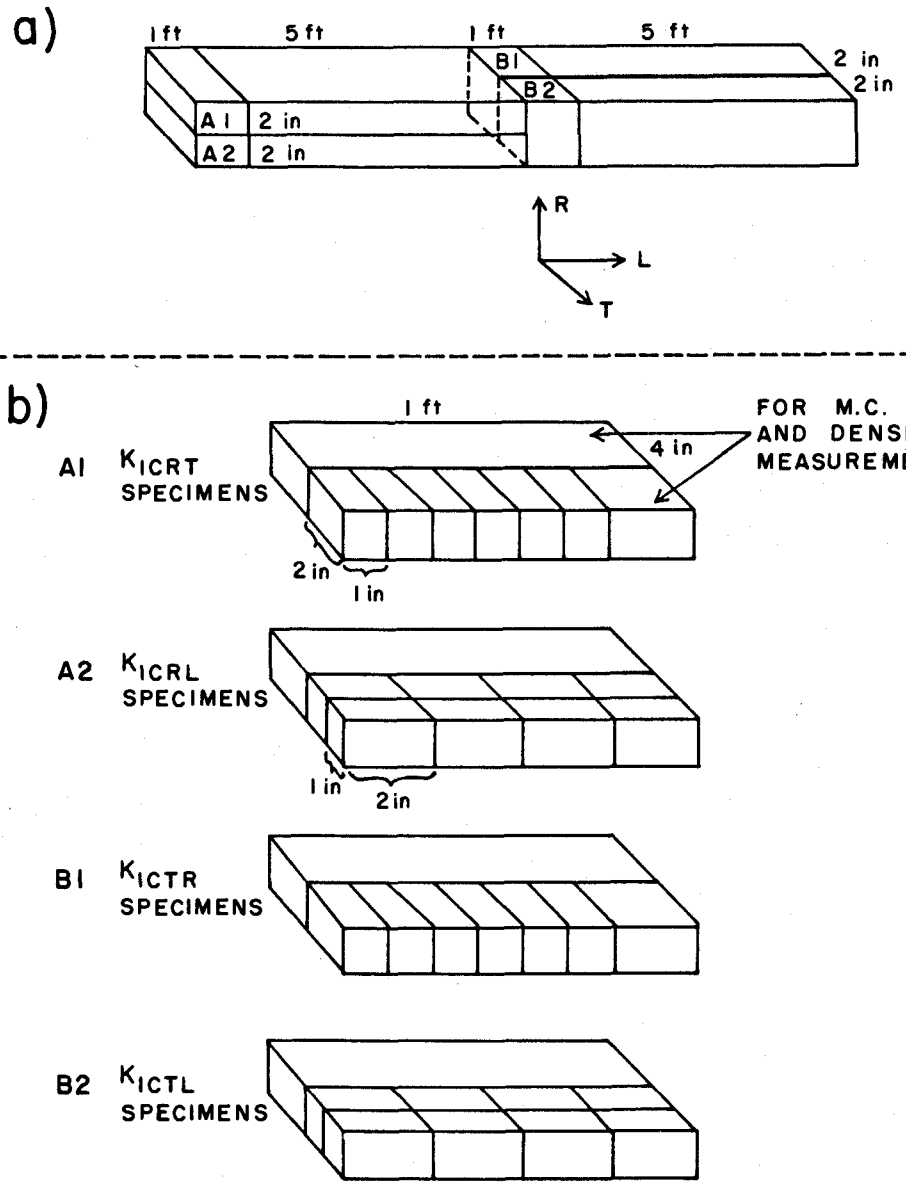

Figure 8. Cutting patterns for a) generating four planks (2 in by 4 in by 6 ft) from each lumber (4 in by 4 in by 12 ft), and b) generating fracture toughness specimens from each plank

tensile load normal to the board plane to investigate wood failure percentage. Full contact between veneers was assumed for the microlam. The conditions ensuring 100 percent wood failure for the phenol-formaldehyde resin (Monsanto R12-3) and the microlams (16 layers of 1/32-inch veneer) manufactured are: 1.35 lb/1000 sq ft resin solids spread rate, 30 minutes assembly time, 325°F in temperature, and a pressure of 250 psi for 10 minutes. Certainly, a higher resin solids spread rate than 1.35 lb/1000 sq ft could be used, but the assembly time has to be increased and the veneer moisture content into the press has to be decreased accordingly.

Experimental Design

Although flake grain orientation, flake dimension, resin solids spread rate, board density, and loading speed were the parameters to be studied, the idea of designing this experiment was to manufacture oriented flakeboards in a manner that the size and frequency of inter-flake voids were monotonically increased from board to board. These oriented flakeboards were then tested to investigate the influence of inter-flake voids and non-bonded areas on their fracture toughness (K_{IC}). The microlams were considered as perfectly aligned flakeboards in which no inter-flake voids and non-bonded areas should be found.

Because of the number of parameters involved, a complete factorial experimental design was not feasible. Therefore, the fracture modes LR and LT were eliminated because their occurrence in a real situation was unlikely for oriented flakeboard. The 1.35 lb/

1000 sq ft was the only resin solids spread rate applied to the high-density board (53 lb/cu ft) because any higher rate would not be beneficial or practical. The flake dimensions were also kept constant because any flake-dimension changes would involve the effect of the three variables, namely, length, width, and thickness. However, the flake length and width effects on the inter-void sizes and distributions in the board still could be studied by comparing the along-fiber sides to the across-fiber sides of the oriented flakeboards.

The summary of experimental design is given in Table 1. In Table 1, the first column is arranged in such a way that the products are in a descending order of assumed increasing effect of inter-flake void size on their fracture-toughness properties.

Oriented Flakeboard and Microlam Manufacturing

In order to test four fracture modes for every product in Table 1, two types of oriented flakeboard or microlam were needed for each product. One type was from flat-grain flakes or veneers to make flat-grain oriented flakeboard or microlam, and the other type was from edge-grain flakes or veneers to make edge-grain oriented flakeboard or microlam. The K_{ICRL} and K_{ICRT} specimens could only be obtained from flat-grain oriented flakeboard or microlam, whereas the K_{ICTL} and K_{ICTR} specimens could only be obtained from the edge-grain oriented flakeboard or microlam.

For the low- and medium-density boards, there were enough flakes to make both types of board (12 in by 12 in by 1/2 in) from each piece

Table 1. Summary of Experimental Design

Product	Variables in product	Variables in test
Microlam	1. Original solid wood 2. Veneer thickness (in) (1/8, 1/16, 1/32)	1. Frature toughness (K_{ICRL}, K_{ICTL}, K_{ICTR}, K_{ICRT}) 2. Loading speed (cm/min) (0.1, 0.01)
High-density (53 lb/cu ft) oriented flakeboard	1. Original solid wood 2. Resin spread rate (lb/1000 sq ft) (1.35)	1. Fracture toughness (K_{ICRL}, K_{ICTL}, K_{ICTR}, K_{ICRT}) 2. Loading speed (cm/min) (0.1, 0.01)
Medium-density (43 lb/cu ft) oriented flakeboard	1. Original solid wood 2. Resin spread rate (lb/1000 sq ft) (1.35, 2.025, 2.7)	1. Fracture toughness (K_{ICRL}, K_{ICTL}, K_{ICTR}, K_{ICRT}) 2. Loading speed (cm/min) (0.1, 0.01)
Low-density (33 lb/cu ft) oriented flakeboard	1. Original solid wood 2. Resin spread rate (lb/1000 sq ft) (1.35, 2.025, 2.7)	1. Fracture toughness (K_{ICRL}, K_{ICTL}, K_{ICTR}, K_{ICRT}) 2. Loading speed (cm/min) (0.1, 0.01)

of lumber (originally 4 in by 4 in by 12 ft). However, for the high-density board, the flakes from a piece of lumber were only enough to make one type of board. Therefore, it took two pieces of 4 in by 4 in by 12 ft lumber to make two oriented high-density flakeboards which could provide the four types of fracture specimens.

The process parameters which were kept constant for manufacturing oriented flakeboards and microlams are:

Oriented flakeboard size: 12 in by 12 in by 1/2 in

Microlam size: 20 in by 2 1/2 in by 1/2 in

Resin: phenol-formaldehyde liquid resin (Monsanto R12-3), 42% solids

Resin temperature when spraying: 76°F

Assembly time: one hour

Mat moisture content into press: 10%

Press temperature: 325°F

Press closing time: 30 ± 10 seconds

Constant pressure maintained: 250 psi

Total press cycle: 10 minutes

There were four items regarding the process parameters which must be noted. The first one concerns the control of resin spread rate. A rotating drum 4 feet in diameter was used as the blender. Resin was sprayed under an air pressure of 60 psi from a single-nozzle air gun in the center of the drum. For flakes, the means to control the resin spread rate was as follows: an exact amount of flakes for a board with a specified density was weighed; the number of flakes weighed was estimated by comparing its weight to an average weight of

a group of flakes each with a known number of flakes. Then the total needed resin weight, in terms of total flake surface area, could be calculated. The amount of resin sprayed on the flakes was controlled by the spraying time which has been determined in a preliminary trial experiment. The actual resin weight on the flakes was finally obtained by substracting the original flake weight going into the blender from the final flake weight coming out of the blender. The resin spread rate controlled by this means enabled us to estimate the resin amount in terms of flake surface area.

It is believed that when a resin is atomized, evaporation can occur from the droplets and change the original percentage of resin solids. In this study, however, no adjustment is made in the calculation of the resin solids spread rate in respect to this evaporation effect.

For spraying resin on the veneers, a movable, hexagonal wooden frame was designed and fitted into the same rotary drum blender. The veneers were attached to the inner face of each hexagonal side by using rubber bands at their ends. The resin was also sprayed by using the air gun while the drum was rotating. The amount of resin applied was controlled by the length of spraying time similar to that of spraying resin on flakes. Very uniform coatings were obtained from veneer to veneer in the same batch.

Secondly, the flakeboard panel size (12 in by 12 in by 1/2 in) was relatively small, especially for the flake size (2 in by 11/16 in by 1/32 in) used. In order to prevent a regular pattern of inter-flake void formation caused by flakes starting or ending at the

inner-edge of the forming-box walls, four pieces of horizontal wired frame were used as a forming box so that flakes at edges of the mat could stick out of the 12 in by 12 in area to maintain the complete randomness of inter-flake void formation even at the edges of the board.

Thirdly, we have the pressure variation in making flakeboard. Although the constant pressure was maintained at 250 psi between the hot-press plates, the closing pressures differed with the density of the board being made. Generally, for the lower-density board the maximum closing pressure needed was 250 psi, whereas for the medium- and high-density boards the required maximum closing pressure was approximately 500 psi and 750 psi, respectively.

Fourthly, it concerns the thickness of microlams. In order to let the microlams made in this study be more comparable in dimension to those of commercial microlams made by Trus-Joist Inc. at Eugene, Oregon, the microlams made in this study were further sandwiched to a final dimension of 20 in by 2 1/2 in by 1 1/2 in. This was accomplished by gluing two one-half inch panels, identical in grain direction and origin to the core microlam, at 220°F and 150 psi for 15 minutes.

After the oriented flakeboards and microlams were hot pressed, they were hot-stacked for one hour, and then moved into the standard conditioning room (72°F, 65% R.H.).

Fracture Toughness (K_{IC}) Specimen Preparation

Specimen dimensions and initial crack introduction are the major concerns regarding the design of fracture toughness specimens for any material. The specimen dimension requirement for testing metals is specified in ASTM Designation: E 399--Standard Method of Test for Plane-Strain Fracture Toughness of Metallic Materials (1974), and the major consideration for the specification is the elimination or reduction of the effect of the plastic zone in front of a crack. However, for woody materials, the discussion on plastic behavior in the literature was limited to bending and compression parallel to the grain of solid wood (Perkins 1967). Tensile strength properties of wood are usually regarded as elastic (Perkins 1967) and brittle "i.e. the relationship between force and deformation is nearly linear to failure" and "failure tends to be sudden and catastrophic" (Schniewind and Pozniak 1971). No two investigators have ever used identical specimen dimensions in testing the fracture toughness of solid wood.

In this study, a specimen length to width ratio of two to one was adopted in reference to the standard compact tension specimen for testing metals (ASTM: E 399). By taking advantage of the loading fixture (next section) used in this study, and assuming that the differences in specimen thickness would not influence the transmission of normal tensile stress to the crack plane, we, therefore, let the specimen thickness be flexible for different types of material because of the convenience in their preparation. The cutting pattern for flakeboards is shown in Figure 9. The actual specimen sizes for

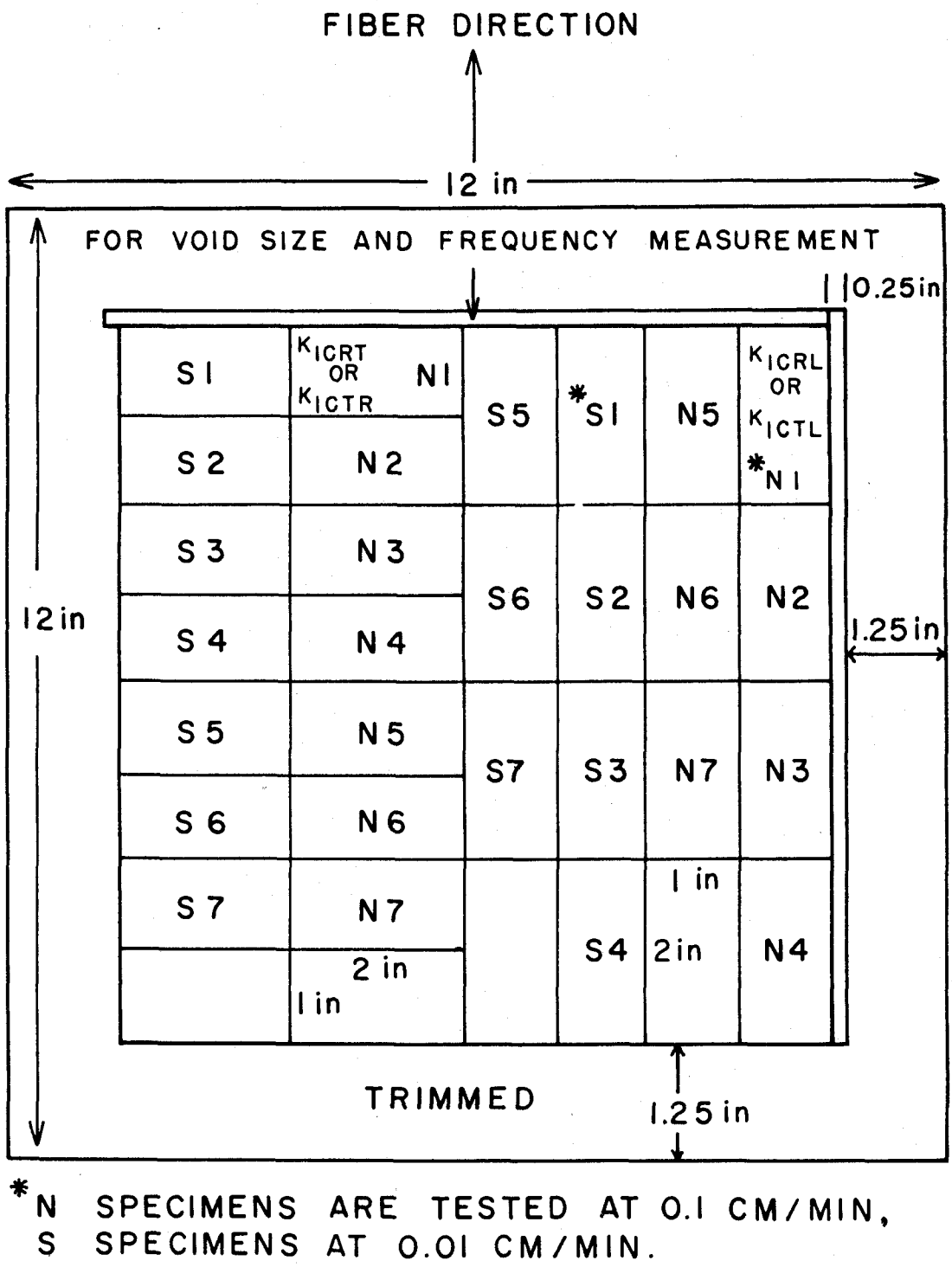

Figure 9. Cutting pattern for oriented flakeboard to obtain K_{IC} specimens and inter-flake void measuring strips

flakeboards, microlams, and solid-wood controls are illustrated in Figure 10.

In the fracture toughness testing, the introduction of an initial crack of known length in the specimen is essential. An ideal initial crack would be a free surface in the material. According to ASTM: E 399, the initial crack is introduced by extending a notched tip by fatigue cracking. This fatigue method is not convenient for testing wood specimens because it takes considerable time to extend a crack, a large number of specimens is usually required to be tested to reveal any consistent wood behavior, and it is difficult to measure the length of a fatigue crack in wood.

The popular method used to introduce the initial crack in wood specimens is to cut a slit into each specimen, either by using a razor blade or a chisel. This method is only suitable for thin specimens. Also, the crack length introduced might be difficult to control or measure due to the split caused by the razor or chisel tip.

In this study, an initial crack length of 0.75 inch was introduced by a two-step band-saw cutting. The first step was to saw a 0.68 inch slit at one side of the specimen with a band-saw blade 0.1 centimeter in thickness. The second step was to finish cutting the 0.75 inch slit by pushing the specimen to a designated stop, with another band-saw blade 0.05 centimeter in thickness with the tooth-tip ground to a very sharp point. Some actual oriented flakeboard K_{IC} specimens are shown in Figure 11. Thus the crack length is 0.75 inch for every specimen. This method of introducing an initial crack

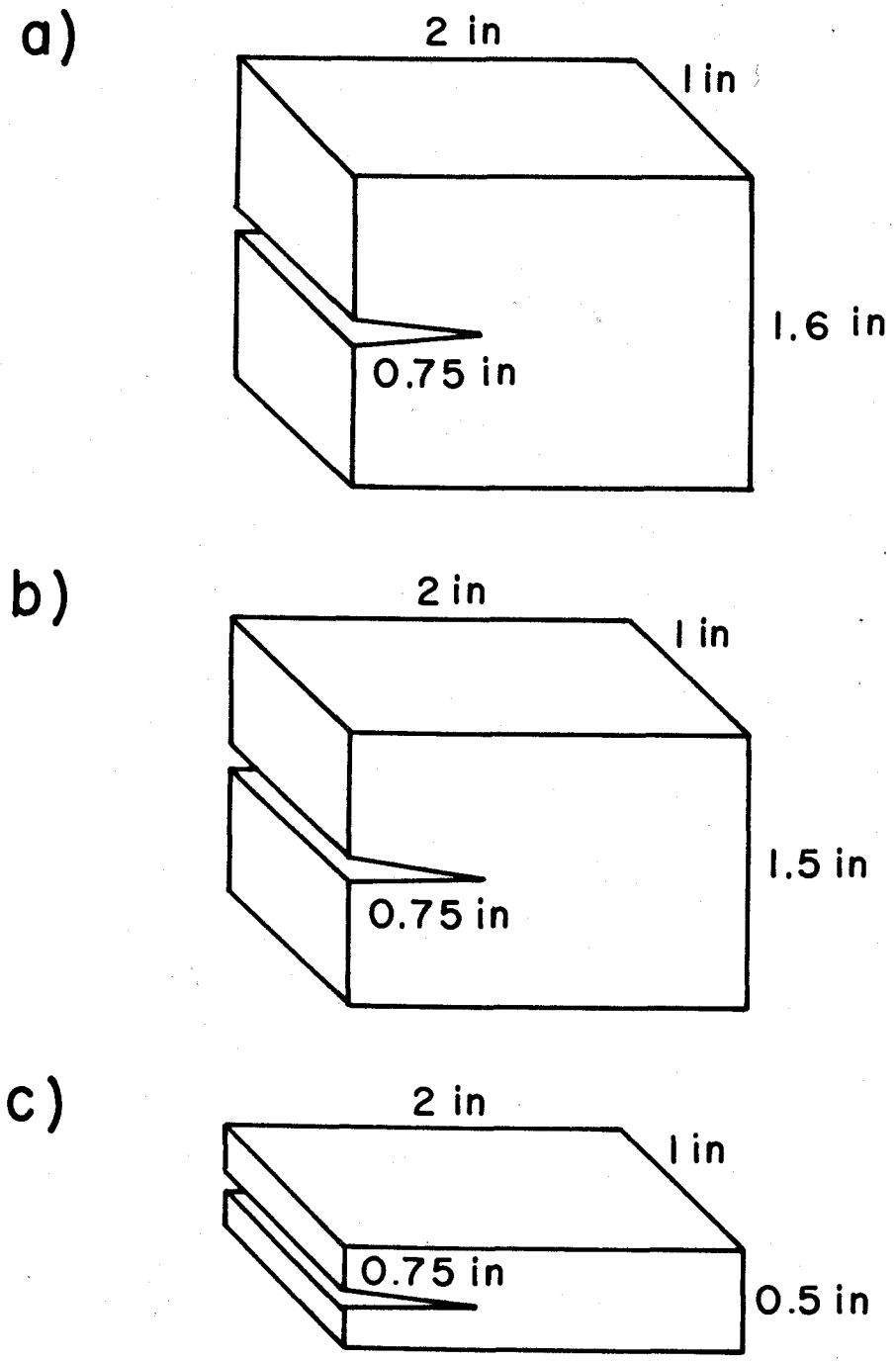

Figure 10. Actual K_{IC} specimen dimensions for a) solid-wood control, b) microlam, and c) oriented flakeboard

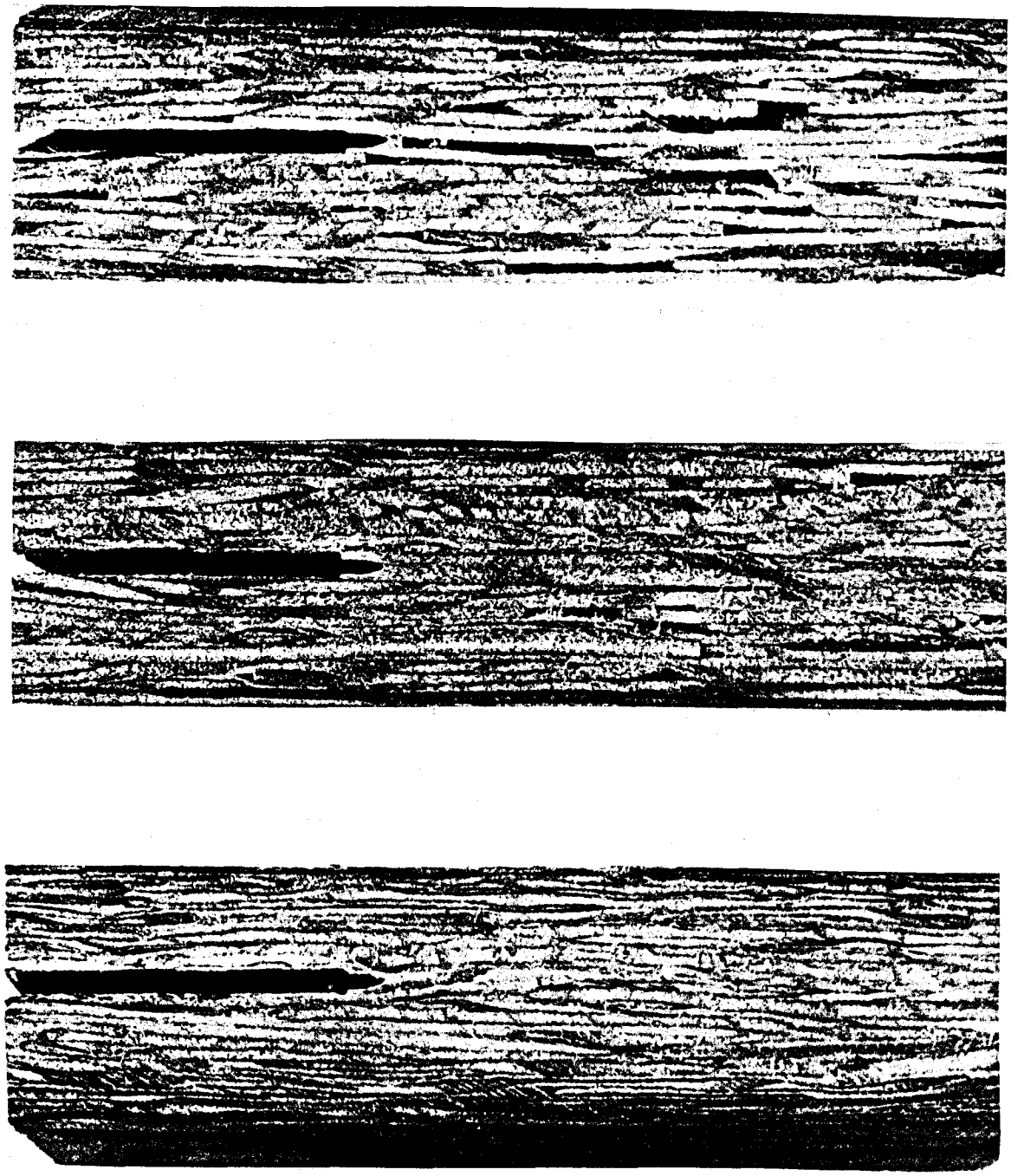

Figure 11. Fracture toughness specimens for low- (34 lb/cu ft), medium- (43 lb/cu ft), and high-density (51 lb/cu ft) oriented flakeboards

length in wood specimens has been observed through a light microscope and found to be to an accuracy of better than hundredth of an inch.

Fracture Toughness (K_{IC}) Testing

Before testing, the data taken were the length, width, and thickness of each specimen to a tolerance of 0.001 inch, the weight of each specimen to a tolerance 0.01 gram, and the moisture content of the designated specimens by the oven-dry method.

Two aluminum loading blocks (Figure 12) were glued to each face of the test specimen as the agency for transmitting a tensile load from the machine to the specimen. The glue used was a hot-melt type donated by Borden Company at Eugene, Oregon. The loading fixture is also shown in Figure 12.

Two loading speeds (0.1 cm/min and 0.01 cm/min) were used to test every type of specimen regardless of the specimen thickness. The selection of the loading speed, considering primarily the thickness of the flakeboard (1/2 inch), was selected from ASTM: E 399 for K_{IC} testing of metallic materials (1974) and from ASTM: D 1037 for testing normal tensile strength of wood-base panel materials (1977). For a specimen thickness of 1/2 inch, the recommended loading speed by the former standard is from 0.023 cm/min to 0.113 cm/min (Young's modulus of Douglas-fir solid wood from Wood Handbook (1974) is used for the calculation of this deformation rate, because the specification in E 399 is in lbf/min), and by the latter standard is 0.102 cm/min.

For each K_{IC} testing, the number of repetitions are 10, 7, and 6 for microlam, flakeboard, and solid wood control specimens

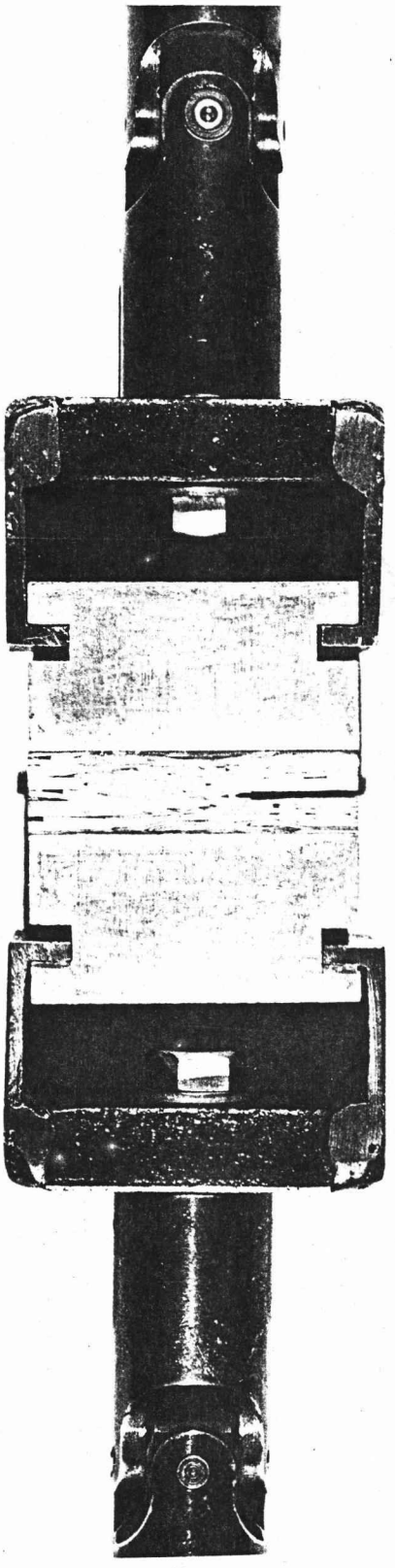

Figure 12. Loading fixture for testing K_{IC} specimens

respectively. Totally, 896 specimens were tested to obtain the ultimate loads. After testing each specimen, the fracture surface was examined immediately, if the crack was not extended from the crack tip, then the test result was abandoned for that specimen. In all, 18 out of 392 flakeboard specimens tested were abandoned because of this limitation. And this situation occurred mostly in low-density flakeboard, and never in microlam or solid-wood specimens. However, there were also test results on microlam specimens that were invalid because delaminations occurred in layers other than at crack tip before crack failure. Totally, 10 out of 240 microlam specimens tested were rejected because of this limitation.

Fracture Toughness (K_{IC}) Calculation

In this study, the oriented flakeboard has been treated as a continuum, and its fracture toughness is evaluated accordingly. Theoretically, the equation used to calculate the K_{IC} of a material is

$$K_{IC} = \sigma_C \sqrt{\pi c} \qquad \text{(Equation (25))}$$

Equation (25) is based on the assumption of idealistic conditions, such as the specimen stressed is an infinite plate with a centered crack, or the material is perfectly linear-elastic and brittle. In order to accommodate various materials or test conditions in the evaluation of K_{IC} which are not idealistic, the equations to obtain K_{IC} are calibrated in accordance with the specimen size, material

properties, and location or type of the crack (Paris and Sih 1965, Brown and Srawley 1966).

The equation used to calculate K_{IC} in this study is adopted from Brown and Srawley (1966) for calculating the K_{IC} of single-edge-cracked metallic plates in tension, it is given by

$$K_{IC} = \sigma_C (c)^{\frac{1}{2}} Y(\frac{c}{W}) \qquad (\text{for } \frac{c}{W} < 0.6) \tag{32}$$

where

$$Y(\frac{c}{W}) = 1.99-0.41(\frac{c}{W})+18.7(\frac{c}{W})^2-34.48(\frac{c}{W})^3+53.85(\frac{c}{W})^4$$

σ_C = maximum force/(W·t)

W = specimen width = 2 inch (in this study)

t = specimen thickness = 1 inch (in this study)

c = crack length = 0.75 inch (in this study)

Equation (32) is constructed by using the experimental compliance method (Srawley et al 1964) which is developed in accordance with the theory of fracture mechanics. Equation (32) is designed for calculating the K_{IC} of metallic materials. Its use is based on the assumption that the plastic region in front of a crack tip is relatively small in comparison with the total volume of the material surrounding the crack tip. If a metal behaves in a brittle manner, then the use of a K_{IC} calibration equation like Equation (32) is supposely independent of Young's modulus of the material (Brown et al 1964, or see Figure 8 in ASTM E 399(1974)). However, the equation is dependent upon the range of the initial crack length ($c/W < 0.6$) (Brown et al 1964). For the metals which have a larger plastic

effect the design of K_{IC}-specimen dimensions should follow the specifications recommended by Brown and Srawley (1966).

Both solid wood and the oriented flakeboards made in this study behave in a brittle manner when they fail in tension. Although the force-displacement curves for the loading of solid wood and oriented flakeboards in tension are not strictly linear-elastic (a slight viscoelastic effect can be observed in the early stage of the loading) like that observed for metals before yielding, by no means do they behave like metals having a so-called plastic (yielding) effect. Therefore, the tension property for solid wood is usually regarded as nearly linear-elastic (Perkins 1967, Schniewind and Pozniak 1971).

The reasons for the selection of Equation (32) to use in this study are: 1. both the solid wood and the oriented flakeboards made in this study behave in a brittle and nearly linear-elastic manner when they fail in tension, so they are assumed to be similar to a brittle metal; 2. no K_{IC} calibration equation has been established for a woody material; 3. the crack-specimen width ratio used in this study ($c/W = 0.375$) meets the specification for use of Equation (32) ($c/W < 0.6$). Schniewind and Lyon (1973) used Equation (32) to calculate the K_{IC} of Douglas-fir solid wood. Johnson (1973), however, applied a different K_{IC} calibration equation to obtain the K_{IC} of western redcedar and Douglas-fir. The equation used by Johnson (1973) was established by a so-called "boundary collocation procedure" (Paris and Sih 1965). This procedure is an alternate method to the experimental compliance method for constructing the K_{IC} calibration equation. The particular equation used by Johnson (1973) is applicable to a wider range of c/W ratio ($0.1 < c/W < 1.0$) than the

range specified for Equation (32) ($c/W < 0.6$). The difference between the resultant K_{IC} values calculated using Equation (32) and those using Johnson's equation is, however, within a few percent.

Substituting values σ_c = 100 psi, W = 2 in, c = 0.75 in into Equation (25), Equation (32), and the equation used by Johnson (1973), we obtain the K_{IC} values equivalent to 153 psi$\sqrt{in}$, 322 psi$\sqrt{in}$, and 310 psi$\sqrt{in}$, respectively. In other words, to obtain the best comparison of K_{IC} values between specimens, the same calibration equation should be used.

Measurement of Inter-Flake Void Sizes and Frequencies

Two strips cut from each of the flakeboards made (Figure 9) were used as specimens for measuring the inter-flake void sizes and frequency of occurrence through the board thickness profile. A binocular microscope with a magnification of approximately 4X was used to traverse an 8-inch span on each strip of the specimen. The traverse or scanning line is 1/32 inch (equivalent to flake thickness) in width and is at the center of each strip. The size of inter-flake voids encountered by the scanning line and the distances between inter-flake voids (Figure 13) were recorded and plotted as frequency histograms.

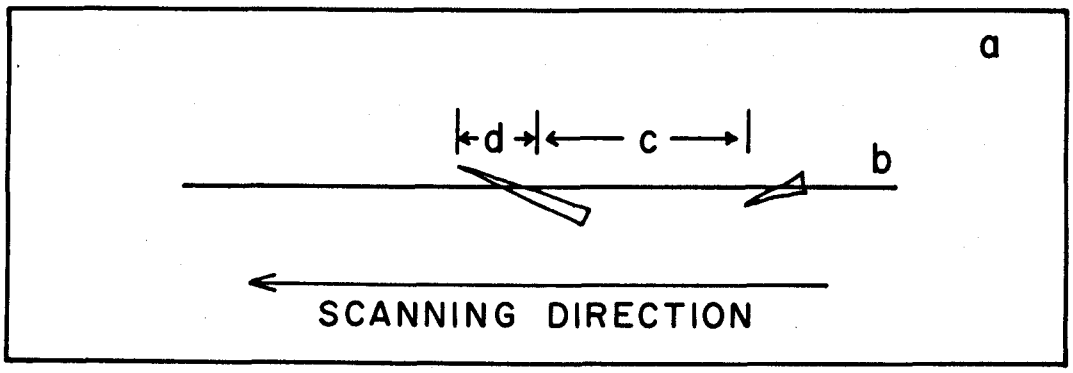

Figure 13. Measurement of inter-flake void and non-void lengths on a scanning strip. a) cross section view of an oriented flakeboard, b) scanning line 1/32-inch wide and 8-inch long, c) distance between voids (non-void length), and d) inter-flake void length

VII. EXPERIMENTAL OBSERVATION AND STATISTICAL ANALYSIS

Fracture Toughness (K_{IC}) of Solid Wood

Effect of Lumber from Different Trees

Eleven pieces of Douglas-fir lumber were used to manufacture the microlams and oriented flakeboards (Table 2). For each lumber, there were 24 solid-wood control specimens to be tested for their four fracture modes of K_{IC} values (six repetitions for each mode). In total, 264 solid-wood specimens were tested for the 11 pieces of lumber. The mean and standard deviation of every fracture mode for each lumber are shown in Table 3.

In order to know whether there were any differences in fracture resistances among the 11 pieces of lumber used, four fracture modes (RL, TL, TR, RT) had to be compared simultaneously. The appropriate statistical method for this kind of testing is the multivariate analysis of variance (Morrison 1967). The statistical-testing program used in this study was from the Statistical Interactive Programming System (SIPS) operating with the OS3 system in the CDC 3300 computer at Oregon State University. The subsystem command MANOVA (multivariate analysis of variance) of SIPS was called to simultaneously compare the four fracture modes among the 11 pieces of lumber. The test statistic is shown in APPENDIX A1.

The statistical conclusion is that at least one of the eleven pieces of lumber is different from the rest at the 1% level in its four modes of fracture resistances. In other words, even within the

Table 2. Relationships Between the Properties of Products (Microlam and Oriented Flakeboard) and Those of Their Original Solid Wood

Original solid wood number	Solid wood density[α] (lb/cu ft)	Product	Product nominal den.[β] (lb/cu ft)	Product actual den.[γ] (lb/cu ft)	Product nominal resin spread rate (lb/1000 sq ft)	Veneer or flake thickness (in)
1	32.78	Microlam 1	--	32.99	1.35	0.125
2	36.15	Microlam 2	--	35.81	1.35	0.0625
3	33.77	Microlam 3	--	35.38	1.35	0.03125
4	32.28	O. flakebd 1a	33	34.44	1.35	0.03125
5	34.84	O. flakebd 1b	33	33.89	2.025	0.03125
6	34.71	O. flakebd 1c	33	35.66	2.7	0.03125
7	32.09	O. flakebd 2a	43	44.21	1.35	0.03125
8	36.65	O. flakebd 2b	43	43.00	2.025	0.03125
9	33.34	O. flakebd 2c	43	44.05	2.7	0.03125
10	29.90	O. flakebd 3a	53	50.62	1.35	0.03125
11	28.47	O. flakebd 3a	53	51.55	1.35	0.03125

α Solid wood density is calculated based on air-dried weight and volume (moisture content = 9 to 10%)

β Product nominal density is calculated based on oven-dried weight and volume (moisture content = 0%)

γ Product actual density is calculated based on kiln-dried weight and volume (moisture content = 5 to 6%)

Table 3. Fracture Toughness (K_{IC}) of 11 Different Pieces of Douglas-Fir Solid Wood (Moisture Content = 9 to 10%)

Original solid wood number	K_{ICRL} ± s.d. (psi$\sqrt{in}$)		K_{ICTL} ± s.d. (psi$\sqrt{in}$)		K_{ICTR} ± s.d. (psi$\sqrt{in}$)		K_{ICRT} ± s.d. (psi$\sqrt{in}$)		Test statistic
1	334[α]	22	286	3	370	37	369	30	
2	355	27	304	7	465	39	407	34	
3	336	15	291	10	422	62	334	25	
4	340	26	312	10	436	29	352	33	
5	379	22	304	15	423	31	390	39	**
6	415	29	323	24	393	18	502	45	
7	326	12	274	6	376	42	328	31	
8	393	34	305	17	387	41	411	44	
9	430	22	309	15	398	34	461	22	
10	381	23	256	21	313	31	353	20	
11	307	18	244	8	369	44	351	25	

[α] Each value is average of six specimens

** The 11 sets of values are significantly different at the 1% level (APPENDIX A1)

same species of solid wood (Douglas-fir), lumber from different trees might have significant differences in fracture resistances.

Effect of Grain Orientation

By pooling the 11 pieces of lumber together, the average K_{IC} value and its standard deviation of 66 specimens for each fracture mode are shown in Figure 14. In Figure 14, one can observe that the fracture resistance of the TL system is distinctly smaller than the others and with the least variation. Whether RL, TR, and RT systems are different is not obvious and has to be determined by statistical comparisons. A series of one-way classification analysis of variance has been carried out to test the difference between fracture modes. The conclusions are: TL mode is significantly smaller than the rest at the 1% level (APPENDIX B1, B2); the probability of RL mode smaller than TR mode is between 95 to 99 percent (APPENDIX B3, B4); TR and RT modes are the same (APPENDIX B5).

A similar trend of grain-orientation effect on solid wood K_{IC} was also observed by Schniewind and Centeno (1973). They, however, used bending specimens to test the Douglas-fir solid wood K_{IC} and found the K_{IC} values to be 373 ± 34 psi$\sqrt{in}$, 284 ± 24 psi$\sqrt{in}$, 323 ± 54 psi$\sqrt{in}$, and 323 ± 46 psi$\sqrt{in}$ for RL, TL, TR, and RT fracture modes, respectively. This difference in K_{IC} values for different fracture modes has been attributed to the effect of varying fracture resistance of different wood anatomical structure (Debaise et al 1966, Schniewind and Centeno 1973).

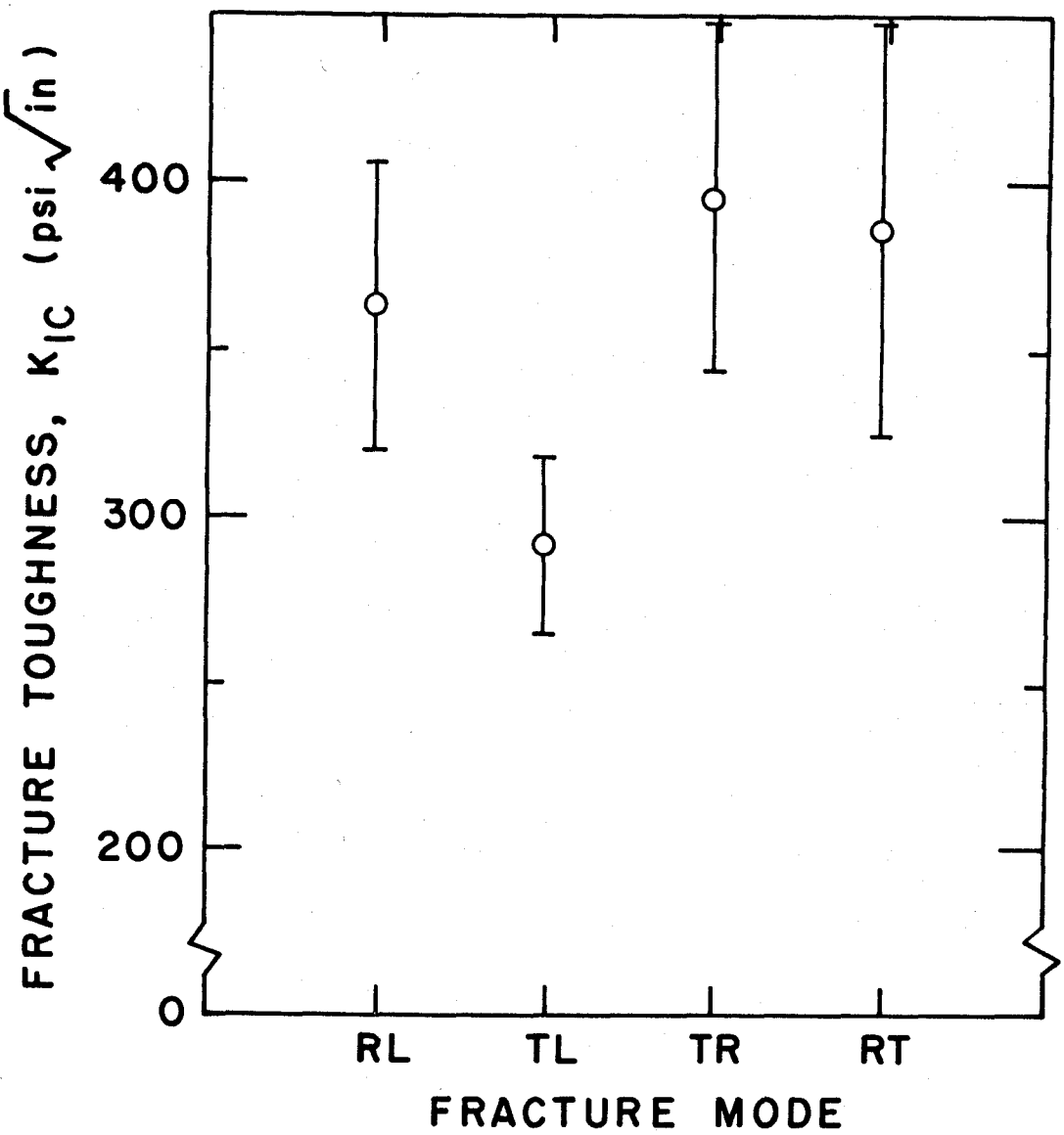

Figure 14. Effect of grain orientation on the fracture toughness (K_{IC}) of solid wood (66 repetitions for each mode)

Effect of Loading Speed

The duration of stress, or the time during which a load acts on a wood member, is an important factor in determining the load that a wood member can sustain. As an approximate indication of the relation between strength and duration of stress, the Wood Handbook (1974) states that as the duration of stress is decreased or increased by a factor of ten, strength may increase or decrease, respectively, by seven to eight percent.

In this study, the fracture toughness of solid-wood specimens was evaluated at two different loading speeds: 0.1 cm/min and 0.01 cm/min. This resulted in loading durations of around 0.5 and 5 minutes respectively before failure. The mean and standard deviation of ten specimens for each fracture mode per loading speed are tabulated in Table 4. There is no significant difference at the 5% level (APPENDIX A2) between the K_{IC} values evaluated at different loading speeds. Similar findings were also reported by Schniewind and Centeno (1973), where only the TL fracture mode was evaluated for loading-duration effect.

Fracture Toughness (K_{IC}) of Microlams

Effect of Veneer Thickness

Three kinds of microlams were made from veneers of different thicknesses, namely 1/8 inch, 1/16 inch, and 1/32 inch. The K_{IC} values are shown in Table 5, for the actual mean value of ten specimens per fracture mode and in terms of the K_{IC} retention of original wood.

Table 4. Effect of Loading Speed on the Fracture Toughness (K_{IC}) of Solid Wood

Loading speed (cm/min)	K_{ICRL} ± s.d. (psi$\sqrt{in}$)	K_{ICTL} ± s.d. (psi$\sqrt{in}$)	K_{ICTR} ± s.d. (psi$\sqrt{in}$)	K_{ICRT} ± s.d. (psi$\sqrt{in}$)	Test statistic
0.1	339[α] 20	318 31	418 54	355 39	N.S.
0.01	343 20	291 12	384 45	323 23	

[α] Each value is average of ten specimens

N.S. Not significant at the 5% level (APPENDIX A2)

Table 5. Effect of Veneer Thickness on the Fracture Toughness (K_{IC}) of Microlams

Microlam veneer thickness (in)	K_{ICRL} (psi$\sqrt{in}$)	Retention[α] (%)	K_{ICTL} (psi$\sqrt{in}$)	Retention (%)	K_{ICTR} (psi$\sqrt{in}$)	Retention (%)	K_{ICRT} (psi$\sqrt{in}$)	Retention (%)	Test statistic
1/8	297[β]	89	273	95	357	96	326	88	
1/16	339	95	288	95	408	88	340	84	**
1/32	360	107	348	120	358	85	385	115	

α K_{IC} retention of original solid wood

β Each value is average of ten specimens

** Three sets of K_{IC} retentions are significantly different at the 1% level (APPENDIX A6)

Because the tip of the notch introduced in the specimen is within the wood veneer instead of in the resin layer for microlam 1 (made from 1/8 inch veneers) and microlam 2 (made from 1/16 inch veneers) (Table 2), one would expect that the K_{IC} values of these microlams would be the same as those of the original solid wood unless there was damage done in the microlam manufacturing process. Statistically, the K_{IC} of microlam 1 and microlam 2 are found significantly lower than those of the original solid wood at the 5% level, but not significant at the 1% level (APPENDIX A3, A4, and Table 5). However, for microlam 3 (made from 1/32 inch veneers), its fracture toughness is statistically stronger than that of the original solid wood at the 1% level (APPENDIX A5). Although the tip of the notch in the specimen for microlam 3 is not always within the wood veneer, it is unlikely for the resin layer or resin-wood joint to have a reinforcing effect on the cell walls to resist crack propagation (White 1976), especially because the amount of resin solids applied was rather small (1.35 lb/ 1000 sq ft). From the concept of fracture mechanics, a possible explanation for this K_{IC} increase of microlam 3 is that the size and number of the inherent flaws (Schniewind and Lyon 1973) in the solid wood might be reduced, either due to the discontinuity of the inherent flaws by the finely spaced glue layers, or due to the sealing of the inherent flaws by the combining effect of resin, heat plastic flow (325°F), and densification (a density increase from 33.77 lb/cu ft of solid wood to 35.38 lb/cu ft of microlam 3 under a pressure of 250 psi).

For the comparison among the three types of microlam (or among the different types of oriented flakeboard in the later sections), it is necessary to minimize the basic K_{IC} differences of the original lumber from which the microlams (or oriented flakeboards) were made, because it is assumed that it is the solid wood that resists the crack propagation in the board. One method to minimize the effect of differing original solid wood K_{IC} is to represent the product K_{IC} in terms of the K_{IC} retention of its original solid wood (K_{IC} of product/ average K_{IC} of original solid wood), then make comparisons between or among the proportions. The validity of the statistical comparison like this, however, is usually concerned with the normality of the data (represented in proportions).

Because the size of the sample involved in each test unit is rather small (repetitions for microlam and flakeboard K_{IC} specimen are ten and seven, respectively), even the actual K_{IC} in each test unit are often not distributed normally. After each product K_{IC} is divided by the average K_{IC} of its original solid wood, the distribution shape of the proportions in each test unit is not changed. Nevertheless, many mathematical transformations (including ln(proportion), arcsin ($\sqrt{\text{proportion}}$), $[\ln(\sqrt{\text{product } K_{IC}})]/[\ln(\sqrt{\text{average } K_{IC} \text{ of original solid wood}})]$, and $\arcsin\{[\ln(\sqrt{\text{product } K_{IC}})]/[\ln(\sqrt{\text{average } K_{IC} \text{ of original solid wood}})]\}$) have been attempted to normalize the proportions. The transformations, however, did not improve the normality of the original distribution. This is checked by comparing the normal plots (Dixon and Massey 1969 P.63) between the original and the transformed distributions by using SIPS. Therefore, no transformation has been

made to the proportions used in this study. In other words, the statistical conclusions made in this study was based on the assumption that the populations of the proportions or the actual K_{IC} are normally distributed.

For the comparison among the microlam 1, 2, and 3 of their K_{IC} retention of the original solid wood, significant differences in K_{IC} retentions (APPENDIX A6) should be found among the three types of microlams due to the increase in K_{IC} values of microlam 3 and the decrease in K_{IC} values of microlam 1 and 2.

Effect of Veneer Grain Orientation

Compared with solid wood, the structure of a perfectly made microlam should not be altered from that of solid wood, except for several thin resin layers interrupting the continuity of wood tissues across the fiber direction. If the crack propagation before failure stays in the wood, then the inherent direction-dependency of K_{IC} as it occurs in solid wood should also occur in microlams. This was true for microlam 1 and microlam 2 (Table 5, APPENDIX B6 and B7), but not for microlam 3 (APPENDIX B8). In other words, the inherent directional effect on the fracture resistance in solid wood disappears in microlam 3 where very thin veneers (1/32 inch) were used to make the product. There is no evidence to show that crack propagates within the resin layer.

There is one more thing that should be noted in Table 5. The TL fracture mode, which is always the weakest in solid wood, consistently

retains the highest K_{IC} percentage of original solid wood.

Effect of Loading Speed

The results of comparing the effect of loading speed on the K_{IC} of microlams are shown in Table 6. There is no statistical difference in K_{IC} values of microlams between loading speeds of 0.1 cm/min and 0.01 cm/min (APPENDIX A7, A8, A9).

Fracture Toughness (K_{IC}) of Oriented Flakeboards

In the discussion of different types of oriented flakeboards, because reference is frequently made to the board density and the resin solids spread rate, it is convenient to use symbols to represent the flakeboard type. Therefore, an arabic number is used to represent board density in such a way that 1, 2, and 3 represent low- (33 lb/cu ft), medium- (43 lb/cu ft), and high-density (53 lb/cu ft), respectively. Whereas, alphabetic letters represent resin solids spread rates in a manner that a, b, and c stand for, respectively, 1.35, 2.025, and 2.7 lb/1000 sq ft. Thus, flakeboard 1a is decoded as an oriented flakeboard with a density of 33 lb/cu ft and a 1.35 lb/1000 sq ft resin solids spread rate. Complete information concerning the types of oriented flakeboards are given in Table 1.

Table 6. Effect of Loading Speed on the Fracture Toughness (K_{IC}) of Microlams

Microlam veneer thickness (in)	Loading speed (cm/min)	K_{ICRL} ± s.d. (psi$\sqrt{in}$)	K_{ICTL} ± s.d. (psi$\sqrt{in}$)	K_{ICTR} ± s.d. (psi$\sqrt{in}$)	K_{ICRT} ± s.d. (psi$\sqrt{in}$)	Test statistic
1/8	0.1	297[α] 22	273 20	357 54	326 27	N.S.
	0.01	281 26	263 18	370 45	332 76	
1/16	0.1	339 63	288 21	408 39	340 39	N.S.
	0.01	351 45	274 20	407 21	316 29	
1/32	0.1	360 50	348 20	358 25	385 50	N.S.
	0.01	330 36	317 24	382 26	365 45	

[α] Each value is average of ten specimens

N.S. Not significant at the 5% level between two sets of K_{IC} values (APPENDIX A7, A8, A9)

Effect of Board Density

In this study, the only comparison made of the effect of board density on K_{IC} values was among the flakeboards with a 1.35 lb/1000 sq ft resin solids spread rate. The averages of K_{IC} values of seven specimens per fracture mode per flakeboard type are tabulated in Table 7.

The fracture resistance of the three different density flakeboards is definitely different when comparing their K_{IC} retentions of original solid wood (APPENDIX A10). However, this difference in board-density effect on K_{IC} values shows a big jump from flakeboard 1a to flakeboard 2a, but only a moderate increase from flakeboard 2a to flakeboard 3a (APPENDIX A11 and A12).

Effect of Resin Solids Spread Rate

The three nominal resin solids spread rates used for oriented flakeboards were: 1.35 lb/1000 sq ft, 2.025 lb/1000 sq ft, and 2.7 lb/1000 sq ft. These spread rates were compared for two different board-density levels: 33 lb/cu ft and 43 lb/cu ft for their K_{IC} retention of original solid wood (Table 8). Statistically, there is no difference in K_{IC} retentions among flakeboard 1a, 1b, and 1c (APPENDIX A13). However, for flakeboard 2a, 2b, and 2c, statistical difference is shown among the K_{IC} retentions (APPENDIX A14). But with further examination of the data, we found that this difference was due to the weaker flakeboard 2b with a 2.025 lb/1000 sq ft in resin solids spread rate (APPENDIX A15 and A16). No statistical

Table 7. Effect of Board Density on the Fracture Toughness (K_{IC}) of Oriented Flakeboards

Product	K_{ICRL} (psi$\sqrt{in}$)	Retention[α] (%)	K_{ICTL} (psi$\sqrt{in}$)	Retention (%)	K_{ICTR} (psi$\sqrt{in}$)	Retention (%)	K_{ICRT} (psi$\sqrt{in}$)	Retention (%)	Test statistic
Flakebd 1a[β]	80[γ]	24	111	36	100	23	89	25	
Flakebd 2a	240	74	255	93	255	68	260	79	**
Flakebd 3a	318	83	234	96	252	68	306	87	

[α] K_{IC} retention of original solid wood

[β] Definition of the code number is in Table 2

[γ] Each value is average of seven specimens

** Three sets of K_{IC} retentions are significantly different at the 1% level (APPENDIX A10)

Table 8. Effect of Resin Solids Spread Rate on the Fracture Toughness (K_{IC}) of Oriented Flakeboards

Product	K_{ICRL} (psi$\sqrt{in}$)	Retention[α] (%)	K_{ICTL} (psi$\sqrt{in}$)	Retention (%)	K_{ICTR} (psi$\sqrt{in}$)	Retention (%)	K_{ICRT} (psi$\sqrt{in}$)	Retention (%)	Test statistic
Flakebd 1a[β]	80[γ]	24	111	36	100	23	89	25	
Flakebd 1b	98	26	155	51	99	23	110	28	N.S.
Flakebd 1c	143	34	116	36	126	32	138	27	
Flakebd 2a	240	74	255	93	255	68	260	79	*
Flakebd 2b	264	67	249	81	252	65	247	60	* N.S.
Flakebd 2c	349	81	329	107	311	78	352	76	*

[α] K_{IC} retention of original solid wood

[β] Definition of the code number is in Table 2

[γ] Each value is average of seven specimens

N.S. Not significant at the 5% level among or between K_{IC} retention (APPENDIX A13 and A17)

* Significant at the 5% level between K_{IC} retentions (APPENDIX A15 and A16)

difference is shown between the boards with a spread rate of 1.35 lb/1000 sq ft and 2.7 lb/1000 sq ft (APPENDIX A17). To explain this, we found that the lumber used to make the flakeboard 2b was much denser than the lumber used to make flakeboard 2a and 2c (Table 2). In other words, relatively less flakes are needed to make a flakeboard of a given density by using denser flakes than by using lighter flakes. This in turn would result in increasing inter-flake void sizes and non-bonded areas in the flakeboard. We also checked the board-manufacturing recordings and found that the average flake weight for four 20-flake groups was 6.07 grams, 7.57 grams, and 5.72 grams, respectively, for flakeboard 2a, 2b, and 2c. From the above observations, we could conclude that a resin solids spread rate above 1.35 lb/1000 sq ft would not contribute advantageously to the K_{IC} values of oriented flakeboard.

Effect of Flake Grain Orientation

Six separate one-way classification analyses of variance were applied to flakeboard 1a, 1b, 1c, 2a, 2b, 2c to test whether there was any difference in K_{IC} values among RL, TL, TR, RT fracture modes within each type of flakeboard. The statistical comparisons are in APPENDIX B9, B10, B11, B12, B13, B14. The average K_{IC} values of the flakeboards are shown in Table 8.

In the results of the statistical analyses, only the TL system of flakeboard 1b is significantly different from the RL, TR, RT systems. In other words, similar to what occurred for microlams made from 1/32 inch veneers, the inherent directional effect of the flake grain

orientation on the fracture resistance tends not to exist for the oriented flakeboards.

Effect of Loading Speed

In the statistical testing (APPENDIX A18 to A24) of the loading-speed effect on the K_{IC} values of flakeboard 1a, 1b, 1c, 2a, 2b, 2c, 3a (Table 9), only flakeboard 3a showed a statistical difference in fracture resistances. Therefore, we can conclude that a strong tendency exists that loading speeds of 0.1 cm/min or 0.01 cm/min will not affect the fracture-toughness values of oriented flakeboards.

Effect of Flake Dimensions

Although the relationship between the fracture toughness and flake dimensions of an oriented flakeboard cannot be explicitly determined because of the experimental design in this study, the effects of a given flake length (2 inches) and flake width (11/16 inch) on the inter-flake void sizes and their frequency of occurrence in an oriented flakeboard can be directly measured.

Because a inter-flake void, as defined in this study, is only related to the ends of the flakes in a board, then conceivably for a given area the cross-fiber side of the oriented flakeboard should include more but shorter inter-flake voids, because the flakes are shorter in this section ((c) and (d) in Figure 15, 16, 17) than on the along-fiber direction ((a) and (b) in Figure 15, 16, 17). This trend can roughly be observed in low- and medium-density boards in Figure 15 and 16. For high density boards (Figure 17), although the smallest

Table 9. Effect of Loading Speed on the Fracture Toughness (K_{IC}) of Oriented Flakeboards

Product	Loading speed (cm/min)	K_{ICRL} ±s.d. (psi$\sqrt{in}$)		K_{ICTL} ±s.d. (psi$\sqrt{in}$)		K_{ICTR} ±s.d. (psi$\sqrt{in}$)		K_{ICRT} ±s.d. (psi$\sqrt{in}$)		Test statistic
Flakeboard 1a[α]	0.1	80	26	111	17	100	27	89	22	N.S.
	0.01	86	36	125	42	82	38	91	35	
Flakeboard 1b	0.1	98	40	155	26	99	16	110	35	*
	0.01	102	25	148	36	134	24	134	58	
Flakeboard 1c	0.1	143	59	116	37	126	38	138	39	N.S.
	0.01	142	67	128	46	93	13	140	27	
Flakeboard 2a	0.1	240	22	255	31	255	53	260	23	N.S.
	0.01	228	29	240	33	247	13	239	14	
Flakeboard 2b	0.1	264	28	249	29	252	24	247	41	N.S.
	0.01	243	40	270	38	296	35	262	43	
Flakeboard 2c	0.1	349	37	329	39	311	63	352	37	N.S.
	0.01	322	35	335	32	326	40	318	30	
Flakeboard 3a	0.1	318	19	234	8	252	12	306	27	N.S.
	0.01	277	20	214	14	229	20	274	29	

[α] Definition of the code number is in Table 2

N.S. Statistically not significant at the 5% level between two sets of K_{IC} values (APPENDIX A18 to A24)

* Statistically significant at the 5% level between two sets of K_{IC} values

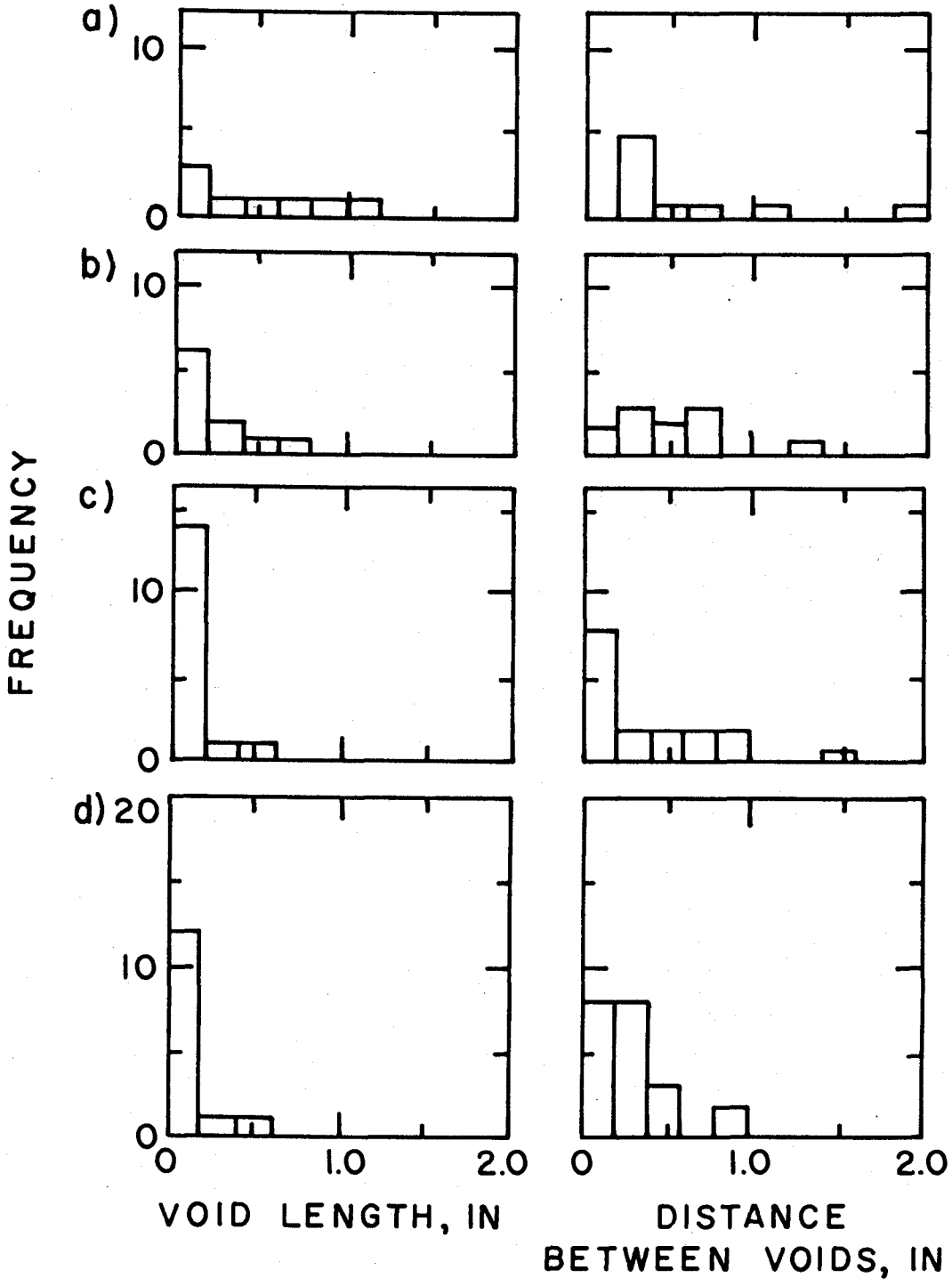

Figure 15. Frequency histograms of inter-flake void and non-void lengths along an 8-inch scanning line for the 34 lb/cu ft oriented flakeboard tested in a) RL mode, b) TL mode, c) RT mode, and d) TR mode

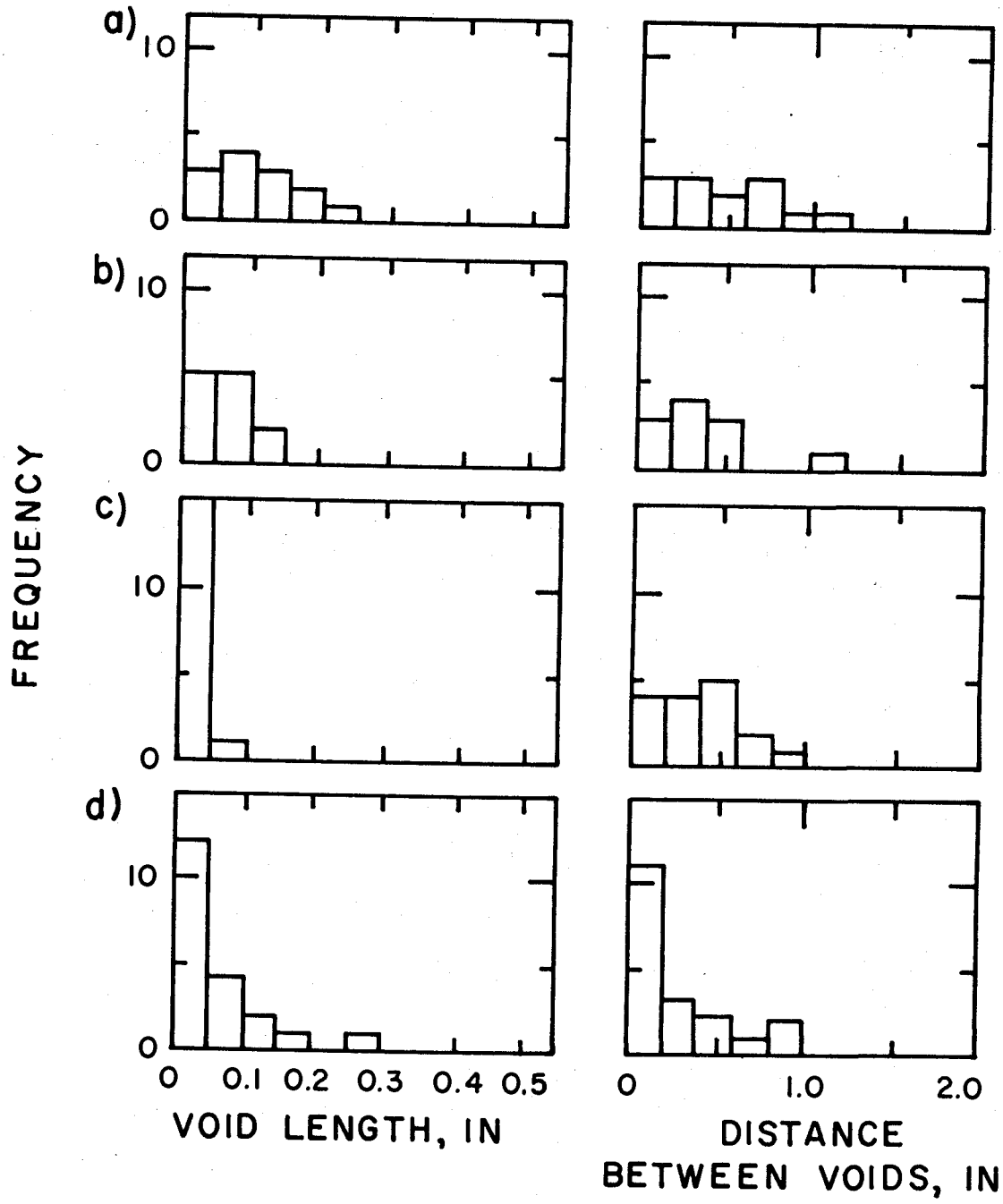

Figure 16. Frequency histograms of inter-flake void and non-void lengths along an 8-inch scanning line for the 43 lb/ cu ft oriented flakeboard tested in a) RL mode, b) TL mode, c) RT mode, and d) TR mode

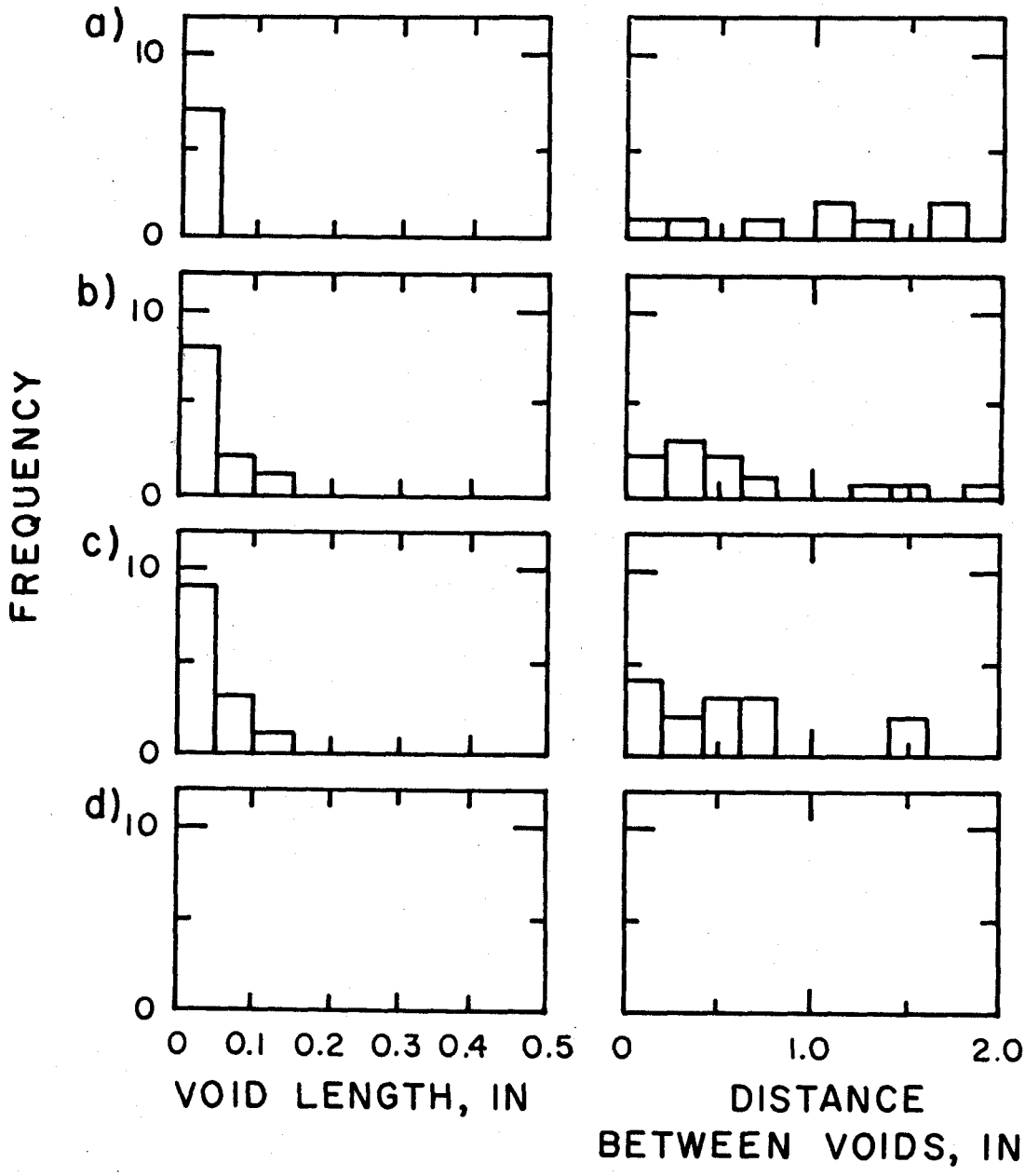

Figure 17. Frequency histograms of inter-flake void and non-void lengths along an 8-inch scanning line for the 51 lb/cu ft oriented flakeboard tested in a) RL mode, b) TL mode, c) RT mode, and d) TR mode

inter-flake void measured was 0.004 inch, most of the voids are sealed due to the dense compaction of the materials. It was even difficult to observe any obvious inter-flake voids in one of the measuring strips (Figure 17(d)).

Effect of Inter-Flake Void Sizes and Their Frequency of Occurrence

Although the objective of designing this experiment is to identify the critical parameters that affect the fracture toughness of the oriented flakeboards, we have hypothesized that the fracture toughness of an oriented flakeboard should be a function of the size and frequency of its processing defects, namely, the inter-flake voids and the non-bonded areas.

Non-bonded areas are not directly measurable before destructive testing, but we can observe from Figure 15, 16, and 17 that the size of inter-flake voids do have a decreasing trend with increasing density in oriented flakeboard (note the divisions on the abscissas are varied in order to better illustrate the inter-flake void size distributions). By further assuming that the microlam 3 (made from 1/32 inch veneers) is a perfectly oriented flakeboard free of inter-flake voids and non-bonded areas, we then can plot the K_{IC} of flakeboard 1a (34 lb/cu ft), 2a (44 lb/cu ft), 3a (51 lb/cu ft), and microlam 3 (35 lb/cu ft) in terms of the K_{IC} retention of its original solid wood. This is shown in Figure 18.

A definite trend is seen in Figure 18. The oriented-flakeboard K_{IC} retention of original solid is a function of their inter-flake void size and frequency of occurrence. The increments of K_{IC}

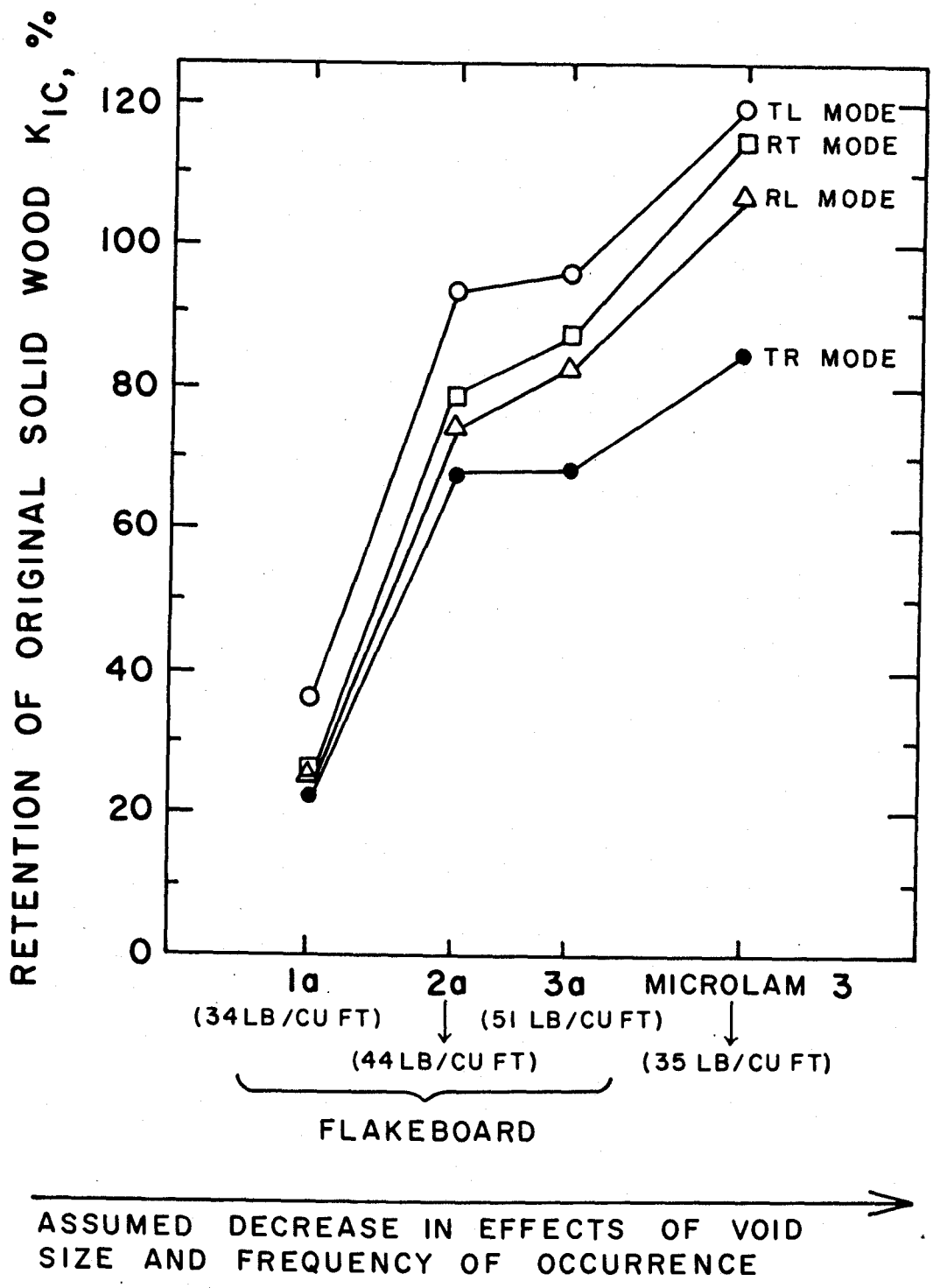

Figure 18. Effect of inter-flake void sizes and their frequency of occurrence upon the oriented-flakeboard K_{IC} retention of the original solid wood

retention from board to board are all statistically significant (APPENDIX A11 and A12).

One more thing should be noted in Figure 18. If the variable on the abscissa is product density instead of void size and distribution, then no consistent trend in K_{IC} retention should exist. In other words, the density of the reconstituted wood composite would not be a consistent indicator of its fracture strength.

Further statistical analysis like multiple linear regression can be done on the individual fracture modes to evaluate the impact of void size on the board K_{IC} retention of original solid wood. In this study, only the TL mode fracture toughness is selected for the analysis because it is the least variant mode (see Table 6 and 9). The variables in the multiple linear regression model are board density (D), resin solids spread rate (R), average void length (V), and their interactions DR, DV, RV, and DRV.

A subsystem command STEPWISE of SIPS was called to select the variables in a sequence of decreasing contribution to the multiple linear model. When the K_{ICTL} values of microlam 3 are included in the analysis with the flakeboards, the sequence is V, DRV, DR, D, R, DV, and RV. In other words, the average void length V is the most significant parameter affecting the product K_{ICTL} retention of original solid wood. The stepwise equations and their corresponding correlation coefficients are shown in APPENDIX C1. The scatter data plotting the K_{ICTL} retention versus average void length and board density, and their fitted regression models are shown in APPENDIX C2 and C3. Because the void length data for each board was obtained by measuring an 8-inch scanning strip near the edge of the board (Figure

9), this might not provide sufficient observations for an unbiased estimation of the average void length for the board. Therefore, in a later experiment additional data is collected to plot K_{ICTL} retention versus the average void length sampled throughout the board, given in APPENDIX C4.

When the ideal oriented flakeboard (microlam 3) is not included with the other flakeboards in the statistical analysis, then the board density becomes a better indicator than the average void length for the board K_{ICTL} retention (APPENDIX C5, C6, and C7). However, it is difficult to analytically model in terms of gross density effect, the board K_{ICTL} retention drop for high density flakeboards.

From the above discussion we conclude that it is logical to analytically investigate the fracture strength of oriented flakeboard in terms of the effects of inter-flake void size and distribution.

Summary of Experimental Results

For solid wood (Douglas-fir):

1. Lumber from different trees might have different fracture resistances.
2. Fracture toughness (K_{IC}) is grain-orientation dependent, and the TL mode is always the weakest among RL, TL, TR, RT modes studied and with the least variation.
3. Loading speeds of 0.1 cm/min or 0.01 cm/min show no significant effect on the K_{IC} values.

For microlam (Douglas-fir):

1. The K_{IC} is affected by veneer thickness. The microlam K_{IC} is higher than that of original solid wood when 1/32 inch-thick

veneers are used, but slightly lower when 1/8 inch- or 1/16 inch-thick veneers are used.

2. No distinction is shown among RL, TL, TR, RT modes of fracture resistance for microlam made with 1/32 inch-thick veneers. However, the distinction is still maintained in the microlams made with 1/8 inch- or 1/16 inch-thick veneers.
3. Loading speeds of 0.1 cm/min or 0.01 cm/min show no significant effect on the K_{IC} values.

For oriented flakeboard (Douglas-fir):

1. The board K_{IC} retention of original solid wood increases with increasing board density, but tends to level off or drop for high-density flakeboard.
2. Within the normal range of resin solids spread rate (1 lb/1000 sq ft to 3 lb/1000 sq ft), there is no significantly benificial effect to the board K_{IC} retention of original solid wood with a spread rate above 1.35 lb/1000 sq ft.
3. No distinction is shown among RL, TL, TR, RT modes of fracture resistance.
4. In comparison with the RL, TR, and RT modes, the TL mode fracture toughness (K_{ICTL}) always has the highest K_{IC} retention of the same mode of the original solid wood.
5. Loading speeds of 0.1 cm/min or 0.01 cm/min show no significant effect on the K_{IC} values.
6. Fracture strength of oriented flakeboard in terms of K_{IC} retention of original solid wood is determined by the lengths and distributions of inter-flake void in the board.

VIII. ANALYTICAL MODEL

To analytically describe the normal tensile strength of an oriented flakeboard we must first identify the critical material parameters which influence the normal tensile strength.

In this study the normal tensile strength was treated as fracture toughness (K_{IC}). The concept of linear-elastic fracture mechanics could then be used to design an experiment for identifying the critical material parameters for flakeboard construction. The sizes and frequencies of inter-flake voids and non-bonded areas in the oriented flakeboard were hypothesized as the critical parameters influencing the K_{IC} of oriented flakeboard. Through the observations of a carefully controlled experiment we were able to verify the hypothesis that the reduction in K_{IC} values, when converting solid wood into oriented flakeboard, was mainly due to the introduction of inter-flake voids (and non-bonded areas--to be verified) into the boards. Although the non-bonded areas in the oriented flakeboard are not directly measurable before destructive testing, it is not difficult to imagine that they must be positively related to the inter-flake void size which is a function of the applied pressure to consolidate the mat, the board density, flake dimensions, and flake density.

Effect of Inter-Flake Void

The following analysis is developed to theoretically quantify the effect of inter-flake void size and frequency of occurrence upon the K_{IC} of an oriented flakeboard. The effect of inter-flake voids can be

visualized in such a way that when an initial crack with a given length c is introduced in a flakeboard specimen, the tip of the initial crack might join with an inter-flake void of expected length Δc. This would lengthen the initial crack c to $c+\Delta c$, thus, reducing the maximum stress needed to fail a flakeboard K_{IC} specimen. This effect of elongating a given initial crack can be further clarified by looking at Equation (32), which can be rearranged to

$$\sigma_C = \frac{K_{IC}}{\sqrt{c}[1.99-0.41(\frac{c}{W})+18.7(\frac{c}{W})^2-34.48(\frac{c}{W})^3+53.85(\frac{c}{W})^4]} \tag{33}$$

where K_{IC}, c, W, and σ_C used here are, respectively, the fracture toughness, initial crack length, specimen width, and maximum stress. Assuming that the K_{IC} of the wood is the same for the original solid wood and the flakes, then, for a given value of K_{IC} in Equation (33), when c is increased to a value $c+\Delta c$, then σ_C must be decreased to a value $\sigma-\Delta\sigma$. Equation (33) can then be rewritten as

$$\sigma_C \text{ (predicted)} = \sigma_C - \Delta\sigma$$

$$= \frac{K_{IC} \text{ (original wood)}}{\sqrt{c+\Delta c}[1.99-0.41(\frac{c+\Delta c}{W})+18.7(\frac{c+\Delta c}{W})^2-34.48(\frac{c+\Delta c}{W})^3+53.85(\frac{c+\Delta c}{W})^4]} \tag{34}$$

where

σ_C (predicted) = predicted maximum normal tensile stress to failure for flakeboard K_{IC} specimen

σ_C = actual maximum normal tensile stress to failure for solid-wood K_{IC} specimen (σ_C=force/(W·t))

$\Delta\sigma$ = stress decrement due to Δc

K_{IC} (original wood) = actual fracture toughness of original solid wood

c = initial crack length in solid wood or flakeboard K_{IC} specimen

Δc = expected inter-flake void length

W, t = width and thickness of K_{IC} specimen

When Equation (34) is used, a limitation would automatically be imposed upon the predicted values of failure stress. The limitation is that the predicted failure stress for oriented flakeboard could never be greater than that of the original solid wood. This limitation, however, is not indicative of what we observed in the EXPERIMENTAL OBSERVATION section--that the σ_c or K_{IC} of a perfectly oriented flakeboard (microlam) could be stronger than that of its original solid wood. The use of K_{IC} (original wood) in Equation (34) as a reference point is from the assumption that the K_{IC} of flakes in the board is equal to K_{IC} (original wood). Although this assumption may not be exactly true, there does not appear to be a better reference point than the K_{IC} (original wood) to predict the failure stress for an oriented flakeboard. A possible means to improve upon this limitation, or to show the occurrence of a better-than-original-wood effect will be discussed in a later section.

Expected Inter-Flake Void Length (Δc)

If Equation (34) is used to predict the maximum stress needed to fail an oriented flakeboard, then the key of the theoretical development is to determine the probability that the tip of an initial

crack will encounter an inter-flake void, and to determine the expected length of this inter-flake void (Δc).

It is not difficult to deduce that a flakeboard should have more smaller cracks than the big ones, especially in the situation of higher density board where the flakes are highly compacted. This deduction can be substantiated by examining the frequency histograms of inter-flake void sizes in Figure 15, 16, 17. We observe that both the lengths of the inter-flake void and the non-void (distance between inter-flake voids) frequency histograms roughly simulate exponential distributions (Figure 19). Because the frequency histograms were obtained by measuring the inter-flake void and non-void lengths along a continuous scanning line, any point of the scanning line has to be either in the state of void or in the state of non-void. For the sake of convenience, we can let

void = state 1

non-void = state 0

We may also let the void length be exponentially distributed with parameter $\mu > 0$, and non-void length be exponentially distributed with parameter $\lambda > 0$. Then it can be shown that the probability $P_{00}(c)$ of being in state 0 at distance c, starting at the c equal to zero at state 0 is

$$P_{00}(c) = \frac{\mu}{\lambda+\mu} + \frac{\lambda}{\lambda+\mu} e^{-(\lambda+\mu)c} \qquad \text{(Karlin 1975 P.154)} \qquad (35)$$

Equation (35) can be used as a beginning to calculate the probability that the initial crack tip introduced at a distance c from one end of a flakeboard specimen would encounter an inter-flake void.

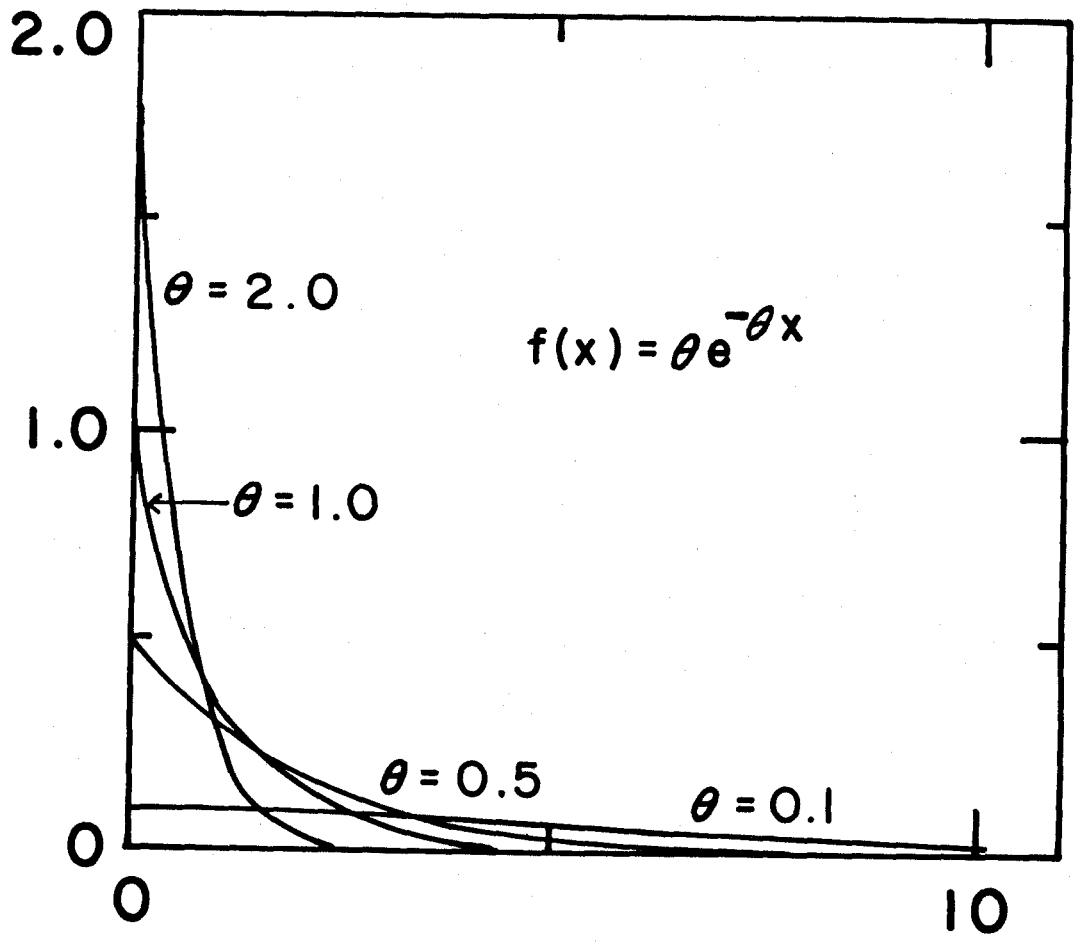

Figure 19. Shapes of exponential distribution in relation to the parameter θ

If we let

$1/\mu$ = average inter-flake void length

$1/\lambda$ = average non-void length

Given $P_{00}(c)$ of Equation (35) in long-hand form,

$$P\{\text{state 0 at c} \mid \text{state 0 at c=0}\} = \frac{\mu}{\lambda+\mu} + \frac{\lambda}{\lambda+\mu} e^{-(\lambda+\mu)c} \tag{35}$$

so

$$P\{\text{state 1 at c} \mid \text{state 0 at c=0}\} = \frac{\lambda}{\lambda+\mu} - \frac{\lambda}{\lambda+\mu} e^{-(\lambda+\mu)c} \tag{36}$$

Similarly, the probability of being in state 1 at distance c, starting at the c equal to zero at state 1 is

$$P\{\text{state 1 at c} \mid \text{state 1 at c=0}\} = \frac{\lambda}{\lambda+\mu} + \frac{\mu}{\lambda+\mu} e^{-(\lambda+\mu)c} \tag{37}$$

so

$$P\{\text{state 0 at c} \mid \text{state 1 at c=0}\} = 1 - \text{Equation (37)}$$

$$= \frac{\mu}{\lambda+\mu} - \frac{\mu}{\lambda+\mu} e^{-(\lambda+\mu)c} \tag{38}$$

At the beginning of a scanning line (c=0), whether the previous state of void or non-void is unknown, the probability to be in state 0 or state 1 at the c equal to zero is a ratio of the average void length to average non-void length. So

$$P\{\text{state 1 at c=0}\} = \frac{\frac{1}{\mu}}{\frac{1}{\lambda}+\frac{1}{\mu}} = \frac{\lambda}{\lambda+\mu} \tag{39}$$

$$P\{\text{state 0 at c=0}\} = \frac{\frac{1}{\lambda}}{\frac{1}{\lambda}+\frac{1}{\mu}} = \frac{\mu}{\lambda+\mu} \tag{40}$$

To combine all the previous situations, the probability of being in a void state at any c is then

$$P\{\text{state 1 at c}\} = P\{\text{state 1 at c=0}\} \cdot P\{\text{state 1 at c} \mid \text{state 1 at c=0}\} + P\{\text{state 0 at c=0}\} \cdot P\{\text{state 1 at c} \mid \text{state 0 at c=0}\}$$

$$= \frac{\lambda}{\lambda+\mu}\left[\frac{\lambda}{\lambda+\mu}+\frac{\mu}{\lambda+\mu}e^{-(\lambda+\mu)c}\right] + \frac{\mu}{\lambda+\mu}\left[\frac{\lambda}{\lambda+\mu}-\frac{\lambda}{\lambda+\mu}e^{-(\lambda+\mu)c}\right]$$

$$= \frac{\lambda}{\lambda+\mu} \tag{41}$$

Because a no aging effect (what happened before does not affect what will happen) is a special property of an exponential distribution, then the expected lengths of inter-flake voids are

$$E(\text{void length} \mid \text{state 1 at c}) = \frac{1}{\mu} \tag{42}$$

and

$$E(\text{void length} \mid \text{state 0 at c}) = 0 \tag{43}$$

So the expected value of an inter-flake void length at any situation is then

$$\Delta c = E(\text{void length}) = \frac{1}{\mu} \cdot \frac{\lambda}{\lambda+\mu} + 0 \cdot \frac{\mu}{\lambda+\mu} = \frac{1}{\mu} \cdot \frac{\lambda}{\lambda+\mu} \tag{44}$$

What Equation (44) says is that the expected inter-flake void length Δc is positively proportional to the average void length and negatively proportional to the average non-void length occurring on a continuous scanning line. The length of the initial crack c does not affect the Δc.

It has to be noted that the $1/\mu$ and $1/\lambda$ defined above are the average inter-flake void and the average non-void lengths, respectively. However, $1/\mu$ and $1/\lambda$ can also be defined as the average inter-flake crack and average non-crack lengths, then

$$\frac{1}{\mu} = \text{average inter-flake void length} + \text{average non-bonded length} \tag{45}$$

$\frac{1}{\lambda}$ = average non-void length - average non-bonded length (46)

One thing should be noted here. Although the effect of an inter-flake void in a oriented flakeboard has been modelled in Equation (34) as a factor which reduces the stress needed to fail the original solid wood, by no means does it imply that oriented flakeboards and solid wood behave the same in terms of fracture resistance. In other words, in accordance with our modelling of the effect of inter-flake cracks, if one introduces an equivalent initial crack length c in both the solid wood and oriented flakeboard K_{IC} specimens, then a crack length of $c+\Delta c$ is used to evaluate the stress required to fail the oriented-flakeboard K_{IC} specimen. If solid wood and oriented flakeboard were the same material but only with different initial crack lengths in their K_{IC} specimens, then their K_{IC} would be the same, because K_{IC} is a material property and its value is independent of initial crack length.

Proportional Variable (g)

In the EXPERIMENTAL OBSERVATION section, both the solid-wood and the oriented flakeboard K_{IC} were evaluated using a constant crack length (c = 0.75 inch) in Equation (32). This automatically assumes a direct relationship between any two pair of σ_C and K_{IC} values, i.e.

$$\frac{K'_{IC}}{K_{IC}} = \frac{\sigma'_C}{\sigma_C} \tag{47}$$

or specifically,

$$\frac{K_{IC}\ \text{(flakeboard)}}{K_{IC}\ \text{(original wood)}} = \frac{\sigma_C\ \text{(flakeboard)}}{\sigma_C\ \text{(original wood)}} \tag{48}$$

However, a new relationship, other than that given in Equation (47), has to be assumed if the K_{IC} of two different materials are calculated using different crack lengths in Equation (32). A possible new relationship in the form of

$$\frac{K_{IC}\ \text{(predicted)}}{K_{IC}\ \text{(original wood)}} = g\ \frac{\sigma_C\ \text{(predicted)}}{\sigma_C\ \text{(original wood)}} \tag{49}$$

or other forms can be assumed. In Equation (49) g is a proportional variable, and σ_C (predicted) is defined in Equation (34). The proportional variable g can only be a function of material fracture properties and crack lengths. It is not derivable mathematically.

Although the mathematical form of g is not known, the variable g, however, can be used to improve upon the limitation imposed on the stress predicted by Equation (34), namely the failure stress of an oriented flakeboard could never be greater than that of the original solid wood. Variable g can be obtained by deduction for improving the predicted K_{IC} values of the flakeboard.

In accordance with the concept of fracture mechanics used in this study, a wood composite would only be weaker than or equivalent to its original solid wood if the original solid wood was flawless (in the previous experiment resin was shown to have no significant reinforcing effect for wood composites). However, in the EXPERIMENTAL OBSERVATION section, we observed that the wood composites could be weaker or stronger than their original solid wood. In other words, the solid wood is not flawless. Actually, most materials have some inherent flaws or defects of certain sizes. Polymeric material like polystyrene has inherent flaws calculated to be a size of 0.043 inch

(Berry 1964). While, calculations for Douglas-fir has shown inherent flaws in a range of 0.1 inch to 0.15 inch (Schniewind and Pozniak 1971, Schniewind and Lyon 1973).

To determine the proportional variable g in terms of the effect of inherent flaws in the solid wood, we need to assume a state in which an oriented flakeboard becomes equivalent to its original solid wood in terms of flaw size, flaw distribution, and fracture resistance, or a state in which the variable g is equal to one. We can assume that this state is reached if the average length of inter-flake crack ($1/\mu$, defined in Equation (45)) is equal to the average inherent flaw (Ω) in solid wood. The simplest mathematical form to depict this state is

$$g = e^{\Omega - \frac{1}{\mu}} \tag{50}$$

where e is Euler's number or the base of natural logarithm. Thus, in Equation (50), when $1/\mu = \Omega$, then $g = e^0 = 1$. Equation (49) becomes

$$\frac{K_{IC} \text{ (predicted)}}{K_{IC} \text{ (original wood)}} = 1 = \frac{K_{IC} \text{ (flakeboard)}}{K_{IC} \text{ (original wood)}} \tag{51}$$

When $1/\mu < \Omega$, then $g > 1$. Thus, g could depict the better-than-original-wood effect of wood composites. For this case, Equation (49) becomes

$$\frac{K_{IC} \text{ (predicted)}}{K_{IC} \text{ (origianl wood)}} = e^{\Omega - \frac{1}{\mu}} \tag{52}$$

In other words, σ_C (predicted) / σ_C (original wood) has been assumed to still have a value of unity although it should have been larger

than unity, because σ_C (predicted) cannot be calculated by Equation (34).

When $1/\mu > \Omega$, then $g < 1$. This negative effect could be helpful for the fact that in lower-density oriented flakeboards, the effects of cracks in the boards tend to be under-estimated by Equation (34). Equation (49) at this condition is then

$$\frac{K_{IC} \text{ (predicted)}}{K_{IC} \text{ (original wood)}} = e^{\Omega - \frac{1}{\mu}} \cdot \frac{\sigma_C \text{ (predicted)}}{\sigma_C \text{ (original wood)}} \tag{53}$$

It should be noted that at the state where the proportional variable g is equal to one, it implies another assumption--inherent flaws no longer exist in the solid-wood constituents at this state. This should be a logical assumption because proper processing conditions of appropriate pressure, resin sealing, and heat plastic flow might very well eliminate the inherent flaws in solid-wood constituents.

Summary of the Model

The establishment of the model consists of two major parts. The first part is to analytically model the effect of an expected inter-flake crack length Δc on the K_{IC} of an oriented flakeboard in terms of the effect of elongating an initial crack length c to $c+\Delta c$, thus reducing the stress σ_C needed to fail an oriented flakeboard K_{IC} specimen to a value of $\sigma_C - \Delta\sigma$. The second part is to incorporate into the model a proportional variable g, which is obtained from pure deduction in accordance with the experimental observation, to remove the limitation imposed on the model that the composite can never be

stronger than the material from which it was derived. The final model is given in terms of K_{IC} retention of original solid wood as

$$\frac{K_{IC}\ (\text{predicted})}{K_{IC}\ (\text{original wood})} = e^{\Omega - \frac{1}{\mu}} \cdot \frac{\sigma_C\ (\text{predicted})}{\sigma_C\ (\text{original wood})} \tag{54}$$

Equation (54) can also be rewritten as

$$K_{IC}\ (\text{predicted}) = e^{\Omega - \frac{1}{\mu}} \cdot \frac{\sigma_C\ (\text{predicted})}{\sigma_C\ (\text{original wood})} \cdot K_{IC}\ (\text{original wood}) \tag{55}$$

where

K_{IC} (original wood) = fracture toughness of solid wood from which the oriented flakeboard is made (obtained by Equation (32))

σ_C (original wood) = maximum normal tensile stress to failure for the original solid-wood K_{IC} specimen (obtained by experimental testing)

K_{IC} (predicted) = predicted fracture toughness of an oriented flakeboard

σ_C (predicted) = predicted maximum normal tensile stress to failure for an oriented-flakeboard K_{IC} specimen (obtained by Equation (44) and (34))

Ω = average length of inherent flaws in solid wood, for Douglas-fir it is in a range of 0.1 to 0.15 inch (Schniewind and Lyon 1973)

$\frac{1}{\mu}$ = average length of inter-flake cracks (defined in Equation (45) and obtained by experimental measurement)

IX. EXPERIMENTAL VERIFICATION

The experimental data needed to evaluate the proposed model are: 1. the average maximum stress needed to fail the original solid wood K_{IC} specimens (σ_C (original wood)); 2. the average length of inherent flaws in the original solid wood (Ω); 3. the average length of inter-flake cracks ($1/\mu$); and 4. the average length of non-cracks ($1/\lambda$). Unfortunately, the data obtained in the previous experiment are not suited for evaluation of the proposed model for the following three reasons: 1. each scanning strip for measuring the void and non-void lengths in an oriented flakeboard was obtained near the edge of each board (Figure 9), where, due to density variation throughout the board, the strip may not be representative of the entire board; 2. each frequency histogram of void or non-void length distributions given in Figure 15, 16, and 17 was collected by scanning an 8-inch measuring strip, and some strips from low-density boards contain less than ten voids on the scanning line, this may not provide enough observations for an unbiased estimation; and 3. no data was collected on non-bonded lengths for the flakeboard of the initial study, because their measurement is a destructive test (see a later section), and there was insufficient material to make this measurement due to the different design purpose of the previous experiment. Therefore, additional oriented flakeboards from which measuring strips can be sampled throughout the entire board are needed for verification of the model.

To simplify the experimental verification, we utilize two previous experimental results to verify the proposed model. First,

is the equivalence in K_{IC} values among RL, TL, TR, RT modes for an oriented flakeboard. In other words, if the TL mode fracture toughness (K_{ICTL}) of an oriented flakeboard could be found by using the proposed model, then the K_{IC} values of other modes should be equivalent. Secondly, the variations of K_{ICTL} values are smaller for the TL mode for a given solid wood or oriented flakeboard than the other modes. Thus, a fewer number of solid wood specimens would be needed to experimentally evaluate the solid wood K_{ICTL}. The solid wood K_{ICTL} value is needed to predict the value for K_{ICTL} of an oriented flakeboard (Equation (34) and (55)). Also, fewer numbers of oriented-flakeboard specimens would be needed to verify the predictions. Thus, to experimentally verify the proposed model a comparison is made of the predicted and actual K_{ICTL} values for the oriented flakeboards.

Experiment

Four oriented flakeboards (1/2 in by 12 in by 12 in) with nominal densities of 37, 40, 43, 47 lb/cu ft (based on ovendry wood weight), a resin solids spread rate of 1.35 lb/1000 sq ft, and edge-grain flakes were manufactured following the experimental procedures of the previous experiment. In order to obtain more measurements of the size of inter-flake voids and non-voids and their frequency of occurrence in each flakeboard, the cutting pattern shown in Figure 20 was used. Five 1/8-inch-thick strips from each board were used to measure the distributions of the inter-flake voids and non-voids, and five additional strips were employed to measure the non-bonded areas.

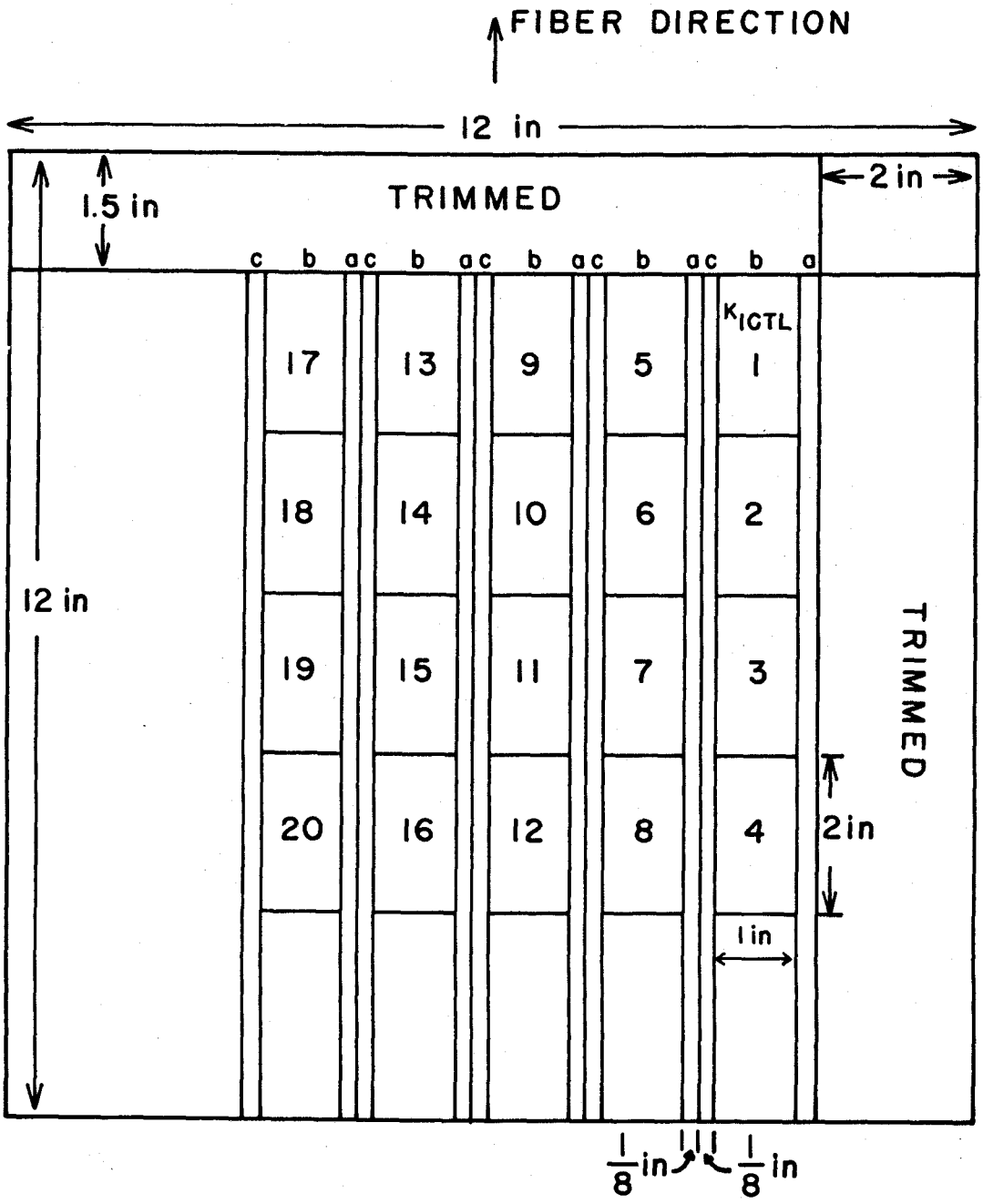

Figure 20. Oriented flakeboard cutting pattern for experimental verification, a) strips for measuring the inter-flake void and non-void lengths and their frequency of occurrence, b) K_{ICTL} specimens, and c) strips for measuring non-bonded lengths

Twenth specimens were tested for the fracture toughness of each board in the TL mode.

The frequency histograms of the inter-flake voids and non-voids for each of the four oriented flakeboards are shown in Figure 21, 22, 23, and 24. The exponential probability density functions used to fit the frequency histograms are also shown in the same graphs.

In this study, the non-bonded area is defined as the tail-part of a triangular (or rectangular) inter-flake void, where no explicit opening can be observed under the microscope and where no resin bond has been found. The method used to measure the non-bonded area was to insert the tip of an x-acto knife into a known-length triangular or rectangular inter-flake void in the 1/8-inch-thick strip. After splitting the void open by an action of twisting the x-acto knife in the void, the total length of the resin-covered area (no wood failure) was measured using a binocular microscope with a calibrated eye-piece. One thing should be noted, the twisting action of an x-acto knife could not split the inter-flake voids in the strips from the denser flakeboards. Pliers were then needed to open the voids in order to measure the resin-covered areas. The non-bonded area expressed in terms of length is thus obtained by substracting the inter-flake void length from the length of total resin-covered length on the surface plane (no resin-bond failure between flakes is assumed).

Results and Discussion

The results for inter-flake void and non-bonded length measurements are given in Table 10. The trend of a decrease in

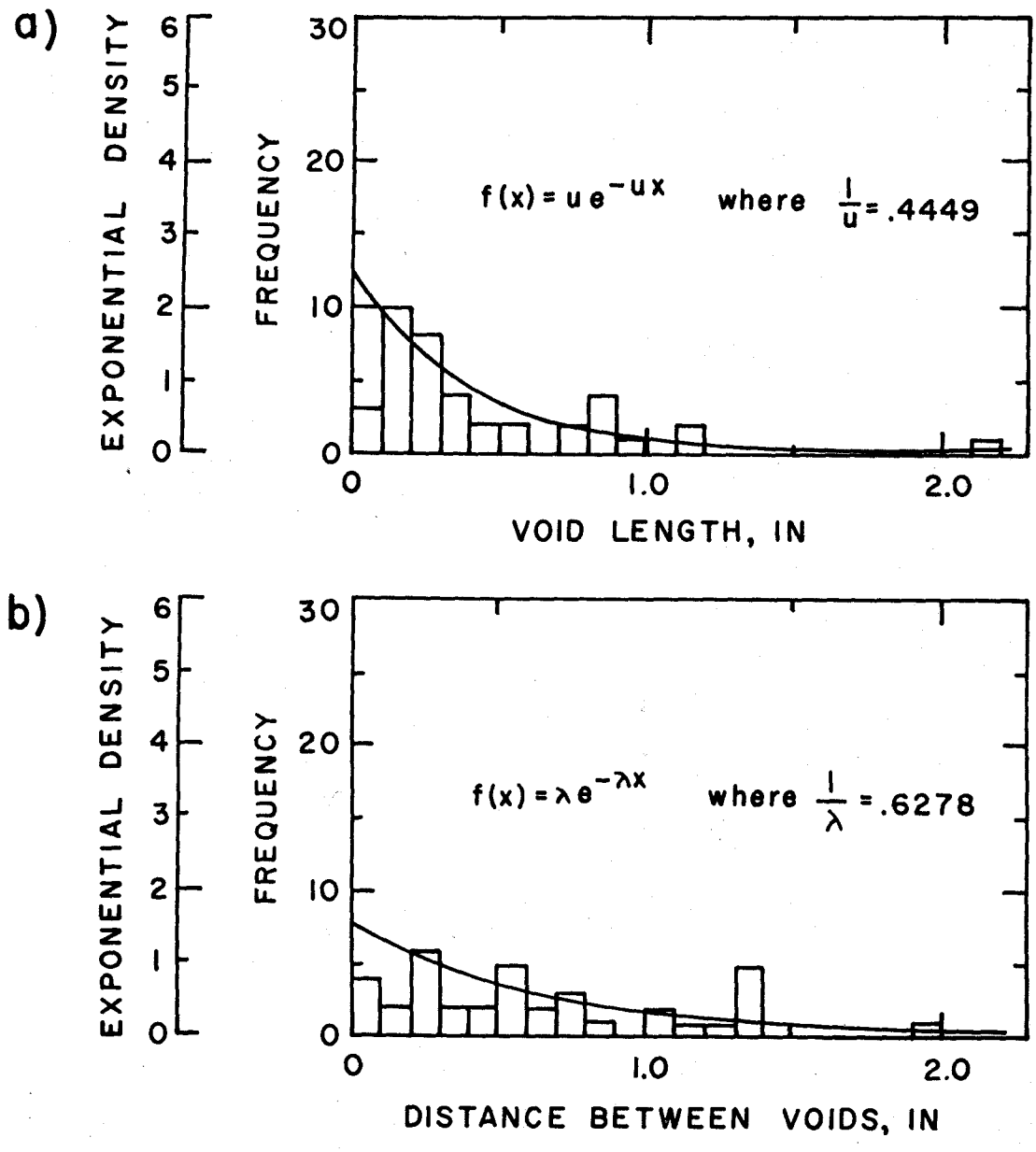

Figure 21. Frequency histogram and its exponential density function of a) inter-flake void lengths, and b) distances between voids of the 38 lb/cu ft oriented flakeboard. ($1/\mu$ = average inter-flake void length, $1/\lambda$ = average distance between voids; data are collected by measuring five 8-inch scanning strips)

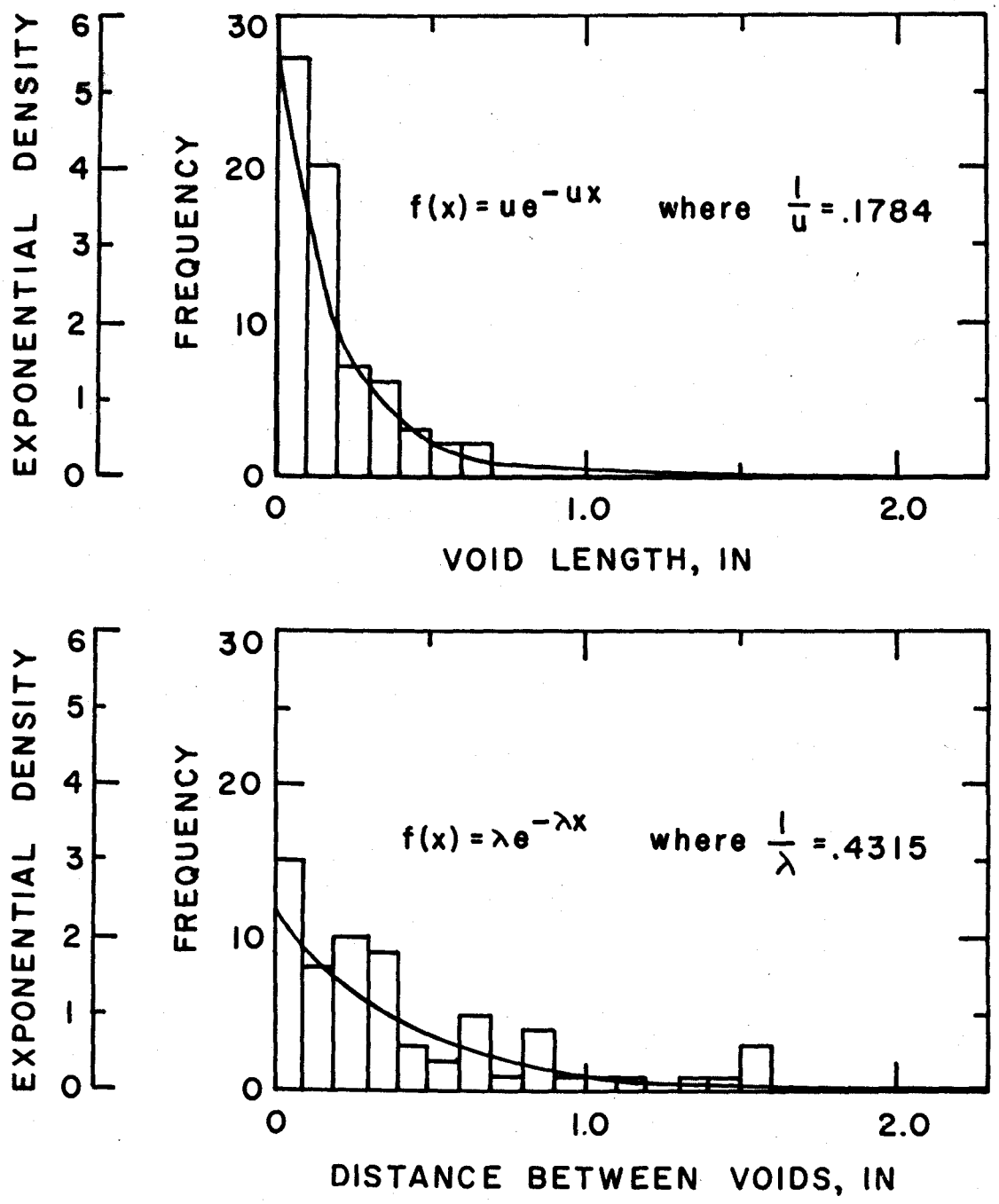

Figure 22. Frequency histogram and its exponential density function of a) inter-flake void lengths, and b) distances between voids of the 39 lb/cu ft oriented flakeboard. ($1/\mu$ = average inter-flake void length, $1/\lambda$ = average distance between voids; data are collected by measuring five 8-inch scanning strips)

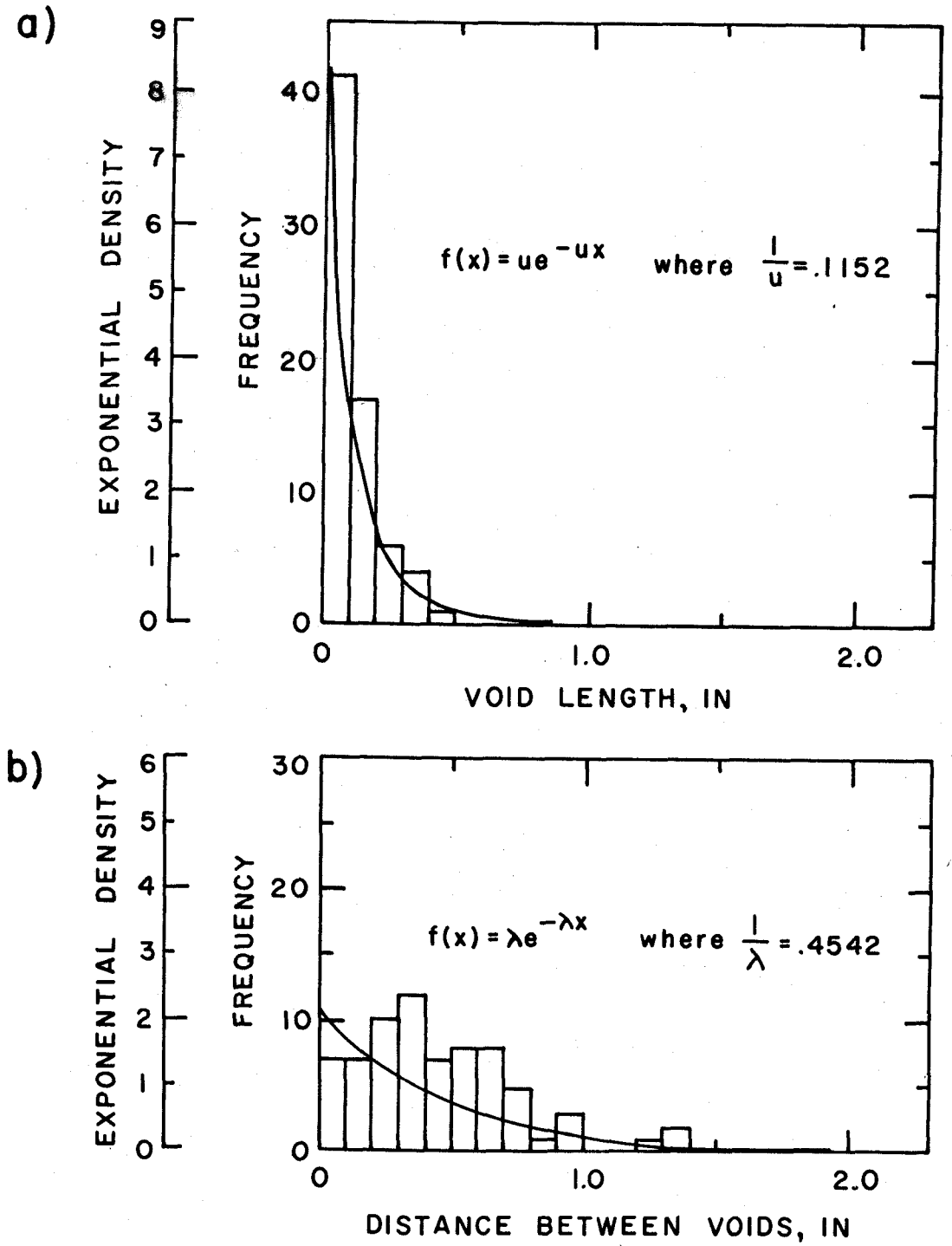

Figure 23. Frequency histogram and its exponential density function of a) inter-flake void lengths, and b) distances between voids of the 42 lb/cu ft oriented flakeboard. ($1/\mu$ = average inter-flake void length, $1/\lambda$ = average distance between voids; data are collected by measuring five 8-inch scanning strips)

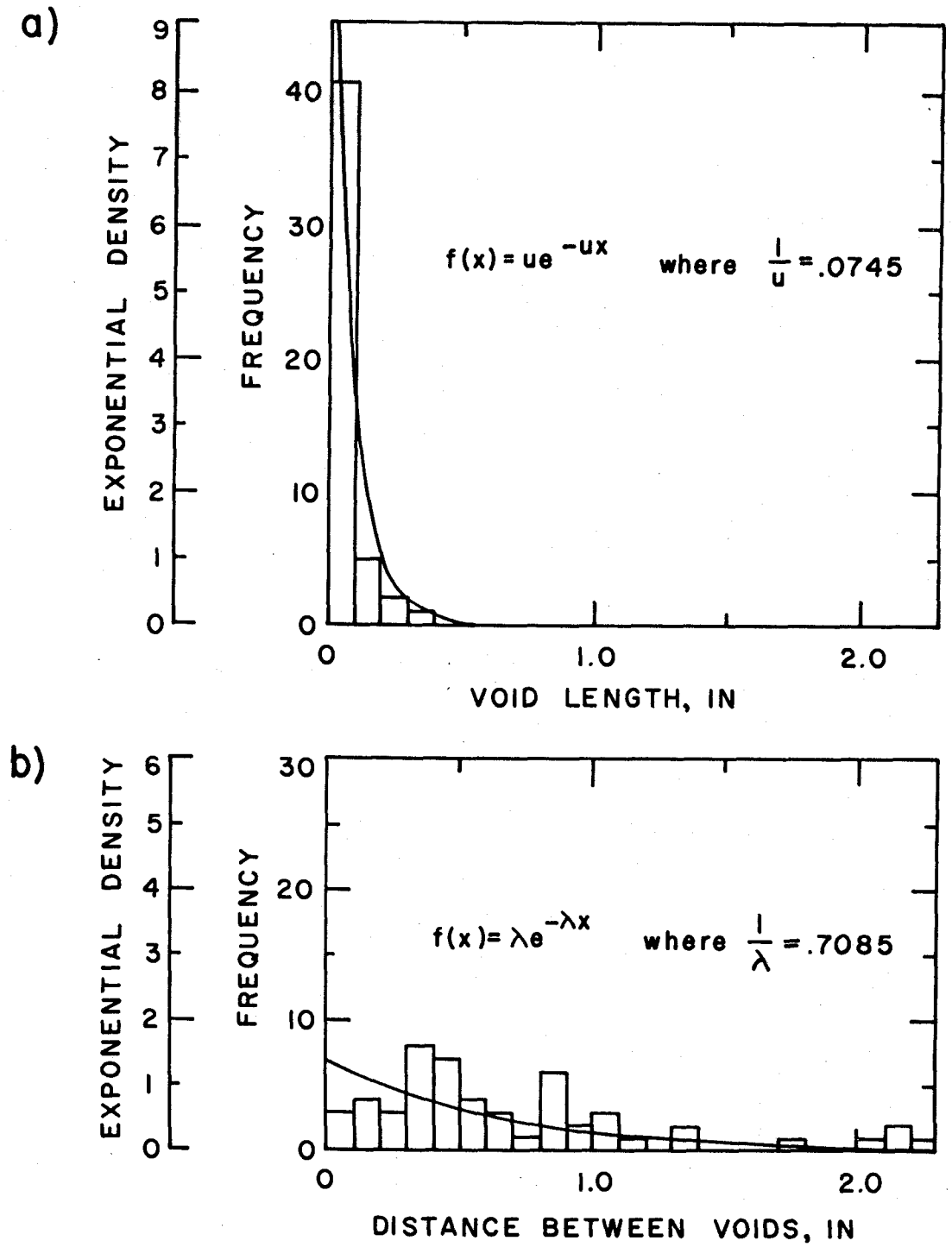

Figure 24. Frequency histogram and its exponential density function of a) inter-flake void lengths, and b) distances between voids of the 48 lb/cu ft oriented flakeboard. ($1/\mu$ = average inter-flake void length, $1/\lambda$ = average distance between voids; data are collected by measuring five 8-inch scanning strips)

Table 10. Average Inter-Flake Void Length, Average Distance Between Voids, and Relationship Between Void and Its Associated Non-Bonded Length in Four Different Densities of Oriented Flakeboard

Nominal flakeboard density[α] (lb/cu ft)	Actual flakeboard density[β] (lb/cu ft)	Average void length (in)	Average distance between voids (in)	Percent of voids without non-bonded lengths (%)	Percent of average non-bonded length to average void length (%)	Average non-bonded length (in)	Average crack length[γ] (in)
37	38.18	.4449	.6278	43.33	13.13	.0584	.5033
40	39.43	.1784	.4315	38.46	26.67	.0476	.2260
43	42.06	.1152	.4542	36.00	27.30	.0314	.1466
47	48.28	.0745	.7058	71.43	0.88	.0007	.0752

[α] Board nominal density is calculated based on oven-dried weight and volume (moisture content = 0%)

[β] Board actual density is calculated based on kiln-dried weight and volume (moisture content = 5 to 6%)

[γ] Average crack length = average void length + average non-bonded length

average inter-flake void length with an increase in board density is demonstrated in Table 10. However, one can observe a relatively big drop in average inter-flake void length between the 38.18 lb/cu ft and 39.43 lb/cu ft flakeboards, where there is only about one-pound difference in board densities. This drop in average inter-flake void length is mainly because denser flakes (37.31 lb/cu ft) were used for making the 38.18 lb/cu ft board than those (32.33 lb/cu ft) used for making the 39 lb/cu ft board (Table 11). For increased flake density, fewer flakes are needed to make a given density flakeboard, thus, due to less compaction, we can expect the occurrence of larger inter-flake voids and non-bonded areas. In other words, if an average inter-flake void length is used as an indicator of any strength property of an oriented flakeboard, then the effect of the original solid wood (or flake) density is automatically compensated for.

Among the 30 inter-flake voids measured in the scanning strips from the 38.18 lb/cu ft flakeboard, there are 13 voids without non-bonded areas. In other words, for the 38.18 lb/cu ft board, about 43 percent of the inter-flake voids could be assessed correctly as actual cracks by using non-destructive measurements with a binocular microscope (Column 5, Table 10). Whereas, the actual crack length of the rest of the voids could be measured correctly only after splitting the voids open. The actual average crack length (inter-flake void plus non-bonded length) for the 38.18 lb/cu ft flakeboard is actually 13 percent larger than the measured average inter-flake void length (see Column 6, Table 10).

Table 11. Comparison Between Actual and Predicted TL Mode Fracture Toughness (K_{ICTL}) of Oriented Flakeboards of Four Different Densities

Original solid wood				Actual oriented flakeboard			Predicted oriented flakeboard with expected void length	Predicted oriented flakeboard with expected crack length[α]
Density[β] (lb/cu ft)	Maximum tensile stress (psi)	K_{ICTL} (psi$\sqrt{in}$)	±s.d.	Density (lb/cu ft)	K_{ICTL} (psi$\sqrt{in}$)	±s.d.	K_{ICTL} (psi$\sqrt{in}$)	K_{ICTL} (psi$\sqrt{in}$)
37.31	93	294	16	38.18	126	38	139	116
32.33	82	260	20	39.43	189	36	213	190
32.33	82	260	20	42.06	206	32	240	226
33.36	96	305	13	48.28	345	42	313	313

[α] Crack length = void length + non-bonded length

[β] Solid wood density is calculated based on air-dry weight and volume (moisture content = 9 to 10%)

The percentage of average non-bonded length to average inter-flake void length given in Table 10 does not show a consistent trend with an increase in board density. Whereas, the actual non-bonded lengths become smaller with an increase in board density, shown in Column 7, Table 10.

Inherent Flaw Size in Douglas-Fir Solid Wood

In the construction of an analytical model for flakeboard we proposed a state (Equation (51)) in which the average inter-flake crack length is equal to the average inherent flaw length of original solid wood from which the flakes were derived. When this occurs, the flakeboard K_{IC} retention of original solid wood then becomes unity. Thus, the average inherent flaw size in the original solid wood can be determined by plotting the average crack length in flakeboard (Table 10) versus the flakeboard K_{IC} retention of original solid wood (calculated from Table 11), and then by locating the average crack length where the K_{IC} retention is equal to unity (100%). This procedure is done in Figure 25, allowing us to determine that the average inherent flaw length is approximately 0.1 inch for the original Douglas-fir solid wood. This value closely matches the values of inherent crack length (0.1 to 0.12 inch) calculated by Schniewind and Lyon (1973) for clear Douglas-fir solid wood, although two entirely different means are used to determine the inherent flaw length.

Accuracy of the Model

The actual and predicted TL mode fracture toughness values (K_{ICTL}) of the different densities of oriented flakeboard made for the experimental verification are shown in Table 11. The predicted K_{ICTL} values were calculated with Equation (34) and (55) by using either the expected void length, or the expected crack (void plus non-bonded) length in Equation (34). The average inherent flaw length used in these calculations (Equation (55)) was 0.1 inch as determined in Figure 25.

The accuracy of the model to determine fracture toughness (K_{IC}) of flakeboard is assessed by averaging the differences between the predicted and actual values given in Table 11. The average error for the predictions is calculated to be 12.2 percent if the expected inter-flake void length is used in Equation (34). However, the average error is only 6.9 percent if the expected inter-flake crack length is used.

Predictions by the use of the expected inter-flake crack lengths expressed in terms of K_{ICTL} retention of original solid wood (or using Equation (54)) are shown in Figure 25. Note that the K_{ICTL} retention of microlam 3 (made from 1/32-inch-thick veneers), which is considered to have inter-flake void or crack of zero length, is also incorporated into Figure 25. Again, the predicted values closely agree to the actual values.

One important thing should be noted when the size of the inter-flake void (or crack) is used as an indicator to evaluate the fracture strength of high-density flakeboard (above 50 lb/cu ft). In the press

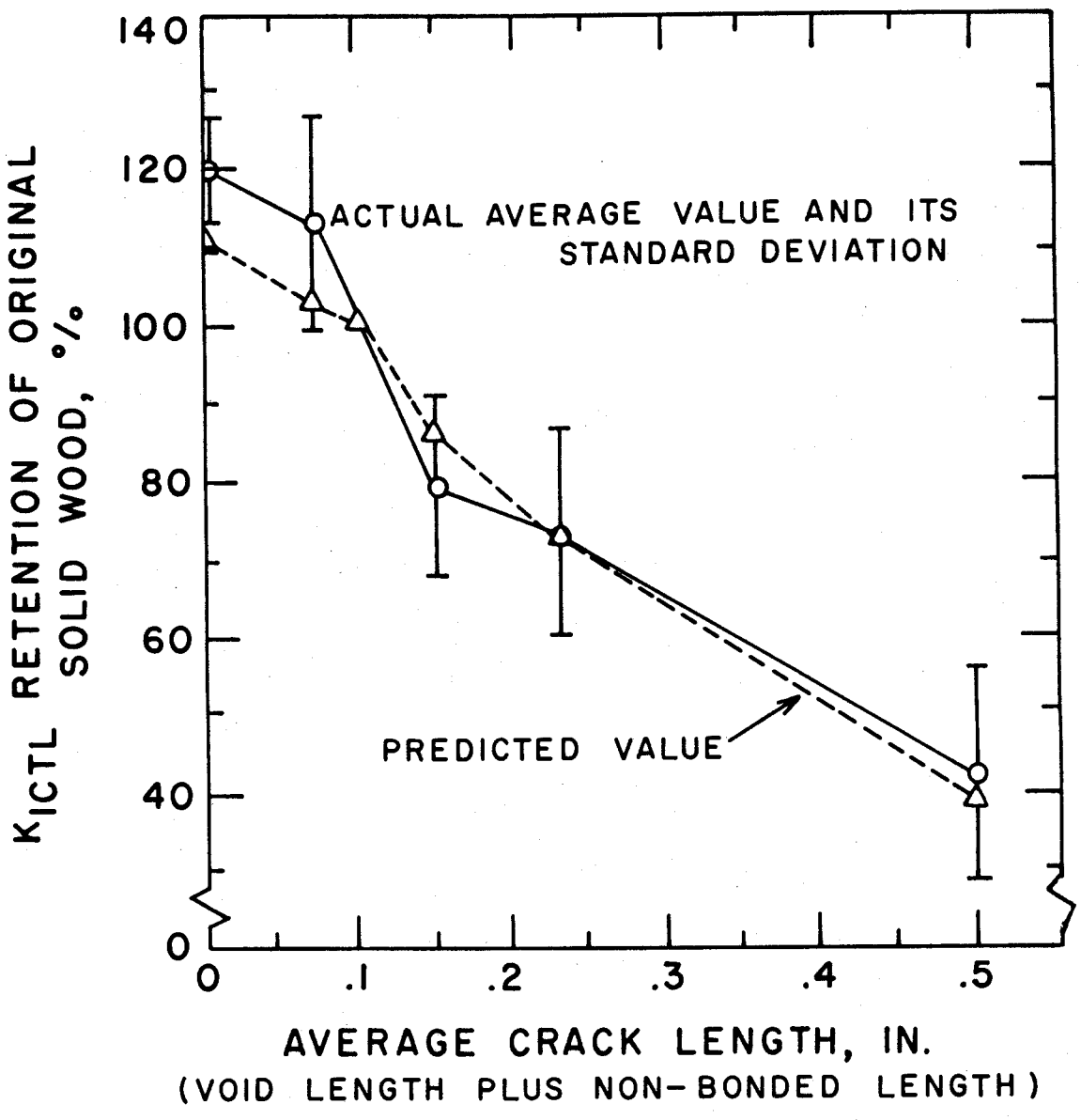

Figure 25. Comparison between the predicted and the actual fracture strength values of oriented flakeboards in terms of K_{ICTL} retention of original solid wood when plotted against average inter-flake crack lengths

cycle for consolidating a high-density flakeboard, if the closing pressure applied to the mat of staggered flakes is near the compression strength of solid wood perpendicular to grain (800 psi for Douglas-fir at 12% moisture content (Wood Handbook 1974)), cracks other than the inter-flake type might occur in the flakeboard due to high-pressure crushing. The detrimental effect of the cracks caused by crushing may offset the beneficial effect of having small inter-flake cracks in high-density boards.

Summary of the Model Verification

The purpose of constructing an analytical model in this study is to depict the effects of the process defects (inter-flake voids and non-bonded areas) in the oriented flakeboards. Once the analytical model has been verified experimentally, then the quantitative impacts of these process defects are identified. The goal is to minimize the influence of the process defects upon the intended used of the board. This can then be considered as the design criterion for specifying manufacturing conditions of oriented flakeboards or other wood composites.

The use of the proposed model as a non-destructive means to predict the K_{IC} of oriented flakeboard is a tedious task at present stage, because the task involves testing the K_{IC} of original solid wood from which the flakes were derived and measuring a large sample of void and non-void lengths. However, the use of the model can be made simplier if the following are established: 1. the average inherent flaw length, average K_{IC} value, and their variations for various wood

species; and 2. the probability relationship between measurements of void and non-void lengths for short scanning lines and entire samples. This information can then be used in conjunction with the model to estimate the K_{IC} or the allowable normal tensile stress of an oriented flakeboard (note that the allowable tensile stress can be obtained by using c = 0.75 inch and $K_{IC} = K_{IC}$ (predicted) in Equation (32)).

X. CONCLUSIONS

In addition to the summary of the experimental findings given on page 91, the following conclusions can be drawn in respect to the analytical model and the experimental verification for the K_{IC} of the oriented flakeboards. This assumes the conditions that the flakes were not severely damaged and that the resin was adequately applied.

1. The K_{IC} of oriented flakeboards are determined by the inter-flake crack length and the distance between inter-flake cracks.
2. When the TL mode fracture toughness (K_{ICTL}) of original solid wood is used as a reference point, the proposed model (Equation (55)) can be used to estimate the K_{IC} of oriented flakeboards within an error of 6.9 and 12.2 percent, respectively, for the use of the expected inter-flake crack length and the expected inter-flake void length in Equation (34).
3. The combining parameter effects of the original wood or flake density, flake dimensions, and board density on the board K_{IC} is reflected by the inter-flake void size and distance between voids in the board, which can be measured non-destructively.
4. The average size of non-bonded areas is directly related to the average size of inter-flake voids in the oriented flakeboards.
5. The concept of linear-elastic fracture mechanics has been proven to be a useful tool to analytically determine the fracture strength of oriented flakeboards.

XI. RECOMMENDATIONS

Although the proposed model can be used to estimate the fracture toughness of oriented flakeboard by predicting the K_{ICTL} of the board, the proposed model by no means depicts the entire fracture mechanism involved in board failure as a result of a tensile stress normal to the board plane. There are several areas of research that can be recommended for the purpose of further understanding the board fracture strength and of designing an optimum oriented flakeboard.

The effect of total crack length on fracture toughness (K_{IC}) is determined by Equation (32), where the coefficients of the polynomial determine the effect of total crack length. Equation (32) is constructed by the experimental compliance method (Srawley et al (1964)). Theoretically, the use of Equation (32) is not dependent on the elastic property of the specimen material (Srawley et al (1964)), but is dependent on the range of the initial crack length. It would be advantageous, however, if Equation (32) could be evaluated by applying the experimental compliance method to solid wood and wood composites.

The understanding of fracture or fracture resistance in a wood composite such as oriented flakeboard is determined by at least three factors: anatomy of the wood (wood constituents), adhesion of the wood constituents, and anatomy of the composite. The study of fracture resistance in terms of anatomical structure of wood has been done by Debaise et al (1966). However, in addition to the inherent fracture resistance of solid wood constituents, the effect of mechanical damage

on the fracture resistance of these wood constituents as a result of production is also critical. The mechanical damage effect has been demonstrated by an experiment done by Echols and Currier (1973). They used rotary-cut veneers to manufacture microlams and then tested their cleavage resistance (fracture by constant displacement). An average cleavage-resistance retention of only 45.5 percent of original solid wood was obtained for the microlams. The cause of this low retention (compared to at least 84 percent in this study) has been attributed to the effect of lathe checks in the veneers. Therefore, methods to describe the mechanical damage of wood constituents, both quantitatively and anatomically, are critically important and should be explored.

Research projects to be done in terms of fracture resistance on the various aspects of the adhesion of wood constituents are numerous. The determination of the relative fracture resistance for the resin layer, resin-wood interphase, and wood constituent are some of them. One should note that the resin spread rate in flakeboard products is usually much lighter than that in plywood. The resin layer between flakes is most likely to be spotty instead of a continuous thick layer. Thus, the effect of resin penetration and wetting which influence the proportions or distributions of the resin layer, the joint-wood interphase and the wood ahead of a crack-front, should also be different in flakeboard than in plywood. The research on the adhesion effect discussed above, together with the research on the anatomy of crack paths in flakeboard should provide information for designing crack arresters in flakeboard to improve fracture strength.

Crack propagation for most materials begins at a low and stable speed. After traveling a given short distance (Δc), the crack-extension force reaches its critical value, then the crack propagates spontaneously. In the given distance (Δc) where the stable crack propagates, the amount of energy consumed is dependent upon the area of the new surface generated. If within a given Δc there exist inherent micro-flaws in the crack propagation path, less energy or a smaller magnitude of applied load is needed to fracture a given material. These micro-flaws should easily occur in the high-density flakeboard which experiences a high consolidating pressure, crushing the wood cells. If this hypothesis is tested by finding Δc and then verified anatomically, it will help to determine the optimum density for an oriented flakeboard.

In this exploratory study of the application of linear-elastic fracture mechanics to explain the fracture strength of oriented flakeboard, clear, straight grain, old-growth Douglas-fir lumber has been used to manufacture the composite products. K_{IC} specimens of exact grain orientation can then be obtained to evaluate four different modes of fracture strength of these composite products. The highlight of this study is, however, at the establishment of an analytical model which exhibits the effect of processing defects (inter-flake voids and non-bonded areas) on the fracture strength of oriented flakeboards, and at the experimental verification of the proposed model. The eventual goal of this type of research is to provide the necessary information to design engineered wood composites from low-grade wood resources. One should realize that it would be difficult to have

perfect grain orientation in the flakes produced from low-grade or fast-growth trees. Therefore, systematical experimental studies on the fracture toughness of flakeboards made from flakes of various grain orientation (flat-grain, edge-grain, and those inbetween) are necessary. However, the analytical effect of the inter-flake void and non-bonded area established in this study is still valid.

The prerequisite of making an oriented flakeboard of optimum density and K_{IC} is that the flakes are not severely damaged, are properly covered by resin, and are distributed uniformly throughout the mat. The flake dimensions of 2 in by 11/16 in by 1/32 in used in this study are quite proper. A decrease in flake thickness could reduce the inter-flake void size but might increase the chance of damaging the flakes and also increase the resin consumptions. However, if the flakes could be produced in such a way that their two ends are properly tapered, then for flakes of a given dimension the inter-flake void sizes in the board should be reduced.

BIBLIOGRAPHY

American Society for Testing and Materials. 1974. Standard method of test for plane-strain fracture toughness of metallic materials. ASTM Desig. E399-74.

American Society for Testing and Materials. 1977. Standard methods of evaluating the properties of wood-base fiber and particle panel materials. ASTM Desig. D1037-72.

Atack, D., W.D. May, E.L. Morris, and R.N. Sproule. 1961. The energy of tensile and cleavage fracture of black spruce. Tappi 44(8): 555-567.

Berry, J.P. 1964. Fracture processes in polymeric solids. In brittle behavior of polymeric solids. ed. B. Rosen. Interscience, 195, New York.

Broek, D. 1977. Elementary engineering fracture mechanics. Noordhoff International Publishing, the Netherlands.

Brown, W.F., and J.E. Srawley. 1966. Plane strain crack toughness testing of high strength metallic materials. ASTM Spec. Tech. Publ. 410.

Brumbaugh, J. 1960. Effect of flake dimensions on properties of particle boards. For. Prod. J. 10(5): 243-246.

Bryan, E.L. 1962. Maximum strength properties for particleboard. For. Prod. J. 12(2): 59-64.

Debaise, G.R., A.W. Porter, and R.E. Pentoney. 1966. Morphology and mechanics of wood fracture. Material Research & Standards 6(10): 493-499.

Dietz, A.G.H. 1971. Composite materials: a general overview. In theory and design of wood and fiber composite materials. ed. B.A. Jayne. Syracuse University Press, 1972.

Dixon, W.J., and F.J. Massey, Jr. 1969. Introduction to statistical analysis. McGraw-Hill, New York.

Echols, R.M., and R.A. Currier. 1973. Comparative properties of Douglas-fir boards made from parallel-laminated veneers vs. solid wood. For. Prod. J. 23(2): 45-47.

Garg, S.K., V. Svalbonas, and G.A. Gurtman. 1973. Analysis of structural composite materials. Marcel Dekker, Inc., New York.

Hanrahan, F.J. 1966. Radial stresses in curved rectangular glue-laminated members. Building Standards Monthly, July 1966: 13-16.

Hunt, M.O. 1970. The prediction of the elastic constants of particleboard by means of a structural analogy. Ph.D. Thesis, Dept. of Wood and Paper Science, N.C. State Univ. at Raleigh.

Irwin, G.R. 1960. Fracture mechanics in structural mechanics. ed. J.N. Goodier and N.J. Hoff. Pergamon Press, New York.

Irwin, G.R. 1962. Analytical aspects of crack stress field problems. T. & A. M. Report 213. Univ. of Illinois, Urbana, Ill.

Johnson, J.A. 1973. Crack initiation in wood plates. Wood Science 6(2): 151-158.

Jones, R.M. 1975. Mechanics of composite materials. Scripta Book Company, Washington, D.C.

Karlin, S., and H.M. Taylor. 1975. A first course in stochastic processes. Academic Press, New York.

Kelly, M.W. 1977. Critical literature review of relationships between processing parameters and physical properties of particleboard. USDA For. Serv. Gen. Tech. Rep. FRL-10.

Keylwerth, R. 1958. Zur Mechanik der mehrschichtigen Spanplatte. (On the mechanics of the multilayer particleboard.) Holz als Roh- und Werkstoff 16: 419-430.

Komatsu, K., H. Sasaki, and T. Maku. 1974. Evaluation of fracture toughness for wood-epoxy adhesive system under external shear force. Wood Research No.57: 10-22.

Komatsu, K., H. Sasaki, and T. Maku. 1976. Application of fracture mechanics to strength analysis of glued lap joints. Wood Research No.61: 11-24.

Kusian, R. 1968. Modell-Untersuchungen uber den Einfluss des Spanformats auf Struktur- und Festigkeitseigenschaften von Spanwerkstoffen. Holztechnologie 9(1968)3: 189-196.

Larmore, F.D. 1959. Influence of specific gravity and resin content on properties of particle board. For. Prod. J. 9(4): 131-134.

Lawn, B.R., and T.R. Wilshaw. 1975. Fracture of brittle solids. Cambridge University Press, Cambridge, London.

Lehmann, W.F. 1970. Resin efficiency in particleboard as influenced by density, atomization, and resin content. For. Prod. J. 20(11): 48-54.

Lehmann, W.F. 1974. Properties of structural particleboards. For. Prod. J. 24(1): 19-26.

Mai, Y.W. 1975. On the velocity-dependent fracture toughness of wood. Wood Science 8(1): 364-367.

McKean, H.B., J.D. Snodgrass, and R.J. Saunders. 1975. Commercial development of composite plywood. For. Prod. J. 25(9): 63-68.

Mindess, S., J.S. Nadeau, and J.D. Barrett. 1975. Slow crack growth in Douglas-fir. Wood Science 8(1): 389-396.

Mindess, S., J.S. Nadeau, and J.D. Barrett. 1976. Effect of constant deformation rate on the strength perpendicular to the grain of Douglas-fir. Wood Science 8(4): 262-266.

Morrison, D.F. 1967. Multivariate statistical methods. McGraw-Hill Book Company, New York.

Moslemi, A.A. 1974. Particleboard. Vol. I and Vol. II. Southern Illinois University Press, Carbondale, Illinois.

National Design Specification for Stress-Grade Lumber and Its Fastening. 1973. National Forest Products Association, Washington, D.C.

Paris, P.C., and C.M. Sih. 1965. Stress analysis of cracks. In fracture toughness testing and its applications. ASTM Spec. Tech. Publ. 381.

Perkins, R.W. 1967. Fundamental concepts concerning mechanics of wood deformation: strength and plastic behavior of wood. For. Prod. J. 17(4): 57-68.

Plath, E. 1971. Beitrag zur Mechanik der Holzspanplatten. (A contribution on particleboard mechanics.) Holz als Roh- und Werkstoff 29: 377-382.

Porter, A.W. 1964. On the mechanics of fracture in wood. For. Prod. J. 14(8): 325-331.

Post, P.W. 1958. Effect of particle geometry and resin content on bending strength of oak flake board. For. Prod. J. 8(10): 317-322.

Post, P.W. 1961. Relationship of flake size and resin content to mechanical and dimensional properties of flake board. For. Prod. J. 11(1): 34-37.

Rackwitz, G. 1963. Der Einfluss der Spanabmessungen auf einige Eigenschaften von Holzspanplatten. (Influence of chip dimensions on some properties of wood particleboard.) Holz als Roh- und Werkstoff 21: 200-209.

Schniewind, A.P., and J.C. Centeno. 1973. Fracture toughness and duration of load factor I. six principal systems of crack propagation and the duration factor for cracks propagating parallel to grain. Wood and Fiber 5(2): 152-159.

Schniewind, A.P., and D.E. Lyon. 1973. A fracture mechanics approach to the tensile strength perpendicular to grain of dimension lumber. Wood Science and Technology Vol. 7: 45-59.

Schniewind, A.P., and R.A. Pozniak. 1971. On the fracture toughness of Douglas fir wood. Engineering Fracture Mechanics Vol. 2: 223-233.

Srawley, J.E., M.H. Jones, and B. Gross. 1964. Experimental determination of the dependence of crack extention force on crack length for a single-edge-notch tension specimen. NASA TN D-2396.

Stayton, C.L., M.J. Hyvarinen, R.O. Gertjejansen, and J.G. Haygreen. 1971. Aspen and paper birch mixtures as raw material for particleboard. For. Prod. J. 21(12): 29-30.

Suchsland, O. 1960. An analysis of a two-species three-layer wood flake board. Michigan Quarterly Bulletin 43(2): 375-393, East Lansing.

Timoshenko, S.P. 1953. History of strength of materials. McGraw-Hill Book Company, Inc., New York.

Tomin, M. 1972. Influence of anisotropy on fracture toughness of wood. Wood Science 5(2): 118-121.

Tsai, S.W. 1966. Mechanics of composite materials. Air Force Materials Laboratory Technical Report AFML-TR-66-149, part 1. U.S. Air Force, Dayton, Ohio.

Turner, H.D. 1954. Effect of particle size and shape on strength and dimensional stability of resin-bonded wood-particle panels. J. of the For. Prod. Res. Soc. 4(5): 210-223.

Vinson, J.R., and T.W. Chou. 1975. Composite materials and their use in structures. John Wiley & Sons, Inc., New York.

White, M.S. 1977. Influence of resin penetration on the fracture toughness of wood adhesive bonds. Wood Science 10(1): 6-14.

White, M.S., G. Ifju, and J.A. Johnson. 1976. Resin penetration--a factor affecting fracture toughness of wood-adhesive joints. Anon. 1976, Proceedings of the Second International Conference on Mechanical Behavior of Materials.

Wood Handbook. 1974. USDA For. Serv. FPL.

Wu, E.M. 1963. Application of fracture mechanics to orthotropic plates. T. & A. M. Report 248. Univ. of Illinois, Urbana.

Wu, E.M. 1967. Application of fracture mechanics to anisotropic plates. J. of Applied Mechanics, Trans. ASME: 967-974.

APPENDICES

APPENDIX A

Models and Test Statistics for Multivariate Analysis of Variance

The use of multivariate analysis of variance in this study is to simultaneously test the equivalence either between two groups of specimens or among three or more groups of specimens in their RL, TL, TR, RT mode fracture toughness (K_{IC}) values.

The model used in testing between two groups of specimens is

$$[A] = [D]\,[B]$$

or

$$\begin{bmatrix} RL_1 & TL_1 & TR_1 & RT_1 \\ RL_2 & TL_2 & TR_2 & RT_2 \end{bmatrix} = \begin{bmatrix} 1 & 1 \\ 1 & 0 \end{bmatrix} \begin{bmatrix} B_{10} & B_{20} & B_{30} & B_{40} \\ B_{11} & B_{21} & B_{31} & B_{41} \end{bmatrix}$$

$$= \begin{bmatrix} B_{10}+B_{11} & B_{20}+B_{21} & B_{30}+B_{31} & B_{40}+B_{41} \\ B_{10} & B_{20} & B_{30} & B_{40} \end{bmatrix}$$

with the null hypothesis

$$H_0: \begin{bmatrix} B_{11} \\ B_{21} \\ B_{31} \\ B_{41} \end{bmatrix} = \begin{bmatrix} 0 \\ 0 \\ 0 \\ 0 \end{bmatrix}$$

and its alternative hypothesis is

$$H_1: \begin{bmatrix} B_{11} \\ B_{21} \\ B_{31} \\ B_{41} \end{bmatrix} \neq \begin{bmatrix} 0 \\ 0 \\ 0 \\ 0 \end{bmatrix}$$

For an α - level test of H_0, the acceptance region is

$$F_\alpha(p,(N-r) - (p-1)) < \frac{1-\Lambda}{\Lambda} \cdot \frac{(N-r) - (p-1)}{p}$$

where

p = number of columns in matrix A

N = number of specimens in each column of matrix A (N is assumed to be equal for every column of matrix A. If any missing data occurs, a special treatment will be automatically adopted by SIPS.)

r = number of columns of matrix D

$\Lambda = \frac{1}{\prod_{i=1} (\lambda_i + 1)}$; where λ_i = eigan values

The model used in testing among three groups of specimens is

$$[A] = [D]\ [B]$$

or

$$\begin{bmatrix} RL_1 & TL_1 & TR_1 & RT_1 \\ RL_2 & TL_2 & TR_2 & RT_2 \\ RL_3 & TL_3 & TR_3 & RT_3 \end{bmatrix} = \begin{bmatrix} 1 & 1 & 0 \\ 1 & 0 & 1 \\ 1 & 0 & 0 \end{bmatrix} \begin{bmatrix} B_{10} & B_{20} & B_{30} & B_{40} \\ B_{11} & B_{21} & B_{31} & B_{41} \\ B_{12} & B_{22} & B_{32} & B_{42} \end{bmatrix}$$

$$= \begin{bmatrix} B_{10}+B_{11} & B_{20}+B_{21} & B_{30}+B_{31} & B_{40}+B_{41} \\ B_{10}+B_{12} & B_{20}+B_{22} & B_{30}+B_{32} & B_{40}+B_{42} \\ B_{10} & B_{20} & B_{30} & B_{40} \end{bmatrix}$$

The test statistic given by the subsystem command MANOVA of SIPS is to be compared with the value x;s,m,n in the multivariate statistical chart (Morrison 1967 P.312-319). For an α - level test of H_0, the acceptance region is

test statistic < x;s,m,n

where

$s = \min(g,p)$

$m = \frac{|g-p| - 1}{2}$

$n = \frac{N-r-p-1}{2}$

g = (number of columns in matrix D) - 1

p = number of columns in matrix A

N = number of specimens in each column of matrix A

r = number of columns in matrix D

The model for comparing more than three groups of specimens is similarly constructed.

A1. Test the equivalence of K_{IC} values among 11 pieces of lumber

test statistic = 0.867

$x_{.01};2,0.5,29 = 0.260$

reject H_0 at the 1% level

A2. Test the equivalence of K_{IC} values of solid wood between specimens tested at loading speeds of 0.1 cm/min and 0.01 cm/min

test statistic = 2.850

$F_{.05}(4,15) = 3.060$

accept H_0 at the 5% level

A3. Test the equivalence of K_{IC} values between microlam 1 and its original solid wood

test statistic = 4.260

$F_{.05}(4,11) = 3.360$

$F_{.01}(4,11) = 5.670$

accept H_0 at the 5% level

reject H_0 at the 1% level

A4. Test the equivalence of K_{IC} values between microlam 2 and its original solid wood

test statistic = 3.930

$F_{.05}(4,11) = 3.360$

$F_{.01}(4,11) = 5.670$

accept H_0 at the 5% level

reject H_0 at the 1% level

A5. Test the equivalence of K_{IC} values between microlam 3 and its original solid wood

test statistic = 20.790

$F_{.01}(4,11) = 5.670$

reject H_0 at the 1% level

A6. Test the equivalence of K_{IC} retention of original solid wood among microlam 1, microlam 2, microlam 3

test statistic = 0.832

$x_{.01};2,0.5,11 = 0.525$

reject H_0 at the 1% level

A7. Test the equivalence of K_{IC} values of microlam 1 between specimens tested at loading speeds of 0.1 cm/min and 0.01 cm/min

test statistic = 0.805

$F_{.05}(4,15) = 3.060$

accept H_0 at the 5% level

A8. Test the equivalence of K_{IC} values of microlam 2 between specimens tested at loading speeds of 0.1 cm/min and 0.01 cm/min

test statistic = 1.394

$F_{.05}(4,15) = 3.060$

accept H_0 at the 5% level

A9. Test the equivalence of K_{IC} values of microlam 3 between specimens tested at loading speeds of 0.1 cm/min and 0.01 cm/min

test statistic = 4.311

$F_{.05}(4,15) = 3.060$

$F_{.01}(4,15) = 4.890$

accept H_0 at the 5% level

reject H_0 at the 1% level

A10. Test the equivalence of K_{IC} retention of original solid wood among flakeboard 1a, 2a, 3a

test statistic = 0.988

$x_{.01};2,0.5,6.5 = 0.640$

reject H_0 at the 1% level

A11. Test the equivalence of K_{IC} retention of original solid wood between flakeboard 1a and flakeboard 2a

test statistic = 148.310

$F_{.01}(4,9) = 6.420$

reject H_0 at the 1% level

A12. Test the equivalence of K_{IC} retention of original solid wood between flakeboard 2a and flakeboard 3a

test statistic = 3.990

$F_{.05}(4,9) = 3.630$

$F_{.01}(4,9) = 6.420$

accept H_0 at the 5% level

reject H_0 at the 1% level

A13. Test the equivalence of K_{IC} retention of original solid wood among flakeboard 1a, 1b, 1c

test statistic = 0.507

$x_{.05};2,0.5,6.5 = 0.540$

accept H_0 at the 5% level

A14. Test the equivalence of K_{IC} retention of original solid wood among flakeboard 2a, 2b, 2c

test statistic = 0.736

$x_{.01};2,0.5,6.5 = 0.640$

reject H_0 at the 1% level

A15. Test the equivalence of K_{IC} retention of original solid wood between flakeboard 2a and flakeboard 2b

test statistic = 6.641

$F_{.01}(4,9) = 6.420$

reject H_0 at the 1% level

A16. Test the equivalence of K_{IC} retention of original solid wood between flakeboard 2b and flakeboard 2c

test statistic = 10.630

$F_{.01}(4,9) = 6.420$

reject H_0 at the 1% level

A17. Test the equivalence of K_{IC} retention of original solid wood between flakeboard 2a and flakeboard 2c

test statistic = 1.300

$F_{.05}(4,9) = 3.630$

accept H_0 at the 5% level

A18. Test the equivalence of K_{IC} values of flakeboard 1a between specimens tested at loading speeds of 0.1 cm/min and 0.01 cm/min

test statistic = 0.170

$F_{.05}(4,9) = 3.630$

accept H_0 at the 5% level

A19. Test the equivalence of K_{IC} values of flakeboard 1b between specimens tested at loading speeds of 0.1 cm/min and 0.01 cm/min

test statistic = 0.744

$F_{.05}(4,9) = 3.630$

accept H_0 at the 5% level

A20. Test the equivalence of K_{IC} values of flakeboard 1c between specimens tested at loading speeds of 0.1 cm/min and 0.01 cm/min

test statistic = 2.430

$F_{.05}(4,9) = 3.630$

accept H_0 at the 5% level

A21. Test the equivalence of K_{IC} values of flakeboard 2a between specimens tested at loading speeds of 0.1 cm/min and 0.01 cm/min

test statistic = 1.753

$F_{.05}(4,9) = 3.630$

accept H_0 at the 5% level

A22. Test the equivalence of K_{IC} values of flakeboard 2b between specimens tested at loading speeds of 0.1 cm/min and 0.01 cm/min

test statistic = 3.276

$F_{.05}(4,9) = 3.630$

accept H_0 at the 5% level

A23. Test the equivalence of K_{IC} values of flakeboard 2c between specimens tested at loading speeds of 0.1 cm/min and 0.01 cm/min

test statistic = 1.901

$F_{.05}(4,9) = 3.630$

accept H_0 at the 5% level

A24. Test the equivalence of K_{IC} values of flakeboard 3a between specimens tested at loading speeds of 0.1 cm/min and 0.01 cm/min

test statistic = 9.280

$F_{.01}(4,9) = 6.420$

reject H_0 at the 1% level

APPENDIX B

One-Way Classification Analysis of Variance and Test Statistics

Null hypotheses H_0: the tested variables are equivalent

B1. Test the equivalence of K_{IC} values of solid wood among RL, TL, TR, RT modes by pooling 11 lumber together

test statistic = 64.504

$F_{.01}(3,260) = 3.780$

reject H_0 at the 1% level

B2. Test the equivalence of K_{IC} values of solid wood among RL, TR, RT modes by pooling 11 lumber together

test statistic = 6.519

$F_{.01}(2,195) = 4.610$

reject H_0 at the 1% level

B3. Test the equivalence of K_{IC} values of solid wood between RL and TR modes by pooling 11 lumber together

test statistic = 14.626

$F_{.01}(1,130) = 6.630$

reject H_0 at the 1% level

B4. Test the equivalence of K_{IC} values of solid wood between RL and RT modes by pooling 11 lumber together

test statistic = 6.350

$F_{.01}(1,130) = 6.630$

$F_{.05}(1,130) = 3.840$

accept H_0 at the 5% level

reject H_0 at the 1% level

B5. Test the equivalence of K_{IC} values of solid wood between TR and RT modes by pooling 11 lumber together

test statistic = 0.822

$F_{.05}(1,130) = 3.840$

accept H_0 at the 5% level

B6. Test the equivalence of K_{IC} values among RL, TL, TR, RT modes of microlam 1

test statistic = 11.636

$F_{.01}(3,36) = 5.390$

reject H_0 at the 1% level

B7. Test the equivalence of K_{IC} values among RL, TL, TR, RT modes of microlam 2

test statistic = 9.340

$F_{.01}(3,36) = 5.390$

reject H_0 at the 1% level

B8. Test the equivalence of K_{IC} values among RL, TL, TR, RT modes of microlam 3

test statistic = 1.232

$F_{.05}(3,36) = 2.920$

accept H_0 at the 5% level

B9. Test the equivalence of K_{IC} values among RL, TL TR, RT modes of flakeboard 1a

test statistic = 2.124

$F_{.05}(3,24) = 3.010$

accept H_0 at the 5% level

B10. Test the equivalence of K_{IC} values among RL, TL, TR, RT modes of flakeboard 1b

test statistic = 3.830

$F_{.05}(3,24) = 3.010$

$F_{.01}(3,24) = 4.720$

accept H_0 at the 5% level

reject H_0 at the 1% level

B11. Test the equivalence of K_{IC} values among RL, TL, TR, RT modes of flakeboard 1c

test statistic = 0.517

$F_{.05}(3,24) = 3.010$

accept H_0 at the 5% level

B12. Test the equivalence of K_{IC} values among RL, TL, TR, RT modes of flakeboard 2a

test statistic = 0.412

$F_{.05}(3,24) = 3.010$

accept H_0 at the 5% level

B13. Test the equivalence of K_{IC} values among RL, TL, TR, RT modes of flakeboard 2b

test statistic = 0.450

$F_{.05}(3,24) = 3.010$

accept H_0 at the 5% level

B14. Test the equivalence of K_{IC} values among RL, TL, TR, RT modes of flakeboard 2c

test statistic = 1.976

$F_{.05}(3,24) = 3.010$

accept H_0 at the 5% level

APPENDIX C

Multiple Linear Regression Models and Nonlinear Models for the Flakeboard K_{ICTL} Retention of Original Solid Wood

Two things should be noted in regard to the construction of the regression models in this appendix. First, the board density value was obtained from each K_{ICTL} test specimen (or seven measurements per board), whereas the values of average void length and resin solids spread rate were only the average per board. Thus, if a definite relationship exists between dependent and independent variables, the regression model with the higher correlation coefficient (R) value might be easier to establish for the former one than for the latter two. Second, the nonlinear models used to fit the scatter data are in a sequence of exponential functions, and quadratic and cubic polynomials. However, one condition has been imposed to the nonlinear models presented with the scatter data. This condition is that the lower-order model is adopted if the higher-order model does not improve the R value by more than 0.03.

C1. Stepwise multiple linear regression models for board K_{ICTL} retention (%) of original solid wood (microlam 3 included), and corresponding R values

Step	Model for board K_{ICTL} retention (%)	R
1	103.01 - 140.23V	.77
2	109.73 - 552.86V + 4.41DRV	.95
3	128.92 - 634.07V + 5.34DRV - .27DR	.96
4	142.17 - 637.67V + 5.38DRV - .21DR - .40D	.96

5	267.21 - 655.67V + 6.04DRV + 1.67DR - 3.13D - 87.05R	.96
6	291.62 - 478.09V + 6.15DRV + 2.25DR - 3.72D - 110.19R - 5.15DV	.96
7	297.50 - 547.98V + 5.30DRV + 2.34DR - 3.87D - 113.62R - 3.87DV + 30.89RV	.96

Degree of freedom (source) = 57

Units = D (lb/cu ft), R (lb/1000 sq ft), V (in)

C2. Scatter data of board K_{ICTL} retention (%) versus average void length V (microlam 3 included), and the fitted nonlinear regression model

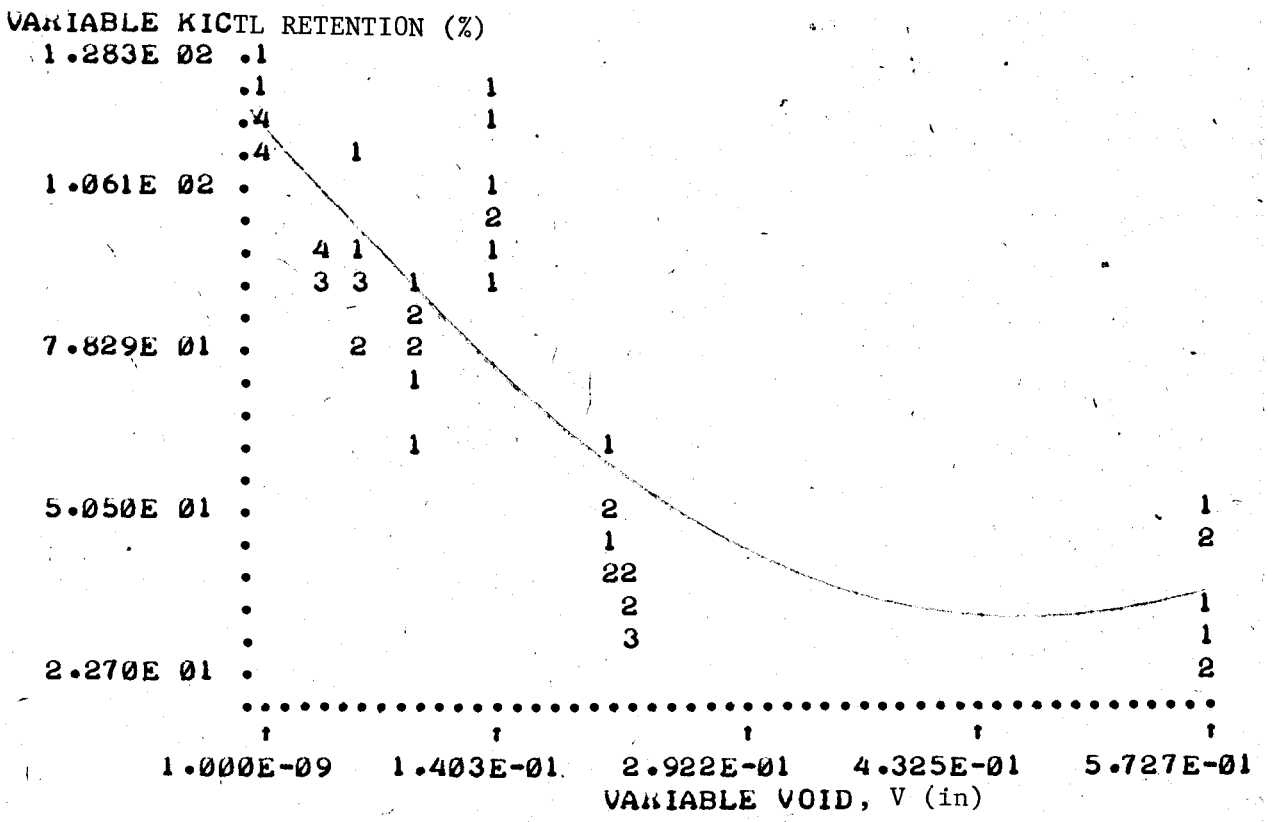

Regression model for K_{ICTL} retention (%) = 118.6 - 378.65V + $407.09V^2$

R = .86

C3. Scatter data of board K_{ICTL} retention (%) versus board density D (microlam 3 included), and the fitted nonlinear regression model

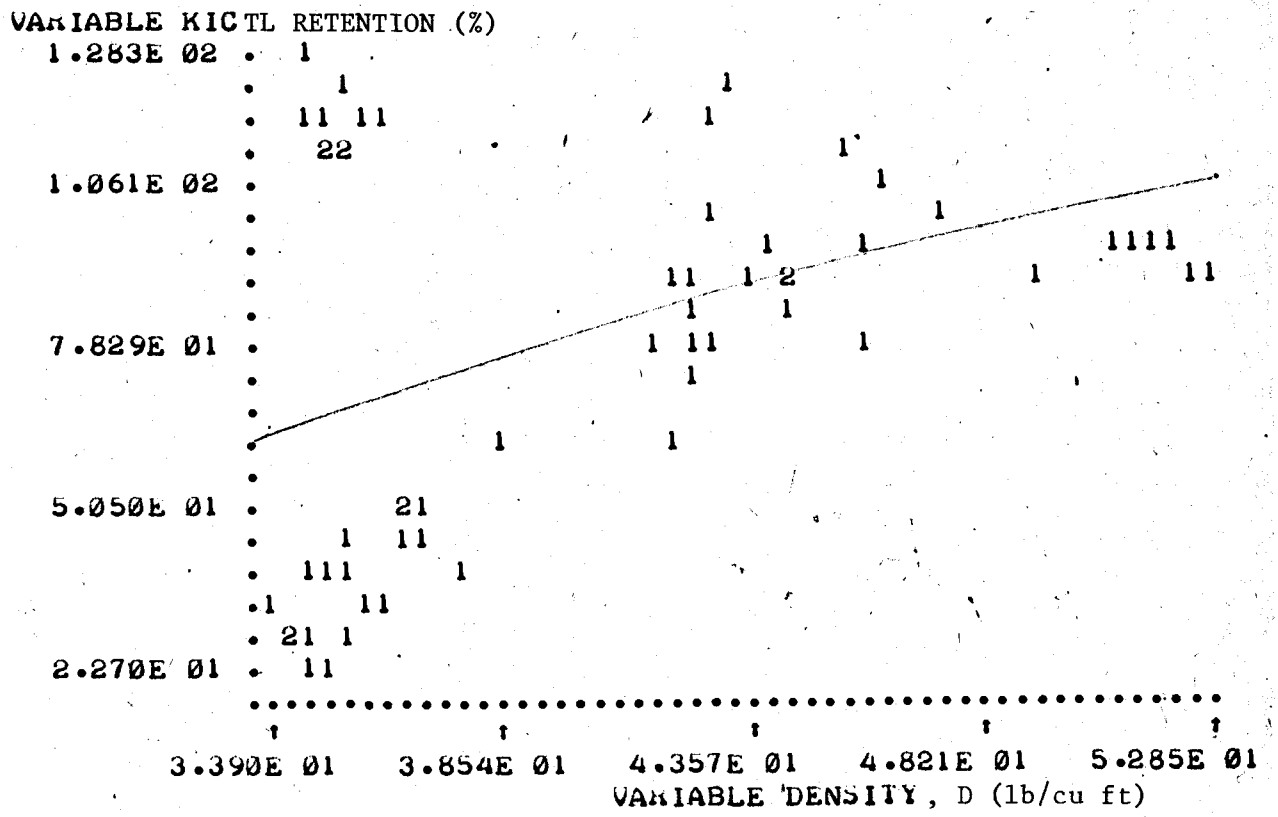

Regression model for K_{ICTL} retention (%) = -271.49 + 95.28 ln(D)

R = .40

C4. Scatter data of board K_{ICTL} retention (%) versus average void length V (microlam 3 included; void length data sampled according to Figure 20), and the fitted nonlinear regression model

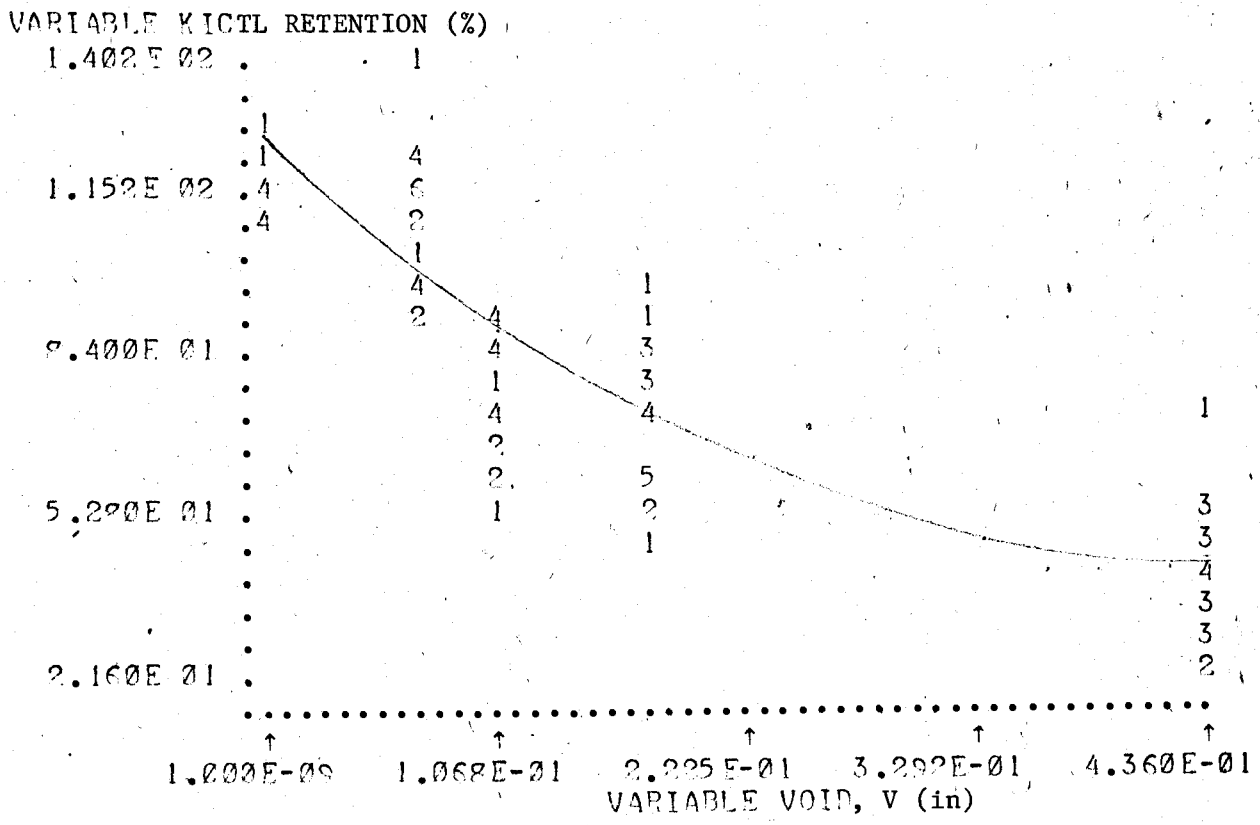

Regression model for K_{ICTL} retention (%) = 126.76 - 377.27V + 422.85V^2

R = .87

C5. Stepwise multiple linear regression models for board K_{ICTL} retention (%) of original solid wood (microlam 3 not included), and corresponding R values

Step	Model for board K_{ICTL} retention (%)	R
1	-106.55 + 4.28D	.84
2	-127.33 + 4.14D + .33DR	.88
3	-48.22 + 2.24D + .54DR - 82.66V	.93
4	66.40 + .70D + .06DR - 436.01V + 3.48DRV	.95
5	188.68 - 1.80D + 1.48DR - 510.09V + 4.57DRV - 69.54R	.95
6	204.17 - 2.15D + 1.70DR - 521.52V + 4.10DRV - 79.12R + 21.56RV	.95
7	209.73 - 2.33D + 1.80DR - 666.49V + 2.41DRV - 82.66R + 80.49RV + 4.21DV	.95

Degree of freedom (source) = 47

Units = D (lb/cu ft), R (lb/1000 sq ft), V (in)

C6. Scatter data of board K_{ICTL} retention (%) versus board density D (microlam 3 not included), and the fitted nonlinear regression model

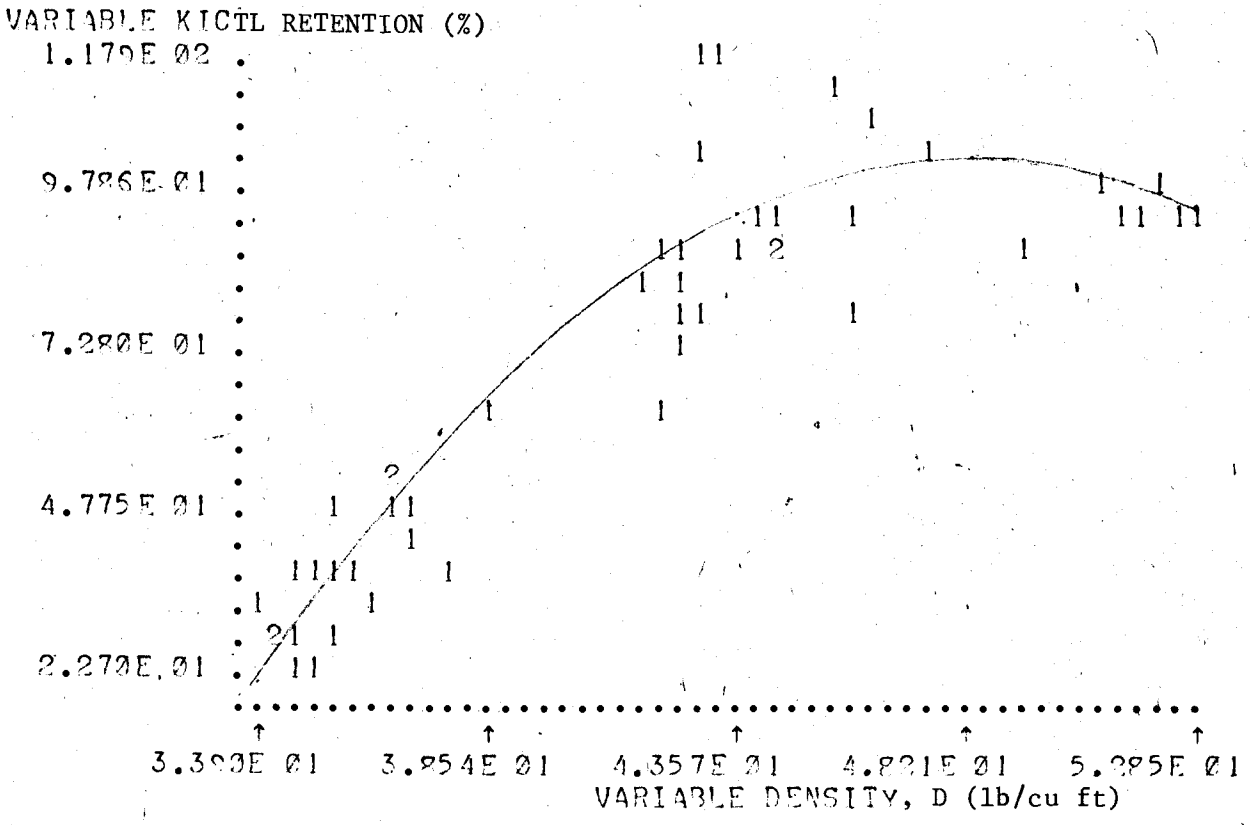

Regression model for K_{ICTL} retention (%) = $-777.92 + 36.22D - .37D^2$

$R = .93$

C7. Scatter data of board K_{ICTL} retention (%) versus average void length V (microlam 3 not included), and the fitted nonlinear regression model

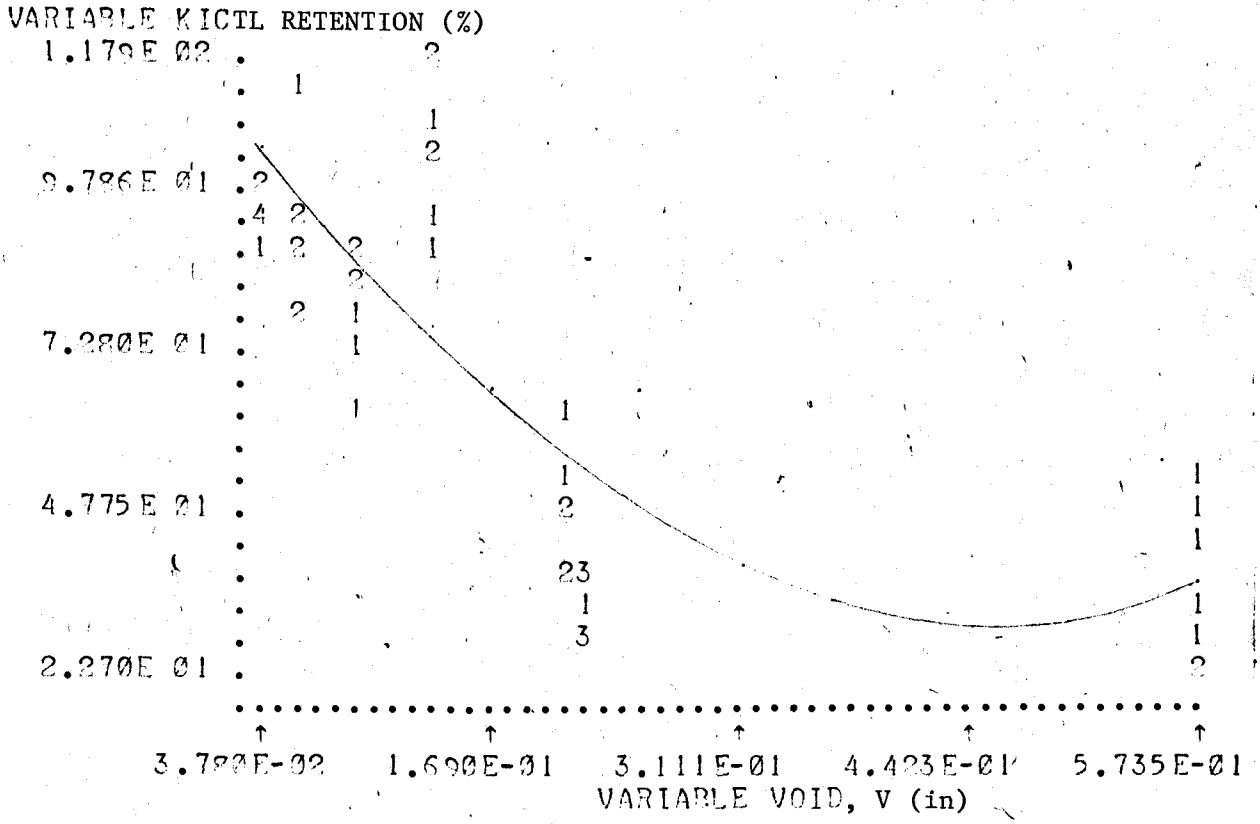

Regression model for K_{ICTL} retention (%) = 117.33 - 367.97V + 392.29V^2

R = .80